Quantitative Analysis and Modeling of Microembolic Phenomena

by

Michael J. Feldstein
B.S. Bioengineering, 2000
University of California at Berkeley

Submitted to the Department of Electrical Engineering and Computer Science in Partial Fulfillment of the Requirements for the Degree of

Master of Science in Electrical Engineering and Computer Science

at the

Massachusetts Institute of Technology

February 2006

Signature of Author: _____
Department of Electrical Engineering and Computer Science
January 20, 2006

Certified by: _____
Elazer R. Edelman
Thomas D. and Virginia W. Cabot Professor of Health Sciences and Technology
Thesis Supervisor

Accepted by: _____
Professor Arthur C. Smith
Professor of Electrical Engineering and Computer Science
Chairman, Committee for Graduate Students

Quantitative Analysis and Modeling of Microembolic Phenomena

by: Michael J. Feldstein

Submitted to the Department of Electrical Engineering and Computer Science on January, 20th 2006 in Partial Fulfillment of the Requirements for the Degree of Master of Science in Electrical Engineering and Computer Science

ABSTRACT

This thesis explores parameters that govern microvascular occlusion secondary to embolic phenomenon. Bulk and individual properties of microembolic particles were characterized using light microscopy, SEM and optically-based particle analysis. Particulate probability distributions were created from imaging data using Matlab. Size distribution, volume, morphology and chemical properties were quantified using in-vivo and model flow systems to correlate particulate characteristics and occlusive efficacy. This study focused on novel expandable/deformable Polyacrylic acid microspheres (PAA-MS) for use as catheter-deliverable therapeutic emboli. These emboli expand in aqueous media such as blood and remain unexpanded in custom delivery media. The techniques developed to investigate therapeutic microemboli were applied to the analysis of clot dissolution byproducts.

PAA-MS expand volumetrically in seconds when placed in aqueous environments. PAA-MS were modified to resist fragmentation based upon failure analysis. Degradation testing demonstrated PAA-MS chemical stability. Charge characteristics inherent to the PAA-MS acid matrix were leveraged to develop low-viscosity media that prevent expansion. Cationic dyes were found that bind the charged matrix within PAA-MS to enhance visualization. Unexpanded PAA-MS were delivered through standard catheters and microcatheters at concentrations that induce durable occlusions. Non-expandable microspheres could not be delivered through microcatheters. PAA-MS required less embolic mass to occlude in-vitro flow systems at significantly higher pressures than non-expandable microspheres. Preliminary biocompatibility tests demonstrated safety and PAA-MS were able to occlude both porcine renal and coronary vasculature in-vivo. An ultrasonic clot dissolution device generated microemboli from synthetic acellular fibrin-only clots and whole blood clots. The average particle size for whole blood clots was less than 100 microns and acellular clots produced larger average emboli than whole blood clots, indicating that cellular components may limit thromboembolic size.

The expandable/deformable properties of PAA-MS allow them to traverse microcatheters when unexpanded. Once in blood, PAA-MS expand 140-fold to create a space-filling, pressure resistant occlusion. These results have implications for intravascular embolization procedures where smaller catheters minimize vasospasm and allow more precise targeting while stronger occlusions resist occlusive breakdown and associated distal embolization. These embolic improvements could reduce procedural complications while increasing efficacy. Future work will solidify correlations between microembolic properties, microvascular occlusion and tissue infarction.

Thesis Supervisor: Elazer R. Edelman
Title: Thomas D. and Virginia W. Cabot Professor of Health Sciences and Technology

Acknowledgements

Firstly I would like to thank my advisor, Professor Elazer Edelman for his guidance and expertise. As an advisor he has directed me toward clinically significant and scientifically interesting quandaries while allowing me the flexibility to explore areas of my own interest. As an MD/PhD who successfully balances clinical duties a successful and prolific laboratory and family life, he is an ideal mentor. I am truly grateful that he has given me the opportunity to work in his lab and I look forward to our future work together.

I am very appreciative that the DuPont-MIT alliance has given me access to their advanced materials and has allowed me to collaborate with their expert scientists. Working with the DuPont embolics team has been a pleasure. I would especially like to thank Garry Figuly who worked with me closely to further develop expandable microsphere embolic technology.

DuPont's funding of this project has been generous and I am thankful for their support. I would also like to thank the Harvard-MIT MD/PhD program and the NIH MSTP grant for funding part of this research.

I would like to thank the members of my lab including Aaron Baker, Haim Danenberg, David Ettenson, Adam Groothuis, Chao-Wei Hwang, Kumaran Kolandaivelu, Kha Le, Andrew Levin, and Peter Wu for their advice, knowledge and inspiring conversations. I would like to thank Jacqueline Brazin for her help studying thromboembolism. The camaraderie engendered by the members of my lab contributes to a pleasant working environment that helps ease the difficulties of academic research.

Without the support of my friends and family I would not have been able to accomplish anything. The good times that I spend with them make all the hard work worthwhile. They give me purpose and are the source of my drive.

Lastly, I would like to dedicate this thesis to my co-worker and friend Tarek Shazly who assisted me with this project and helped carry out many of the detailed and laborious aspects of the work. I truly could not have completed this work without his aid nor would the experience have been as enjoyable without his company.

Table of Contents

Figures

Tables

Chapter 1: Introduction

1.1 Background

1.1.1 What are Microemboli?

Any abnormal mass traveling within the blood stream can be defined as an embolus[1]. However, the fate of that mass, and consequently of the patient, is not fully defined. Many factors contribute to the evolution and destiny of an embolus including but not limited to the size of the mass, its chemical composition, morphology, origin, vascular bed and the activity and vascular health of the patient. Yet, none of these factors alone definitively predict the severity of the response. Large emboli can be catastrophic and of immediate consequences, such as the case of large saddle pulmonary emboli or fat emboli after bone trauma. At the same time, large venous thromboemboli that pass into the redundant network of the lung can remain silent. Microemboli can be similarly silent, even in vascular beds such as the brain and heart that are extremely sensitive to ischaemia. Although detrimental effects may not be instantaneously catastrophic, these microemboli can be an insidious source of destruction[2].

Microemboli by definition are emboli that fall between 1 and 1000 microns and are usually not visible by conventional imaging techniques such as angiography, CT and MRI. The smallest microemboli can infarct tissue if the emboli are thrombogenic or have the capacity to aggregate. Larger microemboli can obstruct critical microcirculatory branches or affect tissues that have heightened sensitivity to ischaemia. In this regard, if the destructive power of microemboli can be understood, controlled and manipulated it could be harnessed for therapeutic applications in areas where blood flow is not desired such as hyper-vascular tumors and arterio-venous malformations. A greater understanding of microembolism could also help prevent complications of embolic procedures and other vascular interventions.

1.1.1 From Thromboembolism to Therapeutic Embolism

For the initial investigations into microcirculatory dysfunction, researchers injected synthetic microemboli into coronary vasculature to recapitulate heart-failure secondary to microembolic events[3]. In a study by Hori et al, 1987, injection of 15-micron spheres mimicked exertional angina with decreased coronary flow reserve while

slightly larger 25 micron spheres caused patchy necrosis, but no decrease in long-term coronary flow reserve. Studies such as these revealed that the size of the particulate has a significant impact on the clinical outcome.

As knowledge of embolization pathophysiology burgeoned, view of these data shifted toward considering microemboli as a potential therapeutic option[4], for example, synthetic microemboli for controlled vascular occlusion. Therapeutic embolization was initially viewed with skepticism because of the potential dangers of injecting an unpredictable foreign material into the blood stream. Prototypical therapeutic emboli were particulate of irregular sizes and shapes made primarily from PVA (poly-vinyl alcohol) [5]. Although PVA achieved some success as an embolic agent for several indications, there are problems associated with the material. Many of the problems are related to the irregular shape of PVA particulate as well as the inability to accurately control size distribution of the particulate[6-11]. Because of these properties, PVA particulate tend to aggregate and occlude delivery catheters[12]. PVA particulate also result in spatially unpredictable vascular occlusion because the particulate can occlude larger arteries if they aggregate or smaller arteries if they do not[13]. Furthermore, PVA particulate occlusions can be temporally unpredictable because the occlusion often depends upon thrombosis around particulate aggregates which may recanalize, causing the occlusion to dissipate[14].

To address some of the problems with PVA particulate, researchers developed microspheres for use in embolization procedures[15]. Spheres had an advantage over PVA in that they did not tend to aggregate. Recanalization of occlusions created with microspheres are less prevalent than with PVA particulate[14]. There are several different types of microspheres that have been used for embolization procedures. The most common are PVA microspheres and tris-acryl gelatin microspheres[11, 16-18]. Another type are Super-Absorbent Polymer (SAP) microspheres[14, 19-21]. These are similar to the tris-acryl spheres except that they expand when introduced into aqueous media. Preliminary studies show that the SAP microspheres perform similarly to tris-acryl microspheres but demonstrate more space-filling within the vasculature, and presumably less thrombosis around the occlusion with less likelihood of recanalization

[21]. However, no quantitative in-vitro tests of these embolic materials have been performed to date.

1.1.2 Uterine Artery Embolization (UAE)

One of the primary indications for therapeutic embolism is uterine artery embolization (UAE) for the treatment of uterine fibroids (also called uterine leiomyoma or uterine myomata)[22]. UAE emerged as an alternative to surgery for the treatment of uterine fibroids in 1995[23]. UAE is minimally invasive and hence far less intrusive than myomectomy or hysterectomy, requires less post-operative care, and retains uterine viability. A growing body of literature reports symptomatic improvement and significant uterine and fibroid shrinkage in approximately 80% of procedures[11]. UAE entails the introduction of a delivery catheter (a long thin polymer tube) into the uterine arteries by way of the large femoral arteries in the legs[24]. Usually the procedure is performed bilaterally to ensure sufficient fibroid vascular occlusion. The interventionalist visualizes the uterine vasculature via x-ray angiography and attempts to embolize as close as possible to the tumor.

Although UAE has favorable results when compared to surgery, there are still complications that must be addressed[12, 25-40]. Frequent complications include: post-embolic fever, non-target embolization, under-embolization, ovarian failure, uterine infarction, relapse of the fibroid tumor, recanalization of occlusion, infection and sometimes even death, [10, 13, 22, 35, 41]. Most of these problems are related to a general lack of occlusive control and/or stability. For example, a major concern is the unintentional embolization of ovarian anastomoses or cervicovaginal branches of the uterine arteries, which can cause ovarian failure or sexual dysfunction respectively. Unfortunately, solutions geared to address one problem can create another. For UAE embolic diameter is recommended to be larger than 500 micron because that is the upper bound of the diameter of ovarian anastomoses[22, 42], thus obligating the use of larger catheters. Larger catheters induce vasospasm in larger vessels and hence prevent close approximation of the delivery catheter to the tumor[12, 13]. Because of this the embolic must be injected more proximally, increasing the chance of unintentionally embolizing proximal branches such as the cervicovaginal. Limitations in the current technology preclude the solution of one problem without creating another.

Identifying procedure endpoint plagues UAE because of complicating factors like vasospasm, thrombosis and the inherent low resolution of angiography. To ensure adequate occlusion, an interventionalist may top-off the uterine circulation with emboli, which can cause over-embolization. Over-embolization of the uterine artery increases collateral damage to healthy tissue and the likelihood of unintended particle migration, especially to the ovarian arteries [11]. On the other end of the spectrum, vasospasm or thrombosis can cause premature end-point determination, resulting in under-embolization, and subsequent survival and persistence of symptomatic fibroids and the need for additional therapy. The procedure endpoint has been described as either flow stasis or markedly reduced flow in the targeted uterine artery[11, 12]. If embolic could be precisely localized and titrated for optimal tumor infarction, many of the complications could be attenuated. Current research is generally empiric, lacking in rational optimization of size, quantity, and morphological characteristics of embolic material. There is no identifiable strategy for providing adequate ischaemia while limiting adverse sequelae such as uncontrolled distal embolization, vasospasm during the procedure or over-embolization leading to healthy tissue destruction.

1.1.3 Embolic Materials

The two most common embolic agents for UAE procedures are non-spherical polyvinyl alcohol (PVA) particulate and tris-acryl gelatin calibrated microspheres (Embosphere®, Biosphere Medical, Rockland, MA)[11, 43]. PVA particulate has the longest history for UAE but is far from an ideal embolic agent, with shortcomings stemming from the irregular particle shape distribution and tendency to aggregate. Tris-acryl gelatin microspheres have consistent shape and size, have lower tendency to aggregate, and allow for more selective pruning of target vasculature[12, 17].

As an incremental improvement to standard microspheres, the DuPont-MIT alliance has developed highly expandable and deformable microspheres principally composed of polyacrylic acid (Expandable/Deformable PAA Microspheres, DuPont, Wilmington, DE). Although there have been some reports of absorbent and expandable microspheres[14, 20, 21, 44-48] and recently Biosphere Medical has announced an expandable product, none have the material properties (up to 140 fold volumetric expansion in seconds) and composition (Poly Acrylic Acid) of the

expandable/deformable PAA microspheres (PAA-MS). Furthermore, there is no evidence in the literature of the in-depth engineering analysis of embolic microspheres.

A major goal of this study is to investigate the properties of PAA-MS and compare it to currently available technology. By quantifying microembolic properties, the key parameters that govern occlusion can be isolated and hopefully manipulated. With this knowledge, optimal occlusion protocols can be designed and embolic protection protocols can be developed to prevent the damage that can be caused from uncontrolled microembolism.

1.2 Theory

1.2.1 Theoretical Benefits of Embolic Expansion/Deformation

There are many aspects of human vasculature that work to prevent infarction and remove any occlusions that may form[49, 50]. This is essential because most organs are extremely sensitive to ischaemia and if the body's efforts to maintain circulation are thwarted, tissue often will die rapidly. Tumors are especially adept at maintaining and adapting their own blood supply[48]. Some biological methods for ensuring tissue perfusion include redundant collateral circulation, innate clot dissolution enzymes, and neo-vascularization. Any method to infarct tissue must overcome these barriers.

There are several reasons why therapeutic embolism, specifically UAE, can fail, but they all relate to uncontrolled embolism[51, 52]. PVA fails often, sometimes even before entering the body, because of aggregation problems and uncontrolled occlusion of vessels and catheters. Tris-acryl gelatin microspheres were developed to address many of the problems with PVA. The tris-acryl gelatin microspheres are smooth and round, enabling ease of delivery and resisting aggregation. A theoretical problem with a material that traverses catheters easily is that it will not produce as strong an occlusion in the body. Smooth microspheres can roll over each other in a rolling without slipping motion[53] and will not form an occlusion until they are deep enough within the vasculature to fill the vasculature from the microcirculation proximally. Microspheres at the more proximal end of such occlusions are resting on top of the more downstream microspheres and can theoretically migrate away from the site of occlusion because there is no force holding them in place.

Occlusive stability is a critical factor for long-term safety and efficacy of embolic therapy. Expandable/deformable microspheres could theoretically create a much more stable occlusion than spheres designed solely for ease of delivery. By expanding within the elastic environment of the target artery the PAA microspheres will exert a normal force on the arterial wall and other surrounding microspheres, resulting in a tightly packed occlusive mass. The resultant recoil force from the arterial wall will pin the microspheres in place by inducing significant frictional forces normal to the vessel surface and between the surfaces of the deformed microspheres[54, 55]. In addition, the recoil pressure forces the packed microspheres into irregular, non-spherical morphologies, maximizing surface interactions and therefore increasing the stability of the occlusion. Deformable microspheres will theoretically assume a nearly rhombic dodecahedron three-dimensional geometry (actual number of faces will approach an average of 13.7 as interstitial space approaches zero) and achieve a much higher packing density[1] (close to 1). (Figure 1-1, Left)

Figure 1-1: Left- Expandable/Deformable PAA-MS in blood deform when juxtaposed and maximize interfacial contact (lines drawn in to highlight surface contact). **Right-** when microspheres are rigid they interact at small areas which can act as pivots for rolling

In comparison, rigid spheres can assume body centered or hexagonal closed pack geometry at best, which yields a packing density of .74048, and for random packing the density is even less at near .6 [56]. Given roughly the same order of magnitude for frictional coefficients for most hydrogels, the fact that deformable/expandable hydrogels

[1] Packing density is defined as the total volume over the volume of particulate and it approaches one as the volume of the interstitial spaces approaches zero

will have orders of magnitude more surface area contact as well as greater normal forces due to expansion will result in far more stable occlusion[57]. The most efficient way for rigid spheres to translocate is to rotate around each other without the need for slipping by forming pivot points at small areas of contact. Deformation will obliterate the rolling without slipping condition which only applies to rigid spheres[53] (Figure 1-1, Right). The space-filling properties of deformable/expandable microspheres will prevent any possibility of recanalization, will prevent rolling of spheres around each other, will increase both frictional forces and surface tension (Van-Der-Waals forces) between spheres and hence should theoretically result in more stable occlusions.

1.2.2 Theory of PAA Microsphere Expansion

Polyacrylic acid is a well known pH-sensitive hydrogel[58-60]. The fixed charge on the hydrogel responds to ionic concentrations in which it is bathed. When spherically encapsulated, the fixed charge can be isolated from the surrounding media. When PAA microspheres are placed in low-pH solutions, the carboxylic acid residues become saturated with hydrogen and assume neutral charge[61]. The lack of charge supplants the thermodynamic drive to isolate charged moieties from one another with an opposite Van-Der-Waals force that brings residues together, resulting in a contracted state for the hydrogel. Uncharged polyacrylic acid residues are less hydrophilic and tend to exclude water and bind to other uncharged residues via Van-Der-Waals forces induced by instantaneous dipoles. When the pH rises above the pKa for the carboxylic acid residues, the acid residues become charged and large coulombic forces drive the residues apart, forcing the hydrogel to expand[62]. In the process, water floods into the polymer to hydrate the exposed charges, shielding them from one another via hydrogen bonding. Organic solvents such as DMSO, ethiodol (poppy seed oil), propylene glycol etc. cannot readily form strong enough dipoles to hydrate exposed charges in polyacrylic acid so PAA microspheres placed in these media do not readily expand. In addition, sodium counter-ions on the polyacrylic acid residues are not readily soluble in the organic solvents and remain associated with the acid when in organic solvents, facilitating neutrality within the contracted hydrogel. High salt solutions prevent expansion by a slightly different mechanism. Dissociated cations in solution prevent expansion of PAA microspheres by forcing the equilibrium constant for the dissociation of the polyacrylic

acid from its counter-ion toward remaining associated. Excess sodium in aqueous solution promotes the formation of the sodium salt of the polyacrylic acid, hindering the coulombic expansion of the hydrogel.

1.3 Thesis Statement

Microembolism and subsequent microvascular occlusion can be a powerful tool to treat tumors and arterio-venous malformations, but can also be dangerous and destructive to healthy tissue. The combination of location, material, size, volume and morphological characteristics of microemboli that induce significant tissue infarction remain enigmatic. The motivation of this work is to elucidate the fundamental characteristics of microemboli that can be life threatening when uncontrolled, or therapeutic when targeted. Using this information, rationale can be established for implementing anti-embolic protocols including intelligently designed embolic protection devices. Furthermore this knowledge can be exploited to design embolic therapies directed toward tumor therapy, arterio-venous malformations and any other application that necessitates controlled occlusion. Theoretically, there exists a minimum embolic load that induces controlled infarction in vascular beds with minimal risk of distal embolization and/or life-threatening necrosis. Expandable/deformable PAA microspheres have theoretical advantages for providing more controlled and stable occlusions with less invasive introduction catheters. In developing a system to study these novel embolic devices, we will also learn more about thromboembolic processes. This research should help expand the knowledge of therapeutic and pathological microembolism in microvascular networks.

Chapter 2: Particulate Analysis System and Probability Distribution Construction

Abstract

Although standard assays such as light microscopy and scanning electron microscopy reveal detailed information about individual micro-particles, generalizing this information to group behavior is not readily possible given inter-specimen heterogeneity and synergy between particulate. To investigate group properties of micro-particulate we chose to use the Beckman-Coulter™ RapidVUE® particle analysis system. We prioritized this system over other particle analysis systems that rely on Doppler shift or impedance differentials because the RapidVUE® system can characterize shape as well as particulate counts and volumes and it can be calibrated to recognize varying particle geometries.

The RapidVUE® system is an optically based micro-particulate analysis system that can analyze 75ml particulate suspension samples with a dynamic range of 20 to 2500 microns. The procedures for cleaning, calibrating and operating the RapidVUE® are outlined in this document along with the theory, specifications, and limitations of the system. We used Microsoft Excel and Mathworks Matlab software for data analysis to create probability distribution models with microembolic population statistics.

2.1 Beckman-Coulter™ RapidVUE® Particle Analysis System

Introduction

Most analyses of microembolic particulate have been qualitative and anecdotal. A more quantitative and rigorous analysis of micro-particulate is needed to establish stronger correlations and causal relationships between micro-particulate properties and in-vivo function. Although standard methods such as light microscopy and scanning electron microscopy reveal a wealth of information about particulate, these methods are limited in that they can only reveal information about a small number of particles at a time. It is imperative to determine the population characteristics of micro-particulate because in-vitro and in-vivo function depends directly on bulk properties rather than the properties of individual particles. To quantify bulk properties of micro-particulate, we chose to implement the Beckman-Coulter™ RapidVUE® particle analysis system. This section describes the specifications, theory, and operation of the RapidVUE® particle analysis system. The choice of this machine for this project is justified and the pertinent features are expounded upon.

Much of the RapidVUE® machine-specific information contained within this section is adapted from the RapidVUE® User's Reference[63], Beckman-Coulter™ part # 8321490B and the RapidVUE® Fluid Sample Module Reference Manual[64], Beckman-Coulter™ part # 8321519. In addition to machine-specific information, this section also outlines general programming and usage of the system as implemented for this thesis work.

Background

The Beckman-Coulter™ RapidVUE® is a commercially available Particle Shape and Size Image Analyzer that can output bulk particulate data to Windows based-PC software for analysis. For this thesis we used version 2.06 of the RapidVUE® software. The RapidVUE® system is available from Beckman-Coulter™ 1950 West 8th Ave, Hialieah, Florida 33010-9015. Technical support for the machine can be accessed by calling 1-800-523-3713.

The RapidVUE® is designed to characterize various shaped particulate, including fibers, rods, and spheres, by capturing images of a flow chamber at a rate of 30 frames per second and analyzing the images in real-time. The user can visualize the shape and size of the material frame by frame as it is being analyzed. In contrast, all other particle analysis systems such as laser-Doppler and standard impedance based Coulter counters do not allow visualization of particles directly and are insensitive to shape. Calibration of the RapidVUE® is therefore more accurate than the calibration of other devices because there is a visual check and corroboration to ensure that the software is counting properly. The machine can be calibrated to digitally filter out particles of the wrong shape type and background image noise. The ability of the RapidVUE® to quantify shape is a unique feature that allows the machine to track sphere integrity and fiber length while increasing count accuracy.

Custom Windows-based software included with the RapidVUE® provides detailed population analysis of the particulate and can be programmed and calibrated to recognize each type of particulate. Detailed information about each particle and statistics regarding the entire run are readily accessible (Figure 2-1). All information gathered can be exported to Microsoft Excel, Matlab or any other data manipulation software.

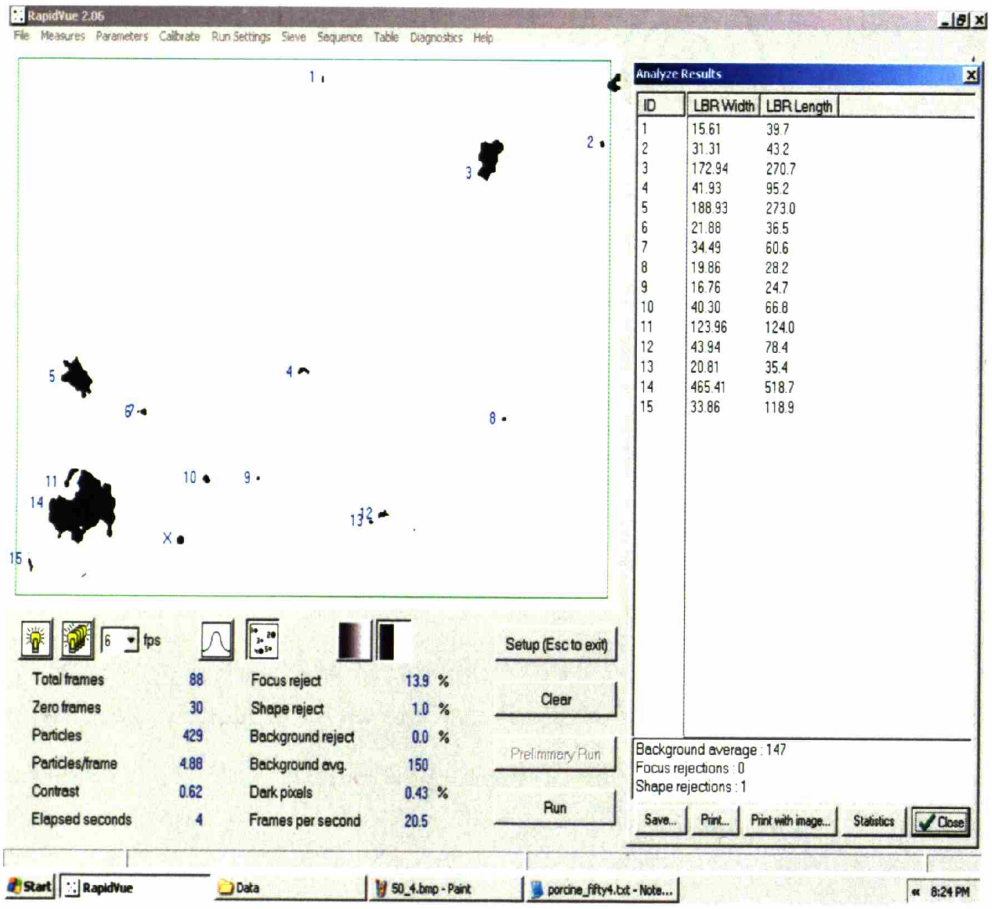

Figure 2-1: Screen shot from the RapidVUE® particle analysis software

Demonstrates how each frame can be analyzed and the particle count analysis is shown at right. By modifying parameters in the software and visually inspecting the analysis, calibration can be optimized.

2.1.1 Specifications

The RapidVUE® has a wide dynamic range, from 20 to 2500 microns, that is much larger than most other particle analysis systems. It is comprised of a fluid sample module and an optical bench. The system has manual controls on the unit and is also interfaced with a Microsoft Windows-based machine. The RapidVUE® system is composed of two main pieces: the optical bench and the sample module.

Optical Bench

The optical bench contains a 0.5 microsecond strobe that projects light through a narrow flow chamber in the sample module to create silhouettes of flowing particles onto a high resolution charge coupled device (640X480 pixels) camera that captures images at up to 30 frames per second. The rate of capture is somewhat dependent on particle

concentration and CPU speed because some of the image processing is performed in real-time and the next image is not taken until basic image processing has been performed on the previous image. The images analyzed contain cross-sections of the actual particles. Because the system is high-resolution and optically based, it can recognize and quantify irregularly shaped particles. The optics and CCD (charge-coupled device) camera interface are designed to analyze particles from 20 micron smallest dimension to 2500 microns in the largest dimension. The lower limit is constrained by the optical magnification settings and the limits of the CCD pixel dimensions. The upper limit is constrained by the field size which is limited by the number of pixels captured at the factory-set optical magnification.

The CCD camera digitizes the projection from the strobe into a 640X480 8-bit grey-scale image by sampling and quantization. Sampling is carried out in space by the layout of the CCD such that 640X480 pixel intensities are captured. Each intensity value is quantized into an 8-bit value between 0 and 255, which correspond to grey-scale intensity. The software then thresholds the image at a user-defined setting between 0 and 256 whereby all pixels lower than the threshold value (darker) are considered to be within a particle. The image is raster scanned from top to bottom, identifying dark segments on each line, and associating them with the segments on the previous line. The segmentation algorithm considers any adjacent particle to be connected within the same particle. This introduces a problem in that overlapping particles can be considered as one large particle. To get around this limitation, filters can be established during calibration to ignore particles that are not of the right shape or that are not in focus. The border is checked for continuity before the particle is considered complete.

The software on the PC conveys threshold, focus, and other rejection criterion to the RapidVUE® before data acquisition begins so that the machine can perform much of the initial calculations for thresholding and segmentation. For each particle, the pixel area, perimeter, halo area around the particle and x-y Cartesian coordinates for the left, right, top, and bottom extremes are all calculated. Using this data, other information can be calculated by the PC software such as focus rejection, sphericity, equivalent circular area diameter or least bounding box. These calculations will be discussed below.

Fluid Sample Module

The fluid sample module is a chemically-resistant one-piece integrated system. The reservoir in the module accepts 75ml samples. A centrifugal pump circulates the fluid through the imaging chamber in a closed loop system at variable speeds between 1 and 20L/minute. The computer is able to estimate the total volume of particulate within the sample by using the speed of the pump and the known fixed volume of the flow chamber to calculate the turn-over rate of the sample. The system is designed for solutions of less than five centipoise in viscosity. This is required because for fluids of greater than five centipoise viscosity, the calculation of flow rate based upon pump speed becomes unreliable.

The fluid chamber can accept many fluids and the materials that the fluid comes into contact with include 316 stainless steel, glass, Teflon hoses and Teflon sample vessel, Kalrez® O-rings, and Parylene coating- providing an inert and durable environment for most solvents including organic solvents. The suspension fluid sample may be top-loaded from the input orifice or it may be pumped into the inlet valve. The suspension fluid drain outlet is controlled by a handle on the side of the machine. The controls for the pump speed are in percent of maximum flow. For all of our experiments the flow speed was set at 30%. This was determined to be an optimal speed in previous studies[65, 66] that allowed for timely analysis of the sample without creating bubbles that could cause artifacts in the analysis. The concentrations of the suspensions are determined by visual inspection such that particles are dispersed enough to minimize overlap and allow adequate luminosity while providing sufficient particulate for a reasonable data rate.

2.1.2 Operation

The following procedure was used for all samples run through the particle analyzer. Turn on the power switch on the right side of the RapidVUE® particle analyzer. If the attached PC computer is not already operational, turn on the computer and load the RapidVUE® software. The default configuration will automatically be loaded. Load in the appropriate configuration for the particulate and suspension to be analyzed. See Calibration and Programming section for information regarding how to configure the software. Adjust the speed of the machine to 30 by pressing the - - - button on the controls on the front of the machine. Empty the reservoir by turning the drain lever on the

right side of the RapidVUE® particle analyzer to the open position. Turn the drain lever to the closed position- the system is now ready to be rinsed as follows.

Rinsing Operation

To rinse the system, approximately 300ml of diluent is flushed through the system by filling the system with 75ml of diluent per run, turning the pump on for approximately 20 seconds, stopping the pump, draining and then repeating three more times. While the system is running, the background particulate count can be monitored on the PC computer to ensure a background of less than 0.4 particles per frame. This number is around the general background noise of most solutions and has been used by other authors[65, 66]. Solutions with higher background noise may require a higher particle per frame value. The rinsing procedure should be repeating until the count is less than .4 particles per frame after 30 seconds of running the machine. Whenever a new suspension fluid is to be used the system should be pre-rinsed as above with the new suspension solution and the background noise should be assessed. If the new suspension solution and the old are immiscible, an intermediate solution in which both new and old suspension solutions are miscible should be used to prevent an emulsion from forming. Before turning the machine off it should be rinsed and cleaned with Coulter-Clenz (available from Beckman-Coulter) and it can be left filled with Coulter-Clenz or distilled water when not in use.

Once the machine has been rinsed thoroughly, the sample suspension can be loaded into the fluid chamber. After the 75ml suspension has been loaded and the top of the fluid chamber has been closed, the machine can be turned on at a speed of 30. The machine should be run for approximately 30 seconds to ensure proper mixing of the suspension and to eliminate bubbles that may have been introduced while loading the sample. While the system is priming, the PC can be used to monitor for bubbles by pressing the preliminary run button in the software and clearing the data after each run. If bubbles are negligible, the sample is ready for analysis. By pressing the Run button in the RapidVUE® software, three successive runs will be performed of 100 seconds each. This is the default run time and can be changed if desired. Depending upon the frame rate during the run, between 2000 and 3000 images will be analyzed. The files will be named sequentially based upon the root name input into the file-name box. This name

must be specified before pressing run, or alternatively the default file name can be used and the files can be renamed afterwards. After a run has been completed, the machine should be rinsed again as in part 5 above. After rinsing, the system is ready for another sample or to be shut down.

2.1.3 Calibration and Programming

The RapidVUE® system is calibrated at the factory to ensure accurate results. The micron/pixel ration, the micron distance that a linear pixel represents, the magnification and the total image size are all determined and input to machine so that accurate correlations can be drawn between image size and actual particle size. The RapidVUE® particle analyzer is periodically serviced and re-calibrated by Beckman-Coulter. The technician uses pre-measured, precision mono-sized microspheres and reticles to make sure that the calibration settings are valid.

In addition to calibration by Beckman-Coulter, we performed our own calibration procedures for each type of sample run in order to tailor the software settings for the specific task. Some of the adjustable values include the threshold value, focus rejection settings, shape rejection settings, border rejection settings, fiber overlap rejection and background intensity rejection.

Threshold Value Determination

The threshold value can have a significant effect on the results, especially if the contrast between particles and background is not sharp. The threshold should be optimized to maximally eliminate background noise without eroding or removing particle data. This can sometimes be difficult to achieve and a compromise may have to be made to optimize signal to noise. For example, if the threshold is set too low, the area of the particles may be underestimated because the borders that are out of focus due to curvature and diffraction will be eliminated from the area calculation while if the threshold is set too high, artifacts or shading in the background may erroneously be counted as particulate.

An absolute threshold value between 0 and 256 can be specified in the software. Alternatively, an adaptive threshold can be specified. The adaptive threshold is a threshold that is a percentage of the background. This method reduces errors associated

with varying levels of luminosity that can be caused by different solvents or higher concentrations of particles. In all of our experiments we used an adaptive threshold value of 56% which has been used by others[65, 66] and produced good results during manual calibration. During manual calibration the threshold value can be adjusted and single frames can be monitored to see how the particle counts are changed.

Experimental Settings

The basic configuration settings for analyzing microspheres were based upon those used by other others[65, 66] for micro-particulate, but were tailored for use with microspheres by manually setting the rejections based upon single image analysis(Table 2-1).

Table 2-1: Standard configuration settings for analyzing microspheres in the RapidVUE® particle analyzer

PARAMETERS	
* Focus rejection	On
* Border rejection	On
Edge correction	Off
* Repetition rejection	On
Fiber overlap rejection	Off
* Shape rejection	On
Background intensity rejection	Off
Background subtraction	Off
Area correction	Off
Shape rejection criteria	Sphericity < 0.90
Focus parameter	500
Minimum particle area	4
Micron/pixel ratio	7.292
Maximum particle area	5000000
Threshold	Adaptive: 56
Magnification	2.74
Image size (microns)	4521 x 3354

Focus rejection was turned on so that out of focus particles would not be counted erroneously. Out of focus particles would give inaccurate size measurements for the particles. The default setting of 500 was seen to be adequate by single-frame manual calibration. Border rejection was turned on so that particles that were interrupted by the border would not be counted. Repetition rejection was turned on to prevent artifacts within the camera or optical system from being counted every frame. One of the most

important rejection criteria for microspheres is the shape rejection setting. Shape rejection was set to reject objects with less than 90% sphericity. This eliminates small debris particles that may be in the background and it also eliminates overlapping spheres. Note: when non-spherical particulate are to be analyzed this setting will often be reversed such that extremely spherical objects are rejected in order to prevent air bubbles from being counted. Other rejection criteria that were not turned on were determined by manual calibration. The minimum and maximum particle sizes used were system defaults used to rule out outliers. These were not adjusted in order to maintain maximum dynamic range. The micron/pixel ratio, the magnification and the image size are all invariants set by factory calibration.

Calibration Experiment

The single frame manual calibration is used to make sure the software is recognizing and measuring particles correctly. In order to further verify the calibration, 66 microspheres were individual counted and suspended in water after dying them with Acridine orange (see material properties chapter for dying protocol) (Table 2-2).

Table 2-2: Calibration counts for 66 individually counted microspheres

Run #	Final Count	Actual Count	Percent Error
Run1	71	66	7.5
Run2	72	66	9.1
Run3	64	66	3

The results show that the percent error is less than 10% for all three runs and the error falls on both sides of the true value. Given that the particle analyzer is not designed to be accurate when measuring small numbers of microspheres, these results are adequate. Although the total volume of particulate is not the most important attribute for microspheres, it is an important value for other types of particulate such as thromboemboli.

2.1.4 Output

The RapidVUE® software provides text output of all measures and settings for each run (Appendix A). This output can be imported into Microsoft Excel or Matlab for analysis. The RapidVUE® software also has analysis capabilities and visual output of

probability distributions and basic statistics in real-time as the particulate are counted. Statistical information such as means, variance, counts, volume and number percentiles, sphericity, probability distributions and performance data are all available as output from the software.

The output gives several different means which are useful for characterizing particle samples with a single number. These means are referred to as the Dpq means where p = 1 to 4 and q = 0 to 4. The standard Dpq definitions apply only to spherical particles.

$$Dpq = [\sum D_i^{\,p} / D_i^{\,q}]^{(1/(p-q))}$$

where i ranges for all particles in the sample and D_i is the i^{th} diameter
For this definition, q is always smaller than p.
The p^{th} power geometric mean, Dpp, is defined as:

$$\log(Dpp) = \sum(D_i^{\,p} \log D_i) / \sum D_i^{\,p}$$

Setting q equal to p in the Dpq dialog box of the RapidVUE® software will generate the Dpp mean. Several values of Dpq can be reported in the output files. The Dpq mean with p=1, q=0 is the standard arithmetic mean of the distribution of the diameters. The surface mean is when p=2 and q=0 and the volume mean is when p=3 and q=0. Dpq with p=3,q=2 relates to the mean of the volume to surface ratio of the particulate and is called the Sauter mean. It is the diameter of the particle whose ratio of volume to surface area is the same as the complete sample.

The spread of the sample can be calculated in several ways. The software automatically outputs the percentiles by number, area and volume. Using the volume percentiles, upper and lower bounds, and the total number of particles the geometric volume standard deviation is estimated by the software using the following formula:

Geometric Standard Deviation = $$\frac{\sum[[D_{v0.5} - (D_{klb} + D_{kub})]/2]N_k}{\sum_k N_k D_{v0.5}}$$

klb = lower bound of bin k
kub = upper bound of bin k
$D_{v0.5}$= Median (50^{th} percentile) diameter
N_k = number of particles in each bin
Note: all of the values necessary for these calculations are in the text output files produced by the software program.

The Relative Span is a measure that relates to the width of the distribution with larger values indicating greater width of a distribution. It is calculated using the following formula:

Relative Span = $$\frac{D_{v0.9} - D_{v0.1}}{D_{v0.5}}$$

$D_{v0.9}$= 90^{th} percentile diameter
$D_{v0.1}$= 10^{th} percentile diameter
$D_{v0.5}$= Median (50^{th} percentile) diameter

2.1.5 Particle Size and Shape Characterization

For spherical particles such as microspheres the strobe projection will be spherical. The RapidVUE® software has several built-in methods for calculating the area of a particle that is assumed a priori to be roughly spherical. The software can calculate the Equivalent Circular Area Diameter, Da, which is equivalent to the diameter of a circle whose area is the same as that of the particle silhouette. The Equivalent Circular Perimeter Diameter, Dp, is the diameter of a circle with the same perimeter as the silhouette of the measured particle. Finally, the Least Bounding Circle Diameter, LBC, is the diameter of the smallest circle that can enclose the entire silhouette. For any shape, Dp is greater than or equal to Da. One definition of a circle is that is has the smallest area for a given perimeter possible, making Da = Dp for perfect circles.

The linear sphericity is calculated by taking the ratio of the diameter of a circle that would generate the area of the particle measured over the diameter of the circle that

would have the same perimeter of the particle measured and is given by the following formula:

$$\textbf{Linear Sphericity} = \frac{\sqrt{(4A/\pi)}}{(P/\pi)} = D_a / D_p$$

A=Area of measured particle
P=Perimeter of measured particle
The linear sphericity generated by the RapidVUE® software. Another method of calculating sphericity is the area-based sphericity which is calculated with the following formula:

$$\textbf{Area-based sphericity} = 4\pi A / P^2$$

The volume of each sphere is estimated from the following formula:

$$\textbf{Volume} = \pi D^3 / 6$$

For rectangular or fiber-like particles the least bounding rectangle properties are calculated rather than a circle. The least bounding rectangle is defined as the rectangle of the smallest area that encloses the silhouette. The software finds this rectangle by rotating a test rectangle based upon the extreme values of the particle by 7.5 degree increments until the smallest orientation is determined. The volume of such a particle is estimated by the estimating the depth of the particle as the average of the dimensions of width and length that encompass the particle as in the following formula:

Approximate Volume = A* (L + W)/2

A = Area of shape as measured from the image
L = Length of enclosing rectangle
W = Width of enclosing rectangle

If a fiber model is assumed, the software is programmed to assume either a cylindrical shape or a flat shape for the fiber. The length and width of fibers is calculated by using

the perimeter and area of the fiber silhouette to estimate an equivalent length and width of a rectangle of the same area and perimeter according to the following formulae:

$$Area = A = L * W$$

$$Perimeter = P = 2 * (L + W)$$

$$Length = L = P/4 + 0.5 * \sqrt{(P^2/4 - 4A)}$$

$$Width = W = A/L$$

Note: Area and Perimeter are measured from the image and the Length and width are then calculated from these values using the equations above. T = Thickness and is specified by the user in the software settings

For the cylindrical fiber model the volume is:

$$V = (\pi * W^2/4) * L$$

For the flat fiber model the volume is:

$$V = L * W * T$$

2.1.6 Accuracy Considerations

Although the particle analyzer is an accurate and quantitative tool for analyzing particulate distributions, there are some potential sources for error inherent to the system, even after proper calibration.

Single particle accuracy can be limited by several factors. The resolution limitation of the CCD limits the size range of the particles. However, the discretization error is most apparent for particulate less than 30 pixels in diameter (roughly 220 micron diameter). For these small particles the software can overestimate the size of the particles by roughening the edges. Small particles can also be affected by diffraction effects as light from the strobe passes around the edges of the particle, causing blurring of the edges resulting in further over-sizing of small particles. If a particle becomes out of focus the reported size can start to vary from the true value. The default settings for focus rejection effectively minimize error related to problems with out of focus particulate. The volume of a single particle is also an estimate because the depth of the particle is averaged from the other two dimensions of the particle. For spherical particles this system works well,

but for other particles it can cause some error. Another issue with volume calculations is that rejection criteria intended to increase the fidelity of population statistics related to size and distribution can reduce the total volume calculated. If volume is of primary concern this must be calibrated or another particle analysis system should be used in conjunction such as an impedance differential based system.

The particle analyzer is designed to determine population characteristics of particulate suspension. A wide range of concentrations is acceptable although suspensions that are too dense will cause light extinction while suspension which are sparse will have low n values and hence larger standard errors of measurement for estimated means and standard deviations. For statistically relevant analysis, the manufacturer recommends a sample size of at lease 5000 particles. The RapidVUE® lens has a dynamic range between 20 and 2500 microns; however, the best accuracy reported by the manufacturer is for measurements above 25 microns and below 1500 microns.

Focus Discrimination

Because the flow chamber that passes in front of the camera and strobe has a finite thickness, some particles may become out of focus if the are either too close or too far from the lens. These particles are not counted because their area will be inaccurate. The RapidVUE® software uses focus discrimination to quantify the sharpness of the particles edges in order to determine whether or not the particle should be rejected. The scan algorithm does this by measuring the magnitude of the intensity gradient across the border of the particle. If there is a large gradient over a short space, the particle is in focus, while if there is a small gradient over a longer space the object will be considered out of focus. To calculate the gradient, a second threshold is established that is at a lower value (i.e. darker) than the general threshold applied to the entire image. Two concentric around the center of the particle are established based upon the threshold levels. Because out of focus particles are darker in the center and become progressively lighter toward their borders, the outer circular diameter will be determined by the higher, general threshold while the inner concentric circle will be determined by the lower, secondary threshold. The difference in threshold values, divided by the pixel distance between these two circles is the gradient calculated by the software. Beckman-Coulter has

determined that the transition slope is linearly proportional to the particles distance from the focal plane and the at the proportionality is independent of particle size for circular shapes[63]. The program creates a well-defined region called the depth of focus that can be adjusted by adjusting the size of the gray level differential between the thresholds. The default focus discrimination parameters were used for all of our studies and showed decent data rates with low percent focus rejection.

A = particle area in pixels
P = particle perimeter in pixels
F = Focus parameter (set by user, default is 500)
T1 = primary threshold set by user
T2 = secondary threshold set by software
A_h = halo area in pixels
W_h = halo width in pixels = A_h / P
G = edge gradient of a particle

$G = (T1 - T2) / Wh = (T1 - T2) P / A_h$

The value of G relates to how focused the particle appears. If G > F the particle is accepted, otherwise the particle is rejected. Since grey-scale intensities change linearly with respect to location the focus test will be independent of the specific values of T1 and T2 because the area of the halo is proportional to T1-T2. The edge gradient calculation is a way of quantifying how fast the threshold changes over a pixel distance. For our studies we used the default focus parameter of 500, which resulted in a low amount of focus rejection with adequate data rates.

2.2 Statistics and Probability Distribution Construction

2.2.1 RapidVUE® output

The RapidVUE® software output the probability distribution in terms of % total volume. The volume is calculated using the shape model input into the settings file. The program also outputs exact data on counts of different diameters. This data can be input into Matlab for manipulation.

2.2.2 Matlab Analysis

Matlab software version 7.1 by Mathworks contains a Statistics toolbox with a distribution fitting tool. This tool was used to construct probability density functions for particulate analyzed by the RapidVUE® system. The distribution fitting tool also calculates the least-mean-square fit of various distributions to the input data and outputs the log-likelihood of the distribution fit. Different distributions can be selected to best fit the given particulate distribution. The distribution statistics can be output to a text file or graph. The calculations involved for probability distribution binning, mean determination, standard deviation and log likelihood can be found in standard probability and statistics texts[67].

2.3 Discussion/Conclusion

Beckman-Coulter™ RapidVUE® particle analysis system gives accurate and quantitative population statistics for a variety of particulate of varying shapes, sizes and distributions. The precision of the system and the flexibility of calibration make it adaptable to many experimental conditions. Although the system has some limitations, careful calibration can maximize the accuracy of this system. Other particulate analysis systems lake the dynamic range and accuracy that this optically-based system provides, which makes it well suited for microspheres and thromboembolic analysis.

Chapter 3: Material Properties of PAA Microspheres

Abstract

Expandable/deformable Poly-Acrylic Acid microspheres were synthesized with varied formulations (Table 3-1). Most of the formulations were designed to be expandable in aqueous media. PAA microspheres expand close to their maximal size in a matter of seconds. Some of the spheres were specifically designed not to expand, while others have properties such as pigmentation, smoothness, or specific filtered size ranges. Methods were established to characterize the material properties of these formulations in order to further understand how material properties might correlate with clinical applications such as endovascular occlusion.

A staining technique using the cationic dye Acridine orange was established to help visualize the microspheres under light microscopy and for particle analysis. The volumetric expansion coefficient from dry to fully hydrated for the PAA microspheres varied between approximately 80 and 140 fold. Several solutions were identified that inhibit expansion. DMSO, DMSO:contrast 7:3, and Propylene Glycol prevented expansion completely while MD-76R contrast and low-pH solutions allowed a small amount of expansion. Based upon these studies, MD-76R contrast may be the most suitable delivery medium because it provides some expansion which allows more deformability, is already approved for endovascular injection, does not adversely affect microsphere properties, and provides intra-procedural visualization.

3.1 Material Formulations

Several variant microsphere formulations were provided by DuPont (Table 3-1). N,N-methylenebisacrylamide (MBA) is a crosslinking agent used in the Microspheres. Divinylbenzene (DvB) is another crosslinking agent. The initial formulations of the microspheres had rough surfaces. After observing that these microspheres fragmented readily, smooth, continuous surface microspheres were developed (see chapter on Quality Control). Microspheres with a reported size range were filtered at DuPont to fall within the indicated range.

Table 3-1: Poly Acrylic Acid microsphere Formulations

Microsphere types-				
Number	Material	Crosslinking	Size range	Description
E108302-12-1	PAA	MBA		
E108302-12-5	PAA	MBA & DvB		
E109317-27	PAA	MBA		smooth surface
E109317-129	PAA	MBA		smooth surface
E109572-25	PAA	MBA		70 gram lot, smooth surface
E109317-45F	PAA	MBA	250-500um	smooth surface
E109572-3	PAA	MBA	250-500um	non-expandable, smooth surface
E105050-75	PAA	MBA	50-150um	smooth surface
E109572-51	PAA	MBA		dyed blue

3.2 Microsphere Visualization & Staining

Unexpanded PAA microspheres are opaque under both light microscopy and to the naked eye. When placed in a medium that does not promote expansion, such as propylene glycol, the spheres remain opaque and visible. However, when PAA microspheres expand in neutral aqueous media, they become translucent and difficult to image by light microscopy. Furthermore, the particle analysis system used to generate statistical size and shape distribution data requires sphere contrast with the flow medium, thus unstained microspheres cannot be analyzed well in pure water. Gross visualization o of expanded microspheres would be an advantage during procedures and for histology. For these reasons a staining method was developed for PAA microspheres.

It was determined that the cationic dye, Acridine orange (AO), sufficiently adheres to the fixed negative charge within the microspheres when they are expanded in

an aqueous medium with an AO concentration of 3 mg/ml. The stain has no effect on swelling properties (as evidenced by light microscopy) Figure 3-1 (A, B).

Figure 3-1 A-B: Light microscopic images of unstained (A) and Acridine orange stained (B) microspheres immersed in water (scale bar 500 micron).

Staining Procedure

To stain E108302-12-1 (MBA crosslinked) PAA Microspheres, first mix 5ml water with 15 mg of Acridine Orange to make a 3mg/ml concentrate. Then add 5mg microspheres and mix well. Capture the microspheres from mixture with a micro-mesh (approx 250 micron pore size) specimen bag and then reconstitute microspheres in 5 ml water.

DuPont provided pre-dyed microspheres E109572-51 that were dyed blue at DuPont in an attempt to incorporate staining into the manufacturing process of the microspheres. There was not enough dye to provide adequate contrast once the microspheres expanded. A higher concentration of dye may provide better results.

3.3 Volumetric Expansion

The primary method used to calculate the volumetric expansion coefficient of PAA microspheres was by comparing a series of light microscopy images of single microspheres prior to and following hydration. This method is useful to determine the expansion of microspheres without the need to include dye for contrast as a confounding agent. This method was corroborated by a using the Beckman Coulter RapidVUE® particle analysis system. This system counts and analyzes large numbers of

microspheres in a flow loop and constructs a probability distribution of the particulate sample. Using this system, population characteristics can be analyzed for a large number of microspheres. This method requires that the microspheres be stained for the machine to be calibrated to recognize microspheres.

DuPont synthesized microspheres with a range of volumetric expansion coefficients (Q) that were media dependent. PAA-MS expanded 140 fold in water. PAA-MS did not appreciable expand in DMSO, Propylene Glycol or DMOS/Contrast(7:3) but they did expand slightly in Acidic solution and to a lesser degree in MD-76R contrast (Table 3-2).

Table 3-2: Calculation of Expansion Coefficient Q for smooth surface PAA-MS

MS E109572-25	6 samples per Medium					
Medium	**Avg Dry Diameter (um)**	**Avg Wet Diameter (um)**	**Avg Dry Vol (um^3)**	**Avg wet Vol (um^3)**	**Avg Q**	**St Dev**
Water	190	980	3.59E+06	4.93E+08	139	22
DMSO	212	214	4.99E+06	5.13E+06	1	0.1
MD-76RContrast	181	291	3.10E+06	1.29E+07	4	0.8
DMSO/Contrast (7:3)	187	194	3.42E+06	3.82E+06	1	0.2
Propylene Glycol	198	200	4.06E+06	4.19E+06	1	0.1
Acidic Aqueous (pH=1.5)	177	361	2.90E+06	2.46E+07	9	4

Microspheres from batch E109572-25 were separated into six samples per medium type on glass slides. The Q values represent the average of the six manual measurements per medium made by light microscopy.

3.4 Optimization of Delivery Solution Properties

Expansion studies have shown that PAA microspheres do not expand in the organic solvent propylene glycol (CH3CHOHCH2OH). However, further experiments revealed that propylene glycol (viscosity 60 cps at 25° Celsius) cannot deliver microspheres through small bore needles and catheters (26 gauge and smaller). To address this dilemma, several candidate solutions were tested to determine a suitable solution for microsphere (MS) suspension that suppresses MS expansion while providing a low-viscosity medium for small-bore catheter or needle based delivery[68]. Adverse biological effects must also be considered when judging the suitability of each carrier solution.

We investigated several systems for preventing microsphere expansion. We chose to test the organic polar solvent dimethyl sulfoxide (DMSO) because it is far less viscous (2.14 cps) than propylene glycol (60cps) but still has similar qualities as an organic solvent.

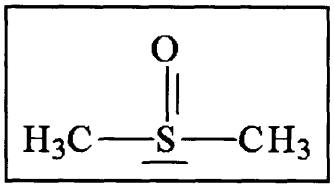

Figure 3-2: Chemical Structure of dimethyl sulfoxide (DMSO)

This organic solvent is polar and displaces water readily. Because it does not form hydrogen bonds like water and is larger than water we posited that it would not form a stable lattice adjacent to the fixed charge within the microspheres and subsequently would not be drawn into the microspheres. This solution should work similar to ETOH dehydration of microspheres, but DMSO may be less destructive to vascular tissue and/or drugs that may be within the spheres than ETOH.

Another possible method for preventing microsphere expansion would be to shield the charge within the sphere such that water will not be favored within the sphere. One method of doing this would be to use a low pH solution. We hypothesized that a low pH solution would neutralize the fixed negative charges within the microsphere, thereby preventing expansion. Solution pH has been used in previous work to modulate the hydrophilic properties of PAA hydrogels[69]. Due to the robust buffer system in the body along with the renal/respiratory handling of acid/base, an acidic delivery system may be preferable because the acid can be neutralized and eliminated from the body rapidly whereas an organic solvent or ETOH may reach locally toxic concentrations and may take much longer to eliminate from the blood stream.

Materials

DMSO study

Type E108302-12-1 expandable/deformable PAA microspheres were stained with Acridine orange. DMSO and Milli-Q distilled, deionized water were used to make solutions.

pH study

Expandable/deformable PAA microspheres types E108302-12-1, E109317-27 were stained with Acridine orange. Acid solutions were made with milli-Q distilled deionized water and hydrochloric acid and basic solution used milli-Q distilled deionized water and Sodium Hydroxide.

Procedure

DMSO study

Nine solutions of increasing water content with DMSO were prepared in 0.5 ml Eppendorf 1.5ml test tubes (Table 3-3).

Table 3-3: % Water Solutions prepared to test expansion in DMSO & Water

Solution	DMSO (ul)	Water (ul)	% Water
1	100	0	0%
2	100	20	17%
3	100	60	38%
4	100	100	50%
5	100	150	60%
6	100	200	67%
7	100	300	75%
8	100	400	80%
9	0	400	100%

Five mg of PAA-MS were added to each solution. The Eppendorf 1.5ml tubes were shaken to submerge all microspheres and then the tubes were allowed three minutes for complete expansion before imaging each solution at five times magnification under light microscopy. The images were qualitatively assessed for level of expansion in each solution.

Particle Analysis of DMSO-treated Hydrated Microspheres

First 20mg PAA-MS were submerged in 10 ml DMSO for 1 hour. The microspheres were then removed from the DMSO and resuspended in an aqueous solution of the cationic dye Acridine orange at a concentration of 3mg/ml in deionized water. After waiting three minutes to allow for complete expansion and absorption, the stained PAA-MS were filtered out using micro-mesh and resuspended in 75 ml deionized water. This sample was then loaded into the RapidVUE® for particle analysis.

pH study

Volumetric Expansion Coefficient

Three solutions of pH 2, 7.1 and 10.2 were prepared by adding HCl or NaOH to water and titrating to desired pH with the aid of a pH-meter. Individual microspheres of type E100317-27 were isolated on cover slides in the dry unexpanded state and images were taken at 20 times magnification. The diameter was recorded. Then a drop of each solution (enough to saturate the microsphere) was added to separate microspheres on individual slides and the imaging was repeated at 5 times magnification and the diameter of the expanded PAA-MS was recorded. The volumetric expansion coefficient was then calculated using the diameters from before and after contact with solution. This procedure was repeated five times for each know pH solution for a total of fifteen trials.

Particle Analysis

Six solutions of pH 2.0, 2.5, 3.5, 4.3, 7.1, and 10.2 were prepared by adding HCl or NaOH to water and titrating to the appropriate pH with the aid of a pH-meter. A 10 mg sample of microspheres (E108302-12-1) was submerged in 5 ml of an Acridine orange solution at 3 mg/ml concentration in water of a known pH. The pH values reported do not take into account any change in pH caused by the cationic dye. Three minutes were allowed for complete expansion before the microspheres were removed, filtered with micromesh and resuspended in a 75ml aqueous solution of the same pH. These samples

were then analyzed in the RapidVUE® particle analyzer. This procedure was carried out for all pH solutions.

Results

DMSO study

Serial Dilution of DMSO-Microsphere Imaging

Microspheres did not expand in DMSO-water solutions until the percent water exceeded 50% (Figure 3-3). This qualitative comparison demonstrates that solutions of high DMSO concentration effectively suppress microsphere expansion (solutions 1, 2, 3). Solution 4 at 50% DMSO is the critical concentration at which microsphere expansion begins. Solutions 5-9 feature an increasing percentage of water; however, the microspheres do not increase in diameter with increasing water percentage indicating that expansion is likely an all or nothing phenomenon.

Particle Analysis of DMSO-treated Hydrated Microspheres

Particle analysis was used to quantify the expansion of microspheres in a pure aqueous solution following a 24 hour pretreatment with DMSO. This is intended to simulate the use of DMSO as a delivery medium for microsphere applications (Figure 3-4, Figure 3-5, and Figure 3-6).

Non-pretreated microsphere populations tend to have more noise near the low-end of diametrical spectrum (Figure 3-4). This is likely caused by microsphere aggregation in DMSO and subsequent adherence of extremely small microspheres to the larger microspheres via static charge interactions. Methods to sieve out these small microspheres are discussed in the Quality Control chapter. It is important to note that when looking at graphs that calculate the PDF based upon percent of total particles rather than percent of total volume, the effect of many small particles may appear exaggerated. When corrected for percent of total volume, small particles are a much smaller proportion of the total volume than their numbers may insinuate. When the particles less than 250 micron are excluded from the estimate of the probability mass function the distributions for the DMSO treated and non-treated virtually overlap (Figure 3-4, Figure 3-5 and Figure 3-6).

Probability density functions comparing pretreated and non-pretreated PAA-MS indicate that pretreatment has no effect on expansion in an aqueous medium (Figure 3-5 and Figure 3-6). The average diameters of the microspheres were calculated for six runs with DMSO-treated and untreated microspheres (Table 3-4).

Table 3-4: Average MS Diameters per Run

Average Diameter per Run (microns)		
	DMSO-treated	Untreated
	590	595
	595	600
	595	610
	595	635
	590	635
	590	635
Average	593	618
Std. Dev.	3	19

Although there was a slight difference in the average of the averages, because the standard deviation for the underlying distributions is roughly 250 microns, there is no statistically significant difference between DMSO-pretreated and untreated distributions (Figure 3-4). These results suggest that DMSO can be used to deliver microspheres without adversely affecting their expansion properties in an aqueous medium.

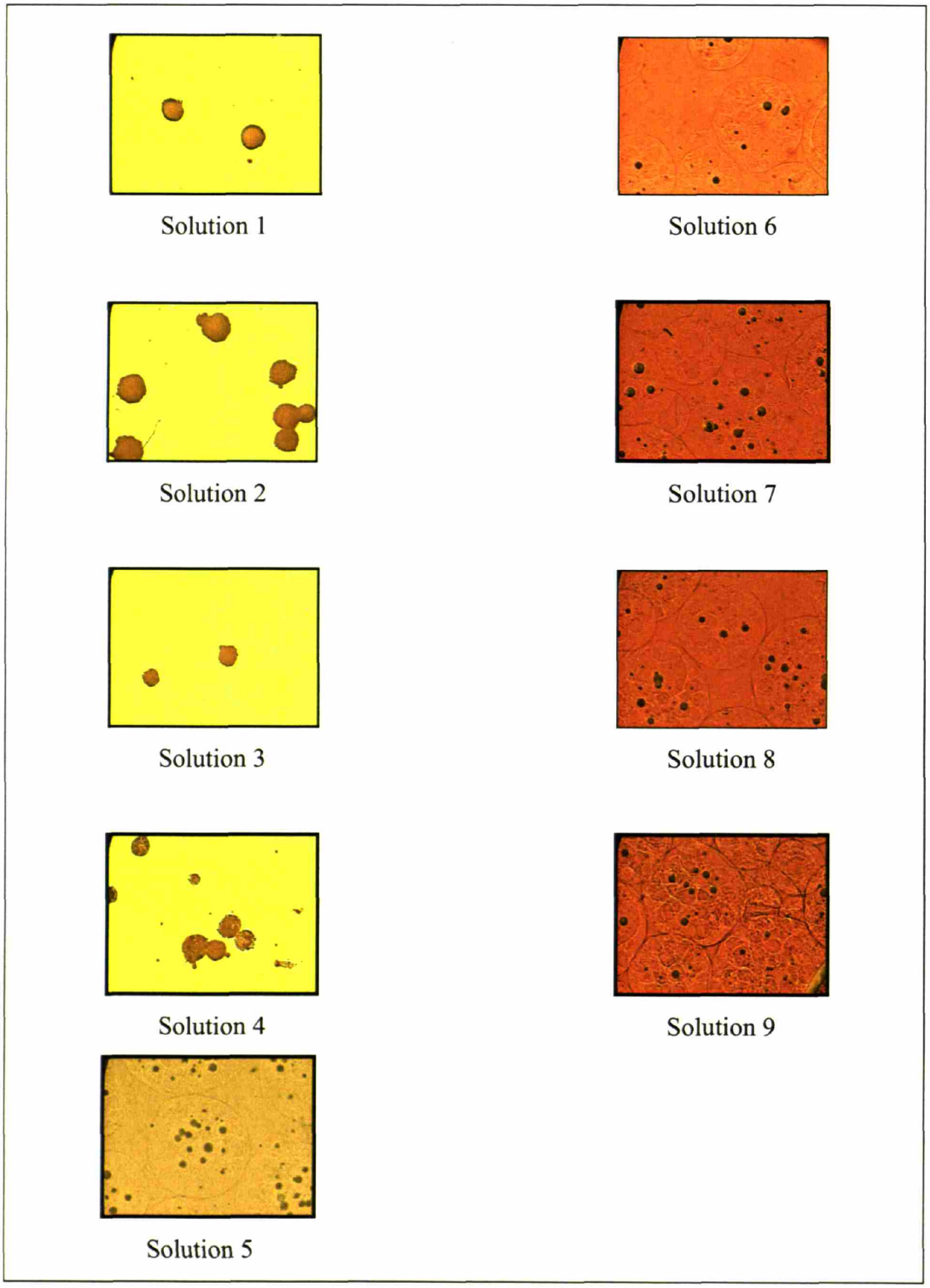

Figure 3-3: Microsphere expansion within serial dilutions of DMSO with water. Field of view: 1.7 x 2.0 mm per image, solutions have increasing percentage water

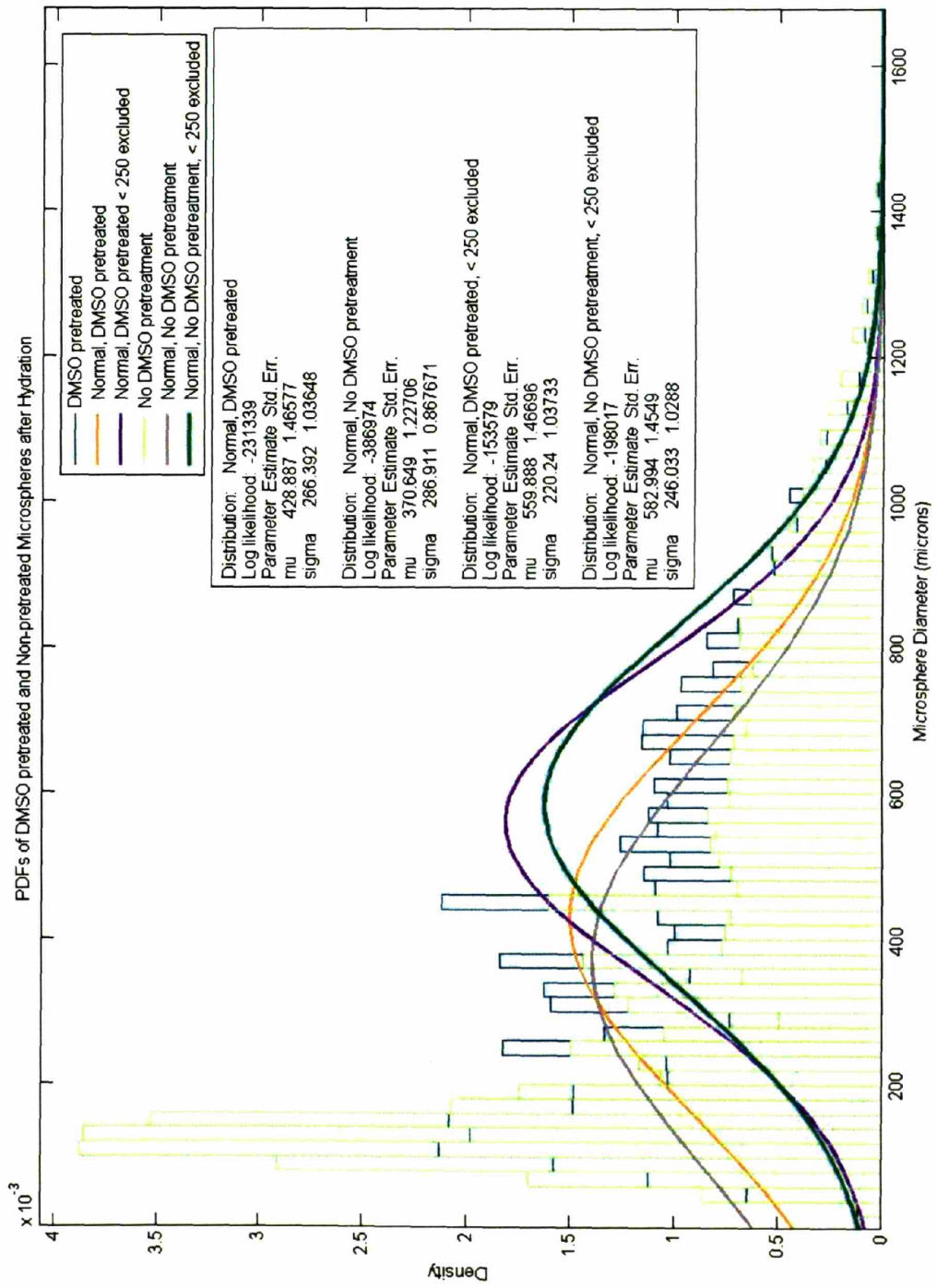

Figure 3-4: PDFs of DMSO pretreated microspheres and non-pretreated microspheres after hydration

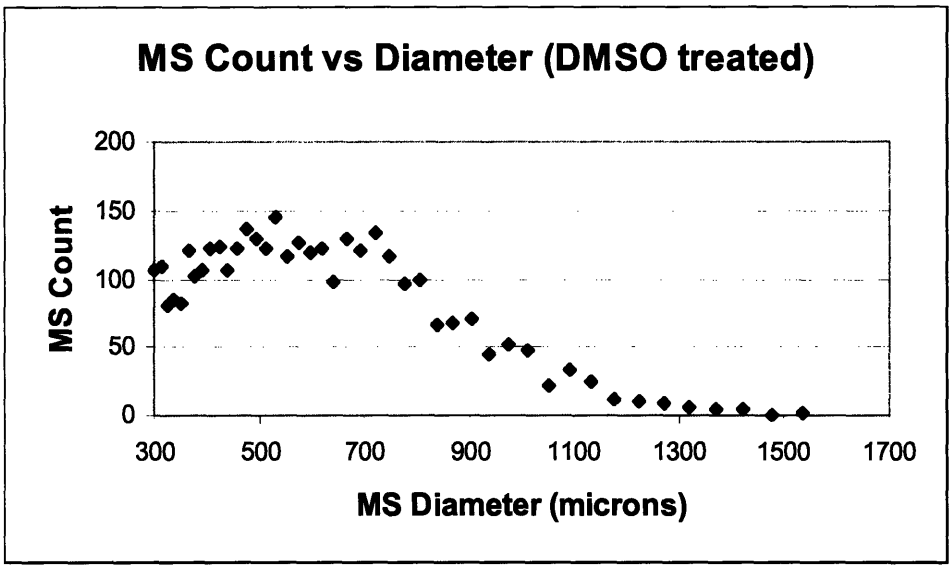

Figure 3-5: Microsphere count versus Diameter for a DMSO treated sample.

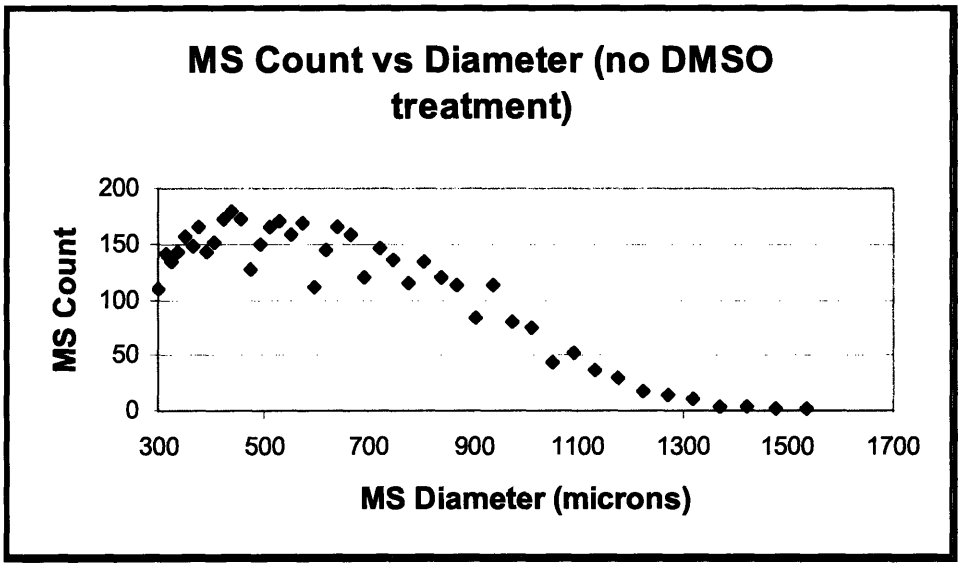

Figure 3-6: Microsphere count versus Diameter for an untreated sample.

pH study

Volumetric Expansion Coefficient

The volumetric expansion coefficients of microspheres in aqueous mediums were measured for different pH solutions. There was a marked reduction in

microsphere expansion in an acidic pH when compared to neutral or basic (error bars denote standard deviation between microspheres within the same media composition) (Figure 3-7, Table 3-5).

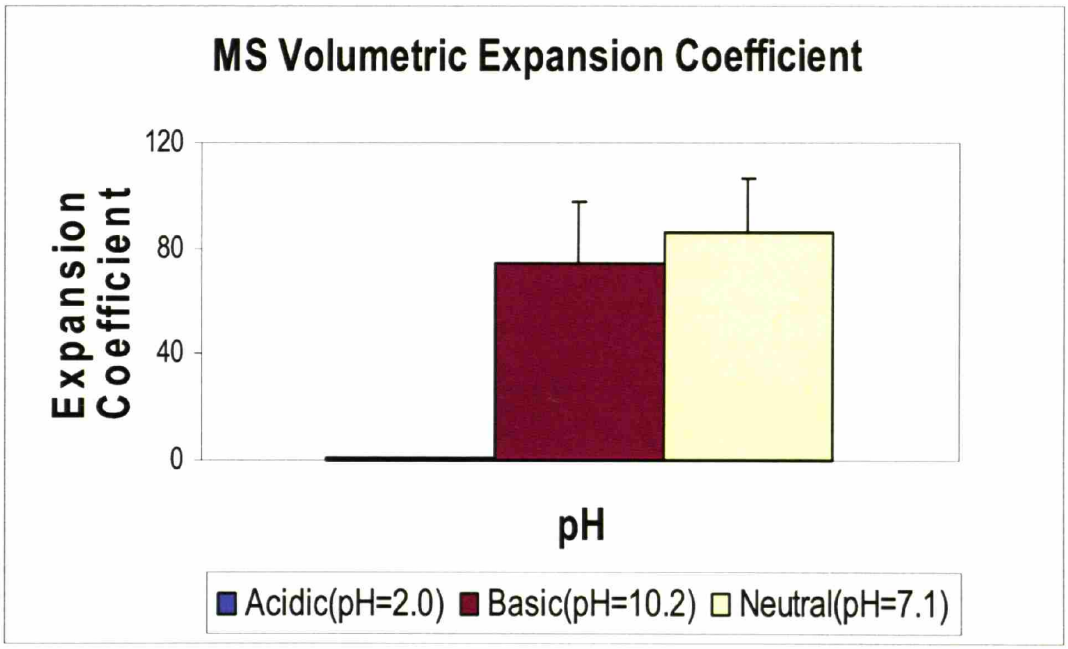

Figure 3-7: Volumetric Expansion of microspheres in various pH solutions.

Table 3-5: Volumetric Expansion Coefficients of Microspheres in various pH solutions

	Acidic	Neutral	Basic
Average Q(n=5)	1.2	85.9	73.9
Standard Deviation	0.1	21.0	23.8

Particle Analysis

A particle analysis study of microspheres in aqueous solutions of varying pH also showed reduced diameter in acidic solutions (Figure 3-8).

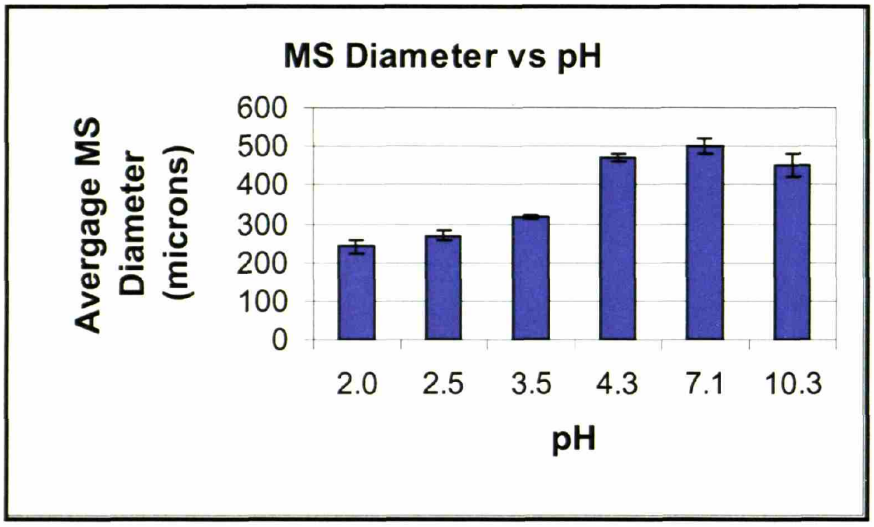

Figure 3-8: Microsphere Diameter in solutions of various pH. (error bars denote standard deviation between particle analysis runs)

Discussion

Most embolics in use are delivered in physiologic saline[22]. PAA-MS expand substantially in saline and thus need a solution of low viscosity that limits expansion. The restrictive viscosity of propylene glycol precludes its use as a delivery medium because it cannot be passed through high-resistance catheters. The results of these studies demonstrate that both DMSO and acidic aqueous solutions have potential to deliver microspheres in the unexpanded or minimally expanded state. By diluting these solutions with water, the level of pre-expansion can be tailored for a given application. In some cases, pre-expansion may be preferred because partially expanded microspheres are highly deformable and may be easier to deliver.

Both low-pH and DMSO based delivery media have low viscosity in addition to causing minimal expansion, allowing for the potential use of small-bore devices such as catheters and needles. Further studies must be conducted to determine the toxicity of each delivery medium in vivo. Intuitively, low pH appears to be a promising medium because the blood buffer should be able to neutralize the medium after insertion, although DMSO acts as a slightly better solution for limiting expansion. Preliminary data indicates that high-salt solutions can also be used to inhibit expansion of microspheres. High salt concentration is the most likely basis for how MD-76R contrast inhibits expansion, which is discussed in the next section.

3.4.1 Contrast Agent MD-76R as a Delivery Medium

Background

Radiopaque contrast agents are used for angiographic visualization of endovascular procedures. Contrast agents typically include chemically bound iodide that distinguishes target tissue from its surroundings under x-ray visualization. Contrast agents are provided as sterile aqueous solutions. Because of the high solute and salt concentration of most contrast agents, it is feasible that they could limit expansion of PAA microspheres. By mixing contrast agents with an agent such as DMSO that prevents expansion, a cocktail may be formed that provides limited expansion while allowing for intra-procedural visualization.

Purpose

Determine if PAA microspheres expand upon suspension in contrast solutions. If expansion does not occur in contrast, determine if microspheres will swell in water when pretreated with a contrast medium. Determine the concentrations of microsphere solutions that can pass through 6 gauge catheters when injected in a contrast solution.

Hypothesis

Due to the salt content of contrast medium MD-76R, PAA microspheres suspended in these solutions will not fully expand. Following contrast pretreatment, microspheres will fully expand in water, as observed following suspension in other restrictive media (high salinity aqueous solutions, low pH aqueous solutions, organic solutions). The low viscosity of MD-76R will allow for homogeneous passage of highly concentrated microsphere solutions through a 6 French catheter.

Materials

Contrast Medium

The contrast medium used in this study is MD-76R, a Diatrizoate Meglumine and Diatrizoate Sodium aqueous solution, supplied by Tyco (Figure 3-9).

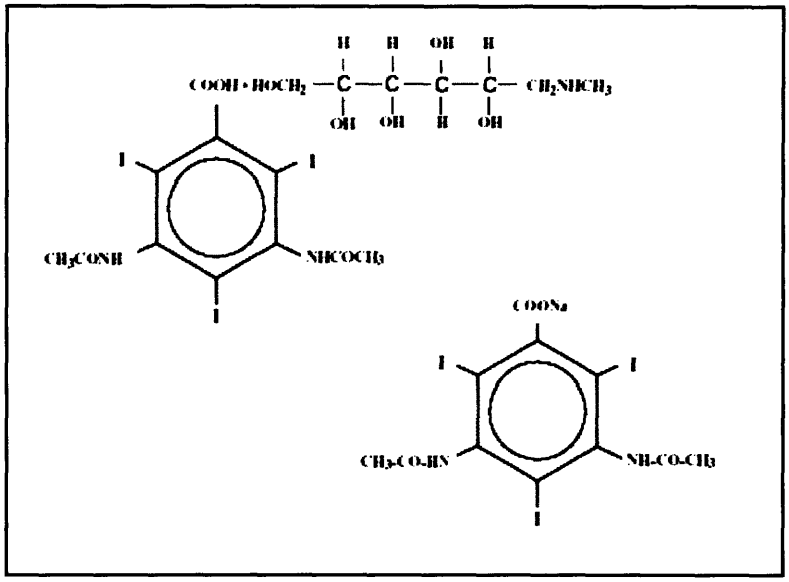

Figure 3-9: Schematics of Diatrizoate Meglumine (top) and Diatrizoate Sodium (bottom)

(Diagram courtesy of Malkinckrodt industries MD-76R package insert available online at: http://imaging.mallinckrodt.com/Products/Product.asp?ProductID=74)

The contrast is buffered with monobasic sodium and is supplied with the pH adjusted to 6.5 – 7.7. The contrast features organically bound iodide, which provides the basis for radiological visualization. The viscosity of the solution is 16.4 cps at room temperature. MD-76R is clinically approved for intravascular arteriography.

Microspheres

The microspheres used in this study are PAA expandable/deformable microspheres. The volumetric expansion and particle analysis studies are conducted with microspheres E109317-129. The catheter passage study incorporates both E109317-129 and E105050-75 microspheres.

Catheters

The catheters used in this study are size 6 French (Z^2 guiding catheters) with an internal diameter of 1.78 mm and a length of 100 cm.

Procedure

Volumetric Expansion

A single, dry microsphere was imaged at 10X magnification with light microscopy-record the diameter. Approximately 0.25 ml contrast medium was then added directly to the slide, suspending the microsphere. Three minutes were allowed for microsphere/contrast contact. The microsphere suspended in contrast was imaged at 5X magnification with light microscopy and the diameter was recorded. The volumetric expansion of the microsphere following suspension in contrast was computed from the diameter measurements. This procedure was repeated six times. The entire process was repeated using water instead of contrast to determine the volumetric expansion following suspension in water and the expansion coefficients in contrast and water were then compared.

Particle Analysis to assess the effect of contrast pretreatment

Five ml of MD-76R contrast and 25 mg microspheres were mixed for 3 minutes with vortex touch mixer at speed 10 for contrast pretreatment. The microspheres were then filtered with a micromesh specimen bag. The microspheres were reconstituted in a homogeneous solution of 10 ml water and 30 mg Acridine Orange (cationic dye) and mixed for 3 minutes with vortex touch mixer at speed 10 for staining. The microspheres were filtered again and resuspended to 75ml water for particle analysis. The procedure was repeated without the contrast pretreatment as a control.

Passage through 6F Catheter

Contrast and microsphere solutions were prepared with a vortex touch mixer at speed ten for three minutes (Table 3-6). Using a 12 ml syringe, an attempt was made to inject each solution through a 6F catheter. Microscopic imaging was used to determine if passed mixtures resulted in microsphere fragmentation.

Table 3-6: Mixtures used for catheter passage experiment

Microsphere Type	Microsphere Mass (mg)	Vol. Contrast (ml)	Concentration (mg/ml)
E109317-129	500	5	100
E109317-129	750	5	150
E109317-129	1000	5	200
E105050-75	1500	5	300

Results

Volumetric Expansion

The results of the volumetric expansion studies of PAA microspheres E109317-129 in contrast and water show that the average expansion coefficient of microspheres in contrast and water are 4.9 and 117.5, respectively (Table 3-7 and Table 3-8).

Table 3-7: Volumetric expansion of PAA microspheres in contrast

Sample	Dry D (mm)	Contrast D (mm)	Dry Vol (micron^3)	Contrast Vol (micron^3)	Vol Exp Coeff
1	0.17	0.26	2.57E+06	9.20E+06	3.6
2	0.18	0.35	3.05E+06	2.24E+07	7.4
3	0.1	0.16	5.24E+05	2.14E+06	4.1
4	0.16	0.28	2.14E+06	1.15E+07	5.4
5	0.18	0.29	3.05E+06	1.28E+07	4.2
6	0.14	0.24	1.44E+06	7.24E+06	5.0

Table 3-8: Volumetric expansion of PAA microspheres in water

Sample	Dry D (mm)	Hydrated D (mm)	Dry Vol (micron^3)	Expanded Vol (micron^3)	Vol Exp Coeff
1	0.18	0.80	3.05E+06	2.68E+08	88
2	0.15	0.67	1.77E+06	1.57E+08	89
3	0.16	0.79	2.14E+06	2.58E+08	120
4	0.17	0.85	2.57E+06	3.22E+08	125
5	0.19	0.98	3.59E+06	4.93E+08	137
6	0.19	1.00	3.59E+06	5.24E+08	146

Particle Analysis

Particle analysis of PAA microspheres with contrast pretreatment suggests that contrast has no significant effect on subsequent microsphere expansion in a pure aqueous medium. The PDFs for the contrast pretreated and no contrast pretreatment groups overlap considerably (Figure 3-10). This result shows that contrast can be used to deliver PAA microspheres without diminishing expansion properties. Particle analysis of filtered microspheres in contrast versus water corroborates the data found on light microscopy (Figure 3-10).

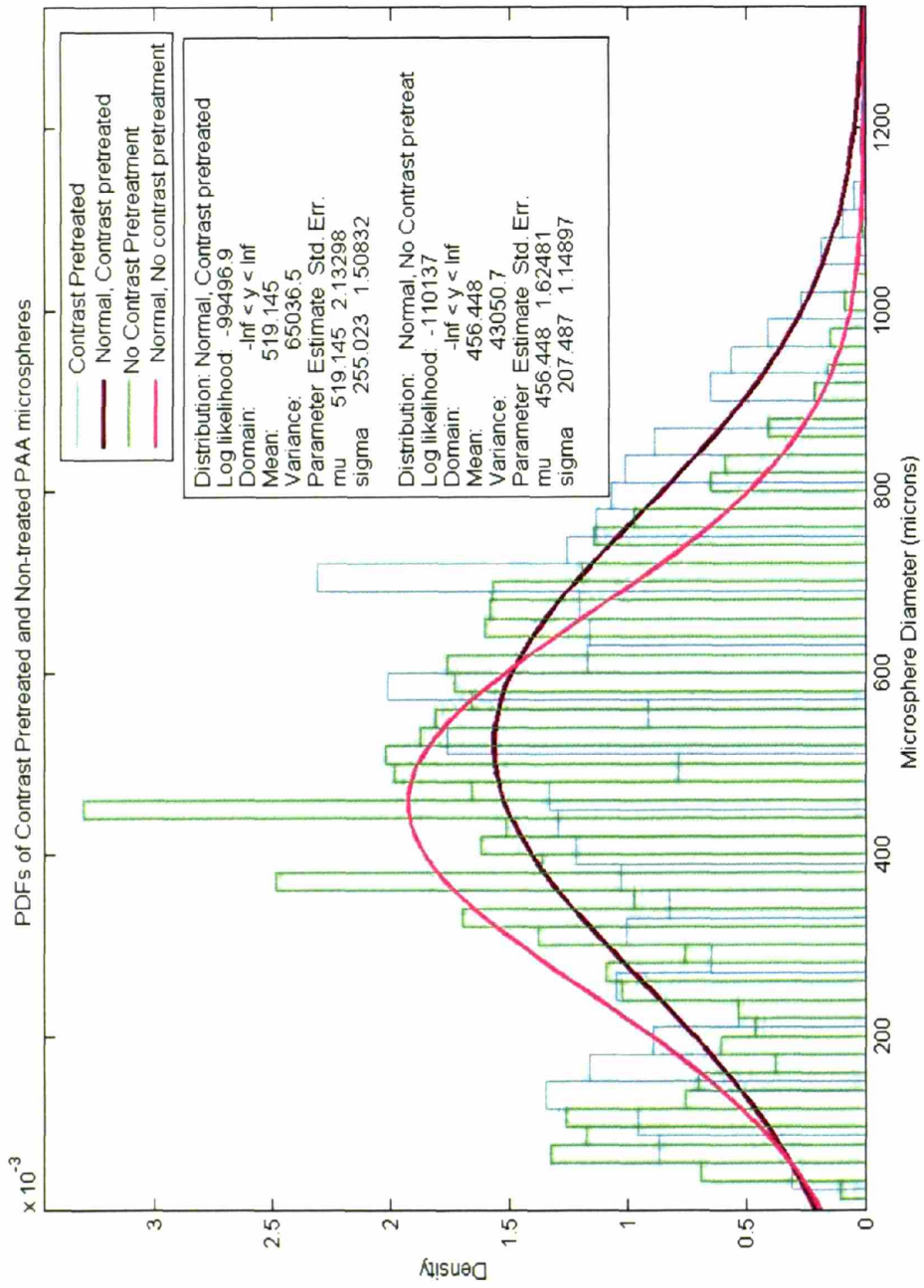

Figure 3-10: PDFs of Contrast Pretreated and Non-treated PAA microspheres

Passage through a 6 French catheter

PAA microspheres were injected with a syringe through a 6 French catheter with contrast medium. The larger (0.15-0.2 mm dry diameter) and variably-sized microspheres (E109317-129) were able to pass through the catheter at a maximal concentration of 150 mg microsphere/ml contrast. The smaller (0.05-0.15 mm dry diameter) microspheres (E105050-75) were sieved and separated according to size and were able to pass at a concentration of 300 mg microsphere/ml contrast. In all cases, no evidence of microsphere fracture following passage was observed with light microscopy (Table 3-9).

Table 3-9: Summary of catheter passage study

Microsphere Type	Microsphere Mass (mg)	Vol. Contrast (ml)	Concentration (mg/ml)	Passage	Fragmentation
E109317-129	500	5	100	Y	N
E109317-129	750	5	150	Y	N
E109317-129	1000	5	200	N	N/A
E105050-75	1500	5	300	Y	N

Conclusion

The results of this study support the use of MD76R contrast as a potential delivery medium for PAA microspheres. Delivering sufficiently concentrated PAA microspheres in contrast would support a readily visible (through angiographic means), sterile and biocompatible catheterization procedure.

Based upon these studies, the MD-76R contrast may be the most suitable delivery medium because it limits expansion, is already approved for endovascular injection, does not adversely affect microsphere properties, and provides intra-procedural visualization. Furthermore, the slight expansion afforded by the MD-76R contrast media may be beneficial for delivery through some catheters because the slight expansion can allow for deformability within the catheter. This expansion can be eliminated if desired by adding DMSO to MD-76R contrast in a 7:3 ratio of MD-76R contrast to DMSO.

3.5 Discussion/Conclusion

This chapter has outlined the material characterization of expandable/deformable PAA microspheres. A staining technique that takes advantage of fixed negative charge in the material by binding cationic dye Acridine orange was established to help visualize the microspheres. The determination of volumetric expansion coefficient to be roughly 100 times and varied between approximately 80 and 140 fold indicates the bounds of expandable technology that will be critical to in-vitro and in-vivo function. One of the crucial discoveries of this chapter was the identification of candidate delivery media including DMSO, DMSO:contrast 7:3, Propylene Glycol, MD-76R contrast and low-pH solutions. MD-76R contrast may be the ideal delivery medium because it provides some expansion and deformability to allow for easier passage through small-bore catheters. It is also approved for endovascular injection, does not adversely affect microsphere properties, and provides intra-procedural visualization. Future work in this area will further explore material properties of PAA-MS including frictional coefficients and radio-opaque treatments in addition to exploring the toxic and biological effects of the candidate delivery solutions.

Chapter 4: Quality Control

Abstract

Embolic microspheres are intended to reproducibly and effectively occlude target vasculature. To ensure that microspheres are able to perform in a consistent manner, quality control measures during and after synthesis must be implemented. The size distribution of the microsphere lots, the expansion properties, the range of size, the sphericity of the microspheres, and the physical integrity of the microspheres should all be monitored and controlled for reproducibly optimal results. The following chapter discusses techniques to monitor and improve upon the quality of microsphere batches.

Sieving methods have been implemented that allow for more precise control over the size range of PAA microspheres. The standard deviation of the PAA microspheres can be reduced significantly by sieving and can be narrowed further than the current standard deviations found in commercially available PVA particulate or tris-acryl gelatin microspheres. Microspheres were tested for degradation in several candidate solutions including air, propylene glycol, saline and water. Degradation was not observed in any of the solutions after four weeks. Light microscopy and SEM (Scanning Electron Microscopy) were conducted to characterize the surface properties of the microspheres. The original batches of microspheres were rough, porous and tended to result in microspheres that were prone to fragment. Modified batches have a smoother, continuous surface and resist fragmentation when exposed to shear stresses commonly encountered in small bore catheters and needles. Resistance to fragmentation allows the use of smaller-bore catheters for a given embolic load, which could potentially result in less invasive procedures and more stable occlusions.

This chapter also describes the preliminary sterilization procedures and cytotoxicity studies used to establish biocompatibility. The PAA microsphere manufacturing process includes a final ethanol wash, which ensures a low initial bioburden. UV sterilization has been shown to not affect microsphere expansion performance or ultra-structure. Microspheres were shown to expand in whole blood to the same degree and just as rapidly as in saline, and therefore will be able to expand within the vasculature. Both a live/dead and an LDL uptake assay indicated that neither intact nor fragmented microspheres are cytotoxic to bovine aortic endothelial cells. These data show that PAA microspheres have passed preliminary biocompatibility and in-vitro functionality tests and are ready to be tested with more detailed methods and within long term animal models.

4.1 Sieving

Representative data plots of the size distribution of a 20mg sample of stained microspheres analyzed in water both before and after filtering show that filtering narrows the standard deviation of the distribution considerably (Figure 4-1). There exists evidence of significant size variation among the initial batches of PAA microspheres that are unfiltered when compared to the sieved batch. Such variation can be potentially dangerous during embolic occlusion as it may lead to incomplete occlusion, recanalization or even unintended microsphere migration throughout the circulatory system. Microspheres that are too small pose a danger as they may cause distal embolization to non-targeted vascular beds while microspheres that are too large may be difficult to deliver or may occlude proximal to the desired target vessel diameter. Unpredictable size distribution within microsphere batches can result in unpredictable occlusions. Because of this, sieving methods have been developed to narrow the size range of the microspheres.

Sieving microspheres with certified sieves can significantly reduce the standard deviation of the microspheres while simultaneously focusing the mean toward a desired range (Figure 4-1). In this case, the range from 125 to 250 microns was chosen because when expanded, these spheres will be large enough that they will be far less likely to embolize down ovarian anastomoses that measure at roughly 500 micron.

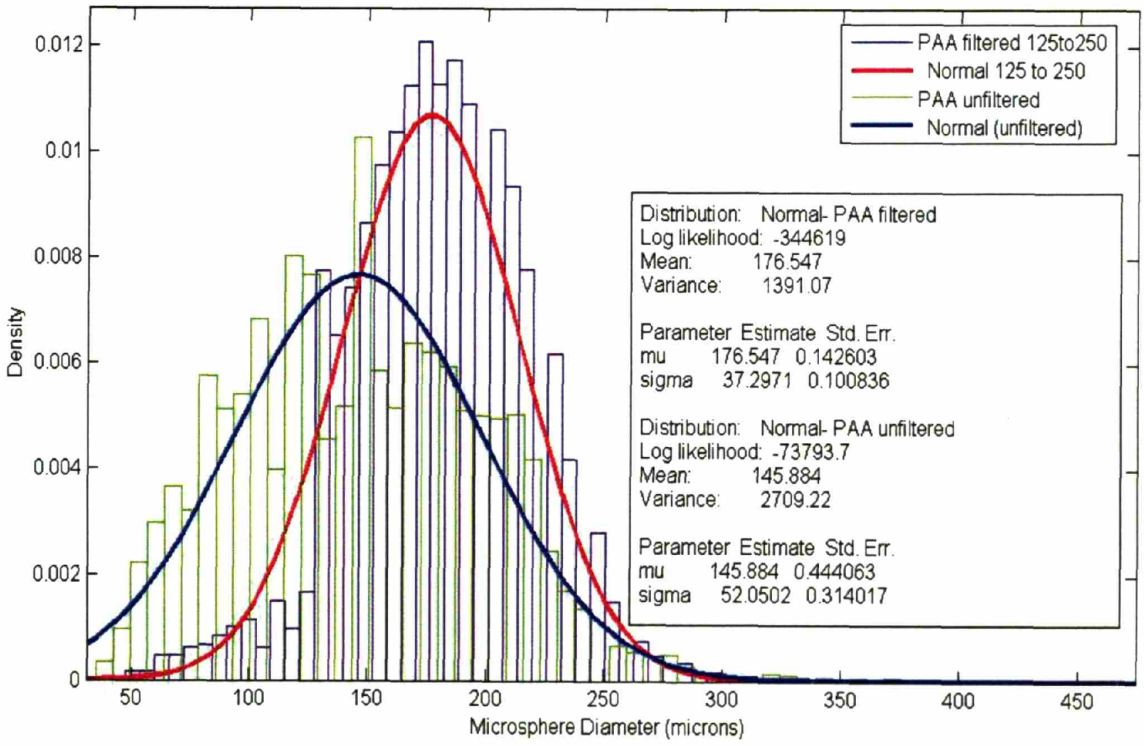

Figure 4-1 Probability density functions for filtered and unfiltered expandable/deformable PAA microspheres in their unexpanded state (while in DMSO).

Filtered sample was filtered using certified sieves between 125 and 250 micron. Variance is significantly smaller when filtered, while the mean is shifted toward a larger, more appropriate diameter for uterine artery embolization.

Commercially available non-expandable tris-acryl gelatin microspheres have a larger standard deviation and a less Gaussian distribution, which may result in more unpredictable performance from the microspheres (Figure 4-2). Furthermore, the tris-acryl gelatin microspheres show a large number of particles appearing toward the smaller size ranges, which are more likely to distally embolize.

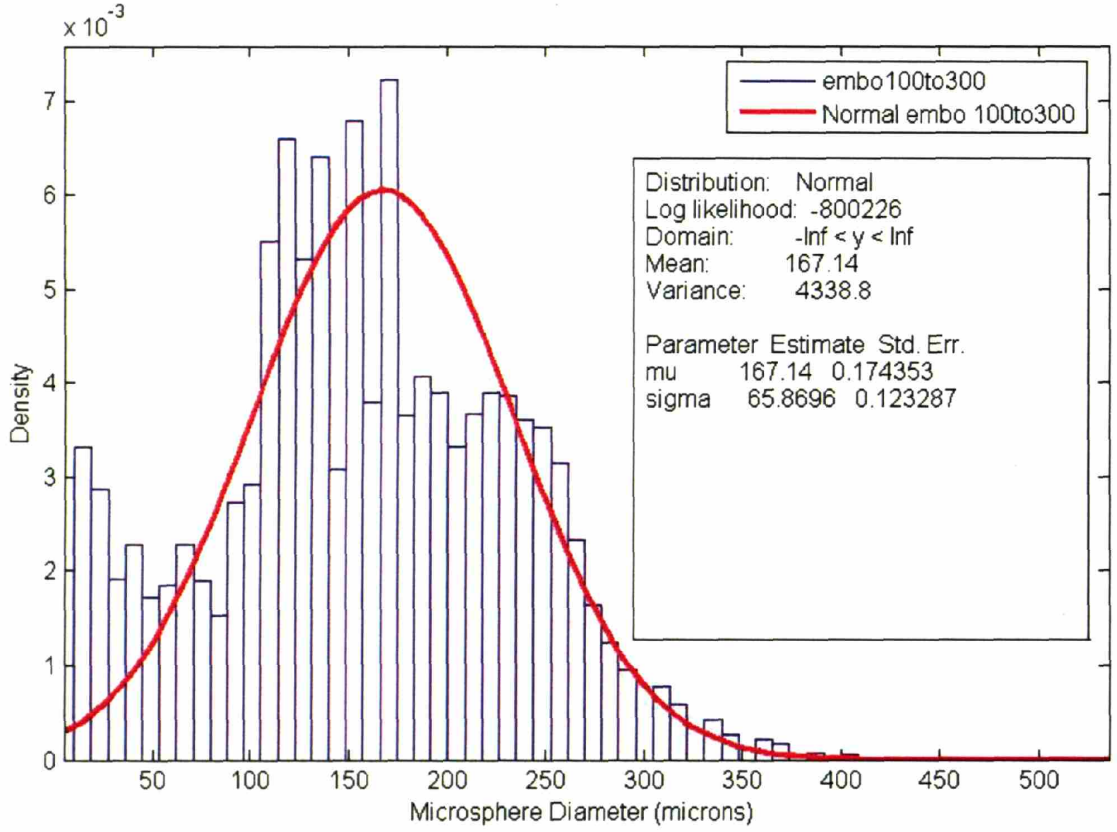

Figure 4-2: Probability density function for tris-acryl gelatin microspheres.

The distribution has a larger standard deviation and is less Gaussian than the PAA expandable/deformable microspheres.

The distribution of PVA particulate, which has the least Gaussian distribution and by far the largest standard deviation of all particulate examined (Figure 4-3), correlates with its reputation as an unpredictable embolic material[5-11, 18, 70, 71].

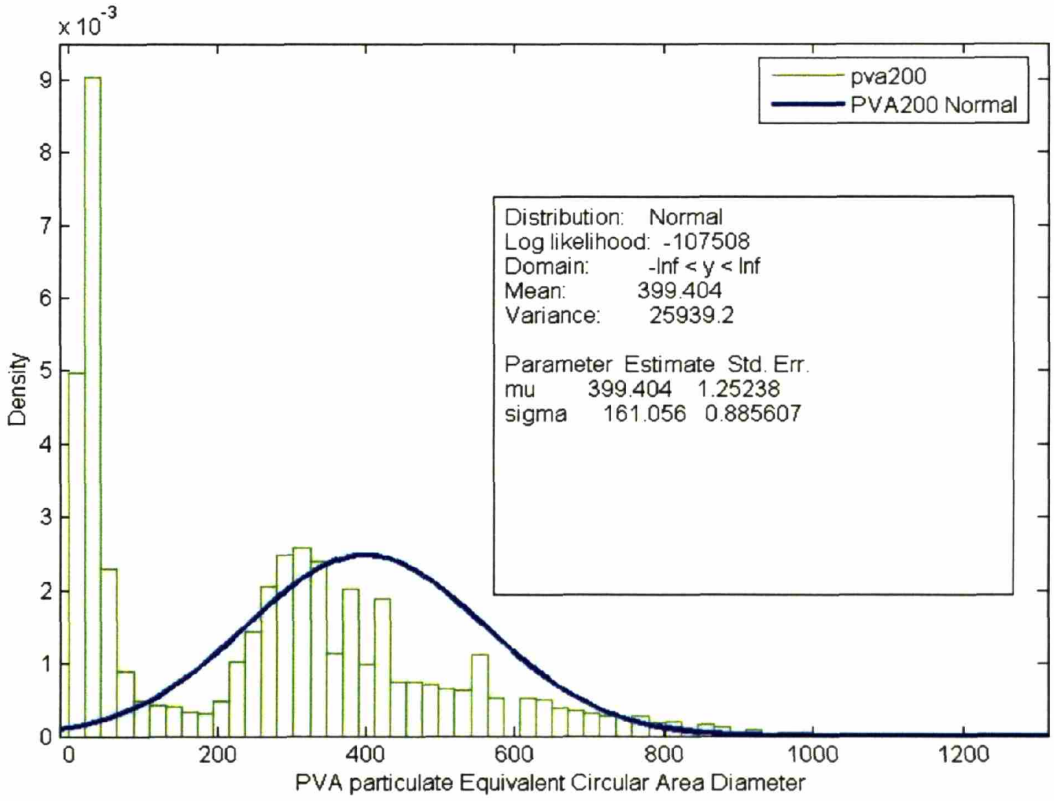

Figure 4-3: Probability density function for PVA particulate

The particulate has a much larger standard deviation and the distribution is non-Gaussian. The normal above was fit by excluding the large amount of particulate in the low diameter region. Diameter is measured in microns.

Procedure for Wet-Sieving Microspheres

One cubic centimeter of Microspheres was suspended in 5 ml DMSO. A sifting stack consisting of VWR U.S.A. Standard testing sieves A.S.T.M E-11 specification was assembled. The number 60 sieve (250 micrometer openings) was placed on top of a No. 120 sieve (125 micrometer openings) followed by a collection container at the bottom of the stack. The solutions were then poured into the top of the stack and followed by rinsing generously with DMSO (approximately 30ml). The samples were collected from the collection container and diluted to 75ml for particle analysis.

Results

The 125 micron to 250 micron filtered samples appeared to be well separated with minimal inclusion of smaller particles. However, smaller particles may be electro-statically bound to larger microspheres and may not be detectable using particle analysis in DMSO. Another limitation of the particle analysis occurs when aggregated microspheres are not reflected in the count due to their low sphericity. Aggregates of smaller particles may be visible after microsphere expansion. The yield of the sieving procedure is also reduced because aggregates of large microspheres are excluded by the larger filter. Finding a solution that promotes aggregation separation may help solve these sieving problems. Possible solutions include deionized water, acidified water, and propylene glycol. Nevertheless, sieving provides a much narrower range of microspheres and a more controlled population than un-sieved microspheres or un-sieved PVA particulate.

4.2 Degradation in various solutions

A four week study was conducted to rate the apparent degradation of the microspheres in four mediums: air, propylene glycol, phosphate buffered saline and deionized water. The samples were maintained at room temperature under static conditions. In all cases, no microsphere degradation was visible with up to 10 time magnification under light microscopy.

4.3 Sphericity

The sphericity of microspheres is an important property to ensure their ease of delivery and limited aggregation when compared to PVA particulate. This is due to the property of spherical objects to roll without slipping along surfaces. Movement by rolling is purely limited by the rotational inertia of the particle and not by frictional interactions, and hence is a faster mode of transport. Both unexpanded and expanded PAA microspheres appear to be spherical (Figure 3-3). To test this on a bulk scale, a 20mg sample of PAA microspheres was suspended in 75ml of water and run through the particle analyzer. A 50mg sample of PAA microspheres was suspended in 75ml of DMSO and run through the particle analyzer. The particle analyzer was configured

identically in both circumstances. The configuration used was our standard for measuring microspheres as given in the chapter on the Particle Analysis System.

The RapidVUE® software can be programmed to report many measures of the particles. For microsphere analysis, the configuration file is set to report Least Bounding Circular Diameter, Equivalent Circular Area Diameter and Sphericity. The calculation of these attributes is described in the section on the function of the RapidVUE® Particle analysis system.

Both expanded and unexpanded PAA microspheres are close to spherical with a sphericity centered near 95% (Figure 4-4). The distributions are not statistically different, demonstrating that expansion is even and does not by itself cause deformation of the microspheres. In this study particulate of less than 90% sphericity was rejected. This is necessary so that background debris and overlapping spheres are not counted as spheres. The value of 90% was determined during calibration of the particle analyzer for microsphere analysis.

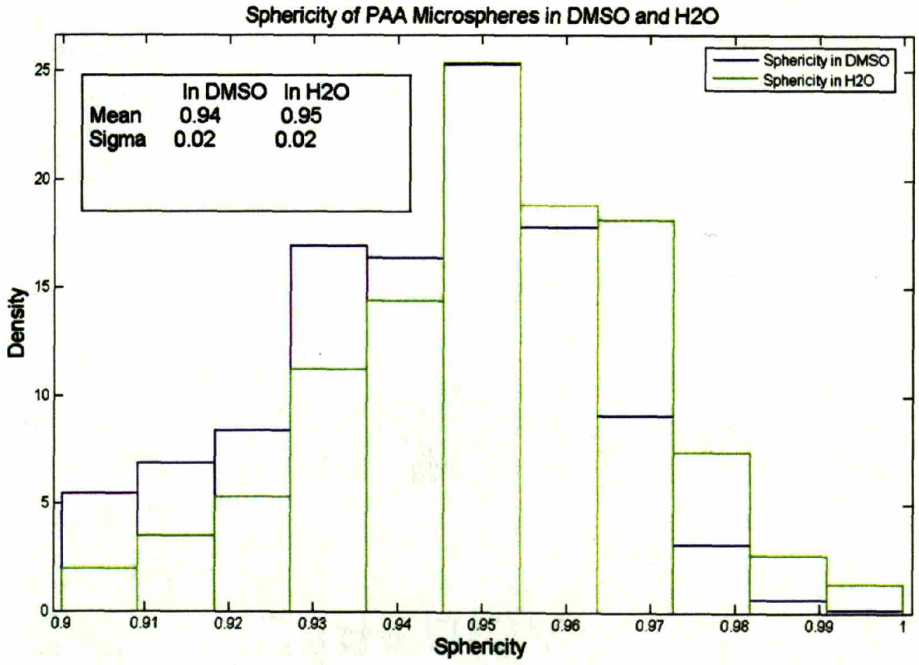

Figure 4-4: Sphericity of PAA microspheres in DMSO and H2O.

The distributions of sphericity are not appreciably different and the distributions are centered near 95% sphericity with a standard deviation of .02

4.4 Fragmentation under SEM and Light microscopy

A scanning electron microscope (SEM) study of the PAA microspheres in the dry state was used to analyze the surface integrity and porosity of the material surface. The images collected in this study revealed that the microsphere surfaces are discontinuous and feature numerous irregular pores (Figure 4-5 A, B). Material friability is a concern as microspheres have been shown to fragment when injected through small diameter needles in aqueous solutions (Figure 4-5 C, D). Microsphere fragmentation could lead to adverse sequelae in the body including but not limited to embolism downstream of target, unwanted inflammatory response, exacerbation of clotting cascade, release of high concentration of drug, and loss of therapeutic occlusion. For these reasons, spheres were designed that are more resistant to fracture. In order to strengthen the microspheres, recommendations were made to increase surface smoothness and/or outer layer thickness by a combination of altering the manufacturing process, increasing cross-linking density, and/or increasing PAA content.

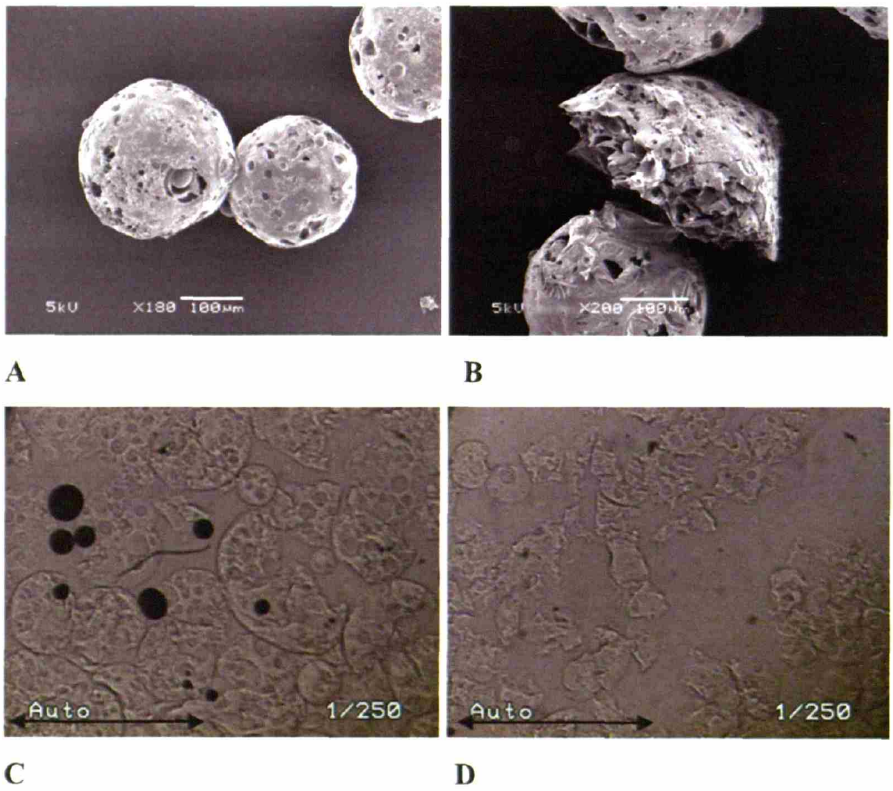

Figure 4-5: A-D: SEM images of dry PAA microspheres (A,B) and light microscopic images (scale bar 1 mm) of expanded PAA microspheres following injection through 21 gauge (C) and 26 gauge (D) needles. Porous surfaces and abundant fragmentation are evident.

4.5 Microsphere Fragmentation due to Injection Shear

Background

A potential advantage of PAA expandable/deformable microspheres is delivery through small bore needles and catheters in the unexpanded or partially expanded state. A clinical concern related to catheter based embolic procedures is fragmentation of the microspheres as they pass through small, non-compliant channels. If fragmented, the occluding capability of the microspheres will be reduced. Furthermore, small particle fragments in the bloodstream may lead to undesirable inflammatory sequelae or unpredictable downstream emboli.

Purpose

Previous experiments using SEM and light microscopy demonstrated that microspheres were fragmenting when passed through small bore needles, but the degree of fragmentation was not quantified. The purpose of this study was to quantify the degree of microsphere fragmentation after injection through small bore needles in both the unexpanded and expanded states. Two different formulations of microspheres were analyzed: the original, porous formulation and an augmented iteration with greater surface smoothness and continuity.

Hypothesis

Microspheres that are passed through small diameter needles in the unexpanded state should not fragment due to their small size (smaller than needle bore) and structural rigidity in the unexpanded state. Unexpanded microspheres should resist shear and compression more than expanded spheres due to the added strength afforded by internal Van-Der-Waals interactions within the polymer matrix. Microspheres that are passed in the hydrated, expanded state will fragment due partly to their large size (larger than needle bore) and partly to the reduction in shear strength associated with hydration and dissociation of internal weak molecular forces. When microspheres expand the polymer matrix is stretched and is the likely mechanism that limits the final expanded size of the microspheres. This places the material in a tension whereby an increase in tension due to shearing may result in rupture of the capsule. Furthermore, the microsphere surface

has holes in it that likely increase in size as the surface area of the spheres increases. This likely decreases the integrity of the capsule further. We posit that a marked reduction in fragmentation will be observed for the smoother and more continuous microspheres when compared to the samples featuring rough and discontinuous surfaces.

Materials and Methods

Two microsphere formations were analyzed in this study. PAA microspheres type E108302-12-1 feature very rough and discontinuous surfaces. The surfaces of these microspheres are highly porous and discontinuous even in the unexpanded state (Figure 4-6). The second formulation of PAA microspheres, type E109317-27, features much smoother surfaces that are virtually continuous and solid (Figure 4-7).

An acidic aqueous solution (pH of 2.1) was used as a low viscosity medium to inject the microspheres in the unexpanded state. This solution was formed by diluting concentrated hydrochloric acid with deionized water and titrating to pH 2.1. Deionized and distilled water (pH of 7.0) was used to deliver the microspheres in the fully hydrated, expanded state.

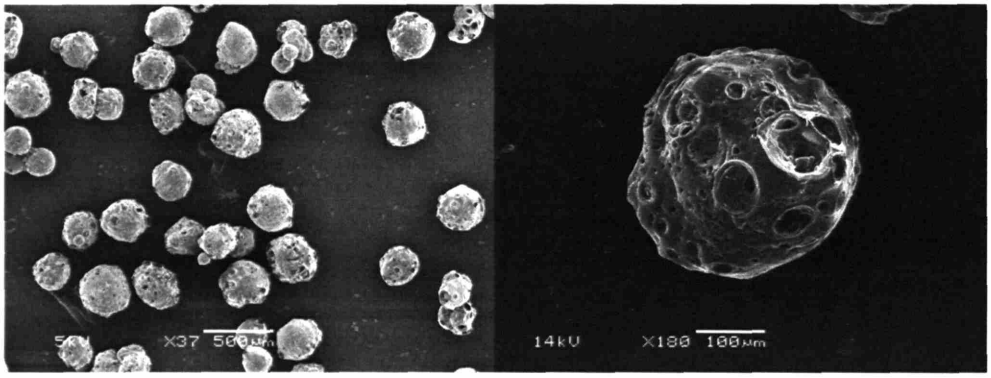

Figure 4-6: SEM images of rough surface microspheres in the unexpanded state (PAA microspheres E108302-12-1).

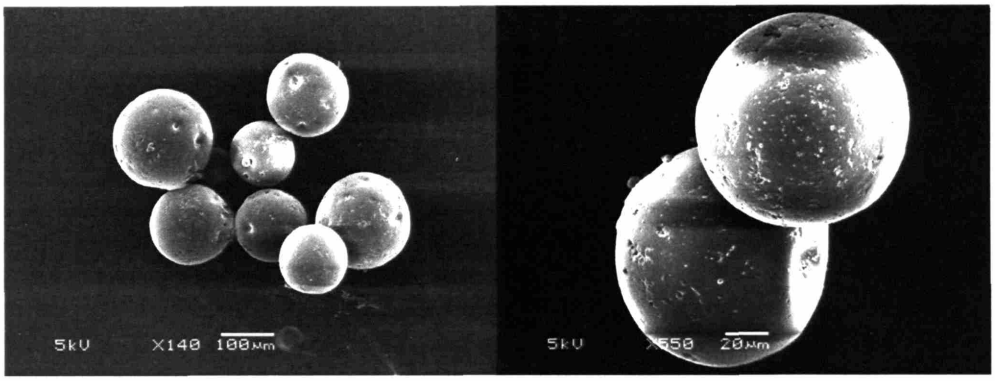

Figure 4-7: SEM images of smooth surface microspheres in the unexpanded state (PAA microspheres E109317-27).

Needle Injection Procedure

E108302-12-1 (rough surface) microspheres and E109317-27 (smooth surface) microspheres were injected though small bore needles and fragmentation was assessed. For both types of microspheres, identical procedures were followed. Two 500 ml samples of deionized water: one at acidic-pH 2.1 and the other neutral-pH 7.00 were prepared by titrating deionized water with HCL of NaOH and validating with a pH meter. 10 ml samples of each solution with 30 mg Acridine orange (cationic dye used to stain microspheres) were prepared and 60 mg of each type of microsphere was added to separate falcon tubes of each solution sample. The microspheres were filtered out with micromesh particulate specimen bags and resuspended in 10 ml of solution with same pH as initially expanded. The solutions were mixed well with a vortex touch mixer. Two ml samples of aforementioned microsphere solutions were injected through 20 and 21 gauge needles (approximately .6mm and .5mm internal diameter respectively) using enough pressure to cause steady flow though the needle. The samples were collected injected in Eppendorf micro tubes. The solutions were diluted to 75ml in the same solutions in which they were originally suspended and then analyzed with the RapidVUE® particle analysis system.

Results

The results of this study demonstrate that the all PAA microspheres undergo a very low level of fragmentation when passed through small diameter needles in the unexpanded state because the means of the distributions before and after injection are not

statistically different. The smoother and more continuous microsphere formulation (E109317-27) undergoes a much lower level of fragmentation when injected in the expanded state relative to the rough/discontinuous microspheres (E108302-12-1)., Microspheres E103302-12-1 showed no signs of fragmentation when injected using acidic media that keeps the microspheres unexpanded (Figure 4-8 and Table 4-1). In the expanded state, there was approximately a 40% reduction in average microsphere particulate diameter following injection through small diameter needles, most likely reflective of significant fragmentation.

Smooth microspheres of type E109317-27 showed some reduction in particulate size when injected in the unexpanded state (Figure 4-9 and Table 4-2). However, the reduction in size of the smooth microspheres (less than 10%) following injection in the expanded state is far less than the reduction in average size of the rough/discontinuous microspheres and is not statistically significant. Given that the standard deviation for the underlying distributions being compared is roughly 50 microns (about 10% of the mean), a less than 10% reduction is within one standard deviation so the means from the distributions are not statistically different according to the t-test. On the other hand, the means between neutral PAA microspheres and acidic PAA microspheres of all types are more than six standard deviations apart, which is well under a p value of .05 to show that the means do not come from similar distributions. Furthermore, the means from the neutral rough type E108302-12-1 microspheres passed through 21 and 20 gauge needles are not statistically different than the means of the microspheres in acidic delivery media, but they are roughly four standard deviations away from the neutral microsphere control that was not passed through a needle. This shows that from a statistical standpoint, the means of rough type E108302-12-1 PAA microsphere distributions change when passed through 21 and 20 gauge needles while the means of smooth type E109317-27 PAA microspheres do not change when passed though small bore 21 and 20 gauge needles.

Table 4-1: Average of means of rough-type microsphere diameters following passage through small bore needles in acidic and neutral aqueous solutions (PAA microspheres type E108302-12-1) as determined by bulk particle analysis.

Delivery Solution	Acid (pH=2.10)			Neutral pH		
Needle Size	no needle	20G	21G	no needle	20G	21G
Run Mean Diameter (microns)	252	258	298	623	367	403
	238	252	269	632	371	422
	226	252	256	644	384	425
Group Average Diameter	**239**	**254**	**274**	**633**	**374**	**417**
Group Standard Deviation	13	4	22	11	9	12

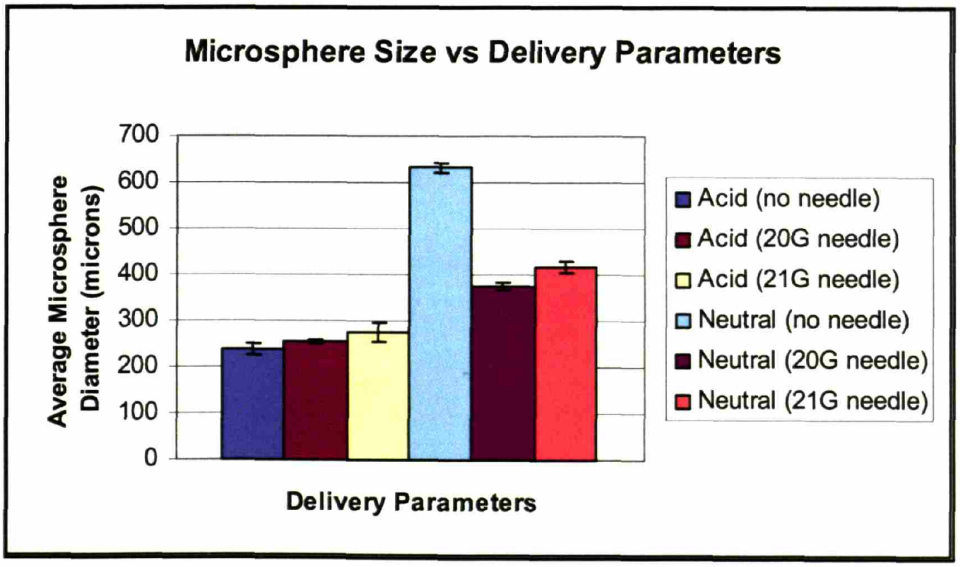

Figure 4-8: Average of mean values of rough-type microsphere diameters following passage through small bore needles in acidic and neutral aqueous solutions (PAA microspheres E108302-12-1) as determined by bulk particle analysis.

Error bars on the graph represent the standard deviations of the means of the samples. The Neutral control that was not passed through a needle is the only distribution significantly different from the others in this graph. The standard deviation for distributions underlying the mean values shown above is roughly 50 microns (Figure 4-1)

Table 4-2: Average of mean values of smooth-type microsphere diameters following passage through small bore needles in acidic and neutral aqueous solutions (PAA microspheres E109317-27) as determined by bulk particle analysis.

Delivery Solution	Acid(pH=2.10)			Neutral pH		
Needle Size	no needle	20G	21G	no needle	20G	21G
Run Mean Diameter (microns)	257	240	235	618	569	545
	251	236	223	627	582	549
	239	225	212	628	586	562
Group Average Diameter	**249**	**234**	**224**	**624**	**579**	**552**
Group Standard Deviation	10	8	11	5	9	9

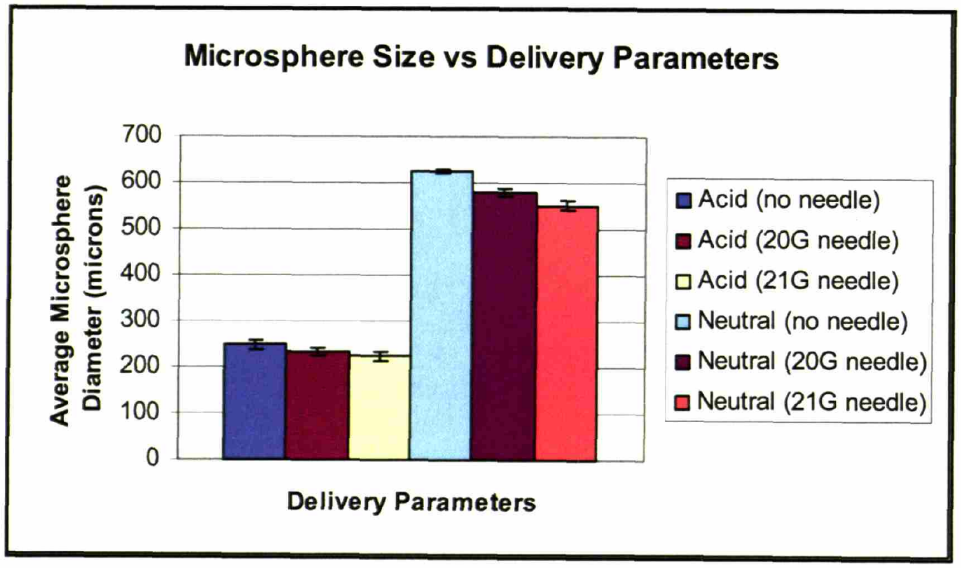

Figure 4-9: Average of mean values of smooth-type microsphere diameters following passage through small bore needles in acidic and neutral aqueous solutions (PAA microspheres E109317-27) as determined by bulk particle analysis.

Error bars on the graph represent the standard deviations of the means of the samples. In this case, the distributions in Neutral solution are not statistically different by t-test, but they are statistically different from the acidic solution distributions. The standard deviation for distributions underlying the mean values shown above is roughly 50 microns (Figure 4-1)

Conclusion

Expandable/deformable microspheres have a benefit over traditional microspheres in that they have potential for delivery through smaller diameter needles and catheters for a given effective embolic load. From a clinical perspective this can facilitate less invasive procedures. The expansion capabilities also may result in more robust occlusion because the spheres can exert radial expansion pressure on vessel walls. However, if the physical integrity of the microspheres is compromised during delivery, the clinical benefit will likely be reduced. The results of this study indicate that smoothness and continuity of the microspheres are significantly influential in determining incidental fragmentation, particularly in the expanded state. For embolic applications, the clinical efficacy will likely increase (mechanical stability will lead to more effective occlusion) and the risk will decrease (minimization of distal embolic formation and/or inflammatory response due to microsphere fragments) with the use of smooth and continuous microspheres.

4.6 Biocompatibility

Assessing biocompatibility of PAA microspheres is an essential step before considering them for long-term intravascular procedures. Biocompatibility must be assessed on biochemical, cellular and whole organism levels. Biocompatibility has been defined as: "biocompatibility is the ability of a material to perform with an appropriate host response in a specific application"[59]. This section will outline the initial investigation into both the host response to PAA microspheres as well as the ability of the material to perform under in-vivo conditions.

4.6.1 Sterilization

Sterilization of implantable materials is essential before implementation within the human body. This is especially important when materials will be used endovascularly, where infection can spread rapidly to distal sites and immune reactions can be systemic. Because of the porous nature and high water content of hydrogel materials, it is imperative that the sterilization procedure prevent seeding by fungal, bacterial or viral pathogens.

Fortunately, the manufacturing process of PAA microspheres includes several steps that preclude the establishment of pathogenic seeding. The final ethanol rinse used to contract the microspheres is an inherent antimicrobial step in the manufacturing process. By extending the ethanol rinse overnight and manufacturing the microspheres in a clean room the initial bioburden within the microspheres can be minimized.

For human use it is imperative that sterility assurance level[2] remains below 10^-6 so that no appreciable pathogens or residual toxins remain in the microspheres. To ensure adequate sterilization, the microspheres should be further sterilized using UV light or ethylene oxide treatment[59]. A concern when using these treatments is the potential for cross-linking or modifying the polymer and adversely affecting material properties of the microspheres.

To assess the effect of UV light on microsphere properties, PAA microspheres were exposed to 260 nm ultraviolet light for a period of 30 minutes in the dry state. Following exposure, approximately half the microspheres were swollen in sterilized water. Both the dry and water-immersed UV sterilized microspheres were observed under light microscopy at 10X magnification, and compared to untreated microsphere samples. In both instances, no difference was observed. Once manufacturing processes for the PAA microspheres have been finalized, UV sterilization will be a good candidate to incorporate as a final step before sterile packaging. If further sterilization is needed as determined by sterility assurance level cultures, ethylene oxide would be the next logical sterilization method to investigate.

4.6.2 Expansion of PAA Microspheres in Whole Blood

Background

PAA microspheres have been shown to expand upon contact with an aqueous medium. Whole blood contains approximately 50% water which is partially saturated with varying concentrations of both inorganic and organic molecules. If expandable PAA microspheres are to induce vascular occlusion, expansion will have to occur in whole

---

[2] The Sterility Assurance level (SAL) is defined as the probability that a product will remain non-sterile after exposure to a specified sterilization process. It is often determined by culturing samples of sterilized material after varying degrees of intensity regarding the sterilization procedure.

59. Ratner, B., et al., *Biomaterials Science*. Second ed. 2004, San Diego, CA: Elsevier Academic Press. P.755

blood. It is important to asses the functionality of PAA microspheres in blood to ensure that they will perform well under in-situ conditions.

Purpose

Qualitatively assess expansion properties of PAA microspheres in whole blood.

Hypothesis

Due to the high water content, neutral pH and low salinity (.9%) of whole blood, PAA microspheres will expand fully and immediately upon immersion in this medium.

Materials and Methods

Microspheres

The microspheres used in this study were expandable PAA microspheres E109317-129. The microspheres were submerged in whole blood in the dry, contracted state.

Blood

Whole blood was extracted from a white New-Zealand male rabbit and stored in a 15 ml polypropylene tube (Falcon tube). The microspheres were suspended in the blood approximately 30 minutes after it was taken from the rabbit. At this time, some minimal amount of clotting was already visible in the blood sample. A small allotment of microspheres (approximately 10 mg) were suspended in a 5 ml blood sample for 3 minutes and then observed with light microscopy.

Results

The results of this study demonstrate that PAA microspheres expand upon suspension in whole blood (Figure 4-10). Similar images of dry microspheres, (Figure 4-11), and microspheres submerged in pure water, (Figure 4-12), demonstrate that microspheres suspended in whole blood have a qualitatively similar expansion response to those in pure water solutions. Furthermore, the time-course of expansion was roughly the same; the spheres expanded fully in seconds. Expanded microspheres were deformed and space between microspheres was filled even with no pressure acting on the spheres.

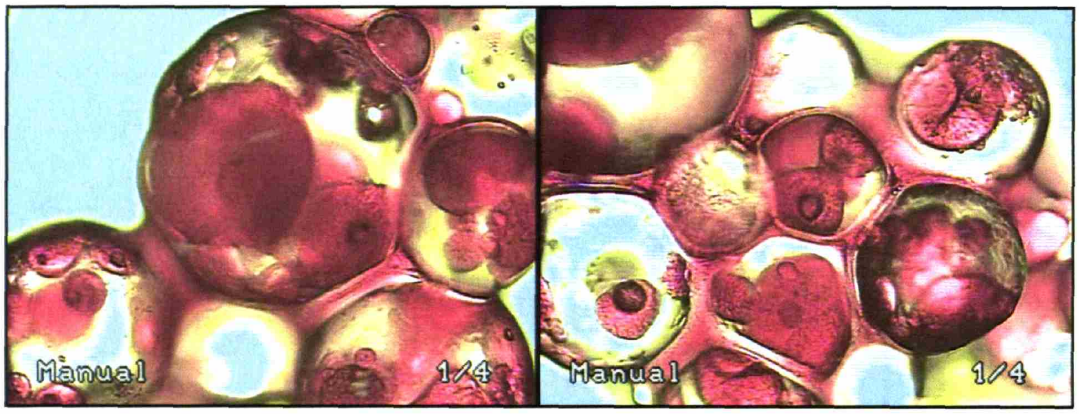

Figure 4-10: PAA microspheres following suspension in whole blood. Note space filling properties

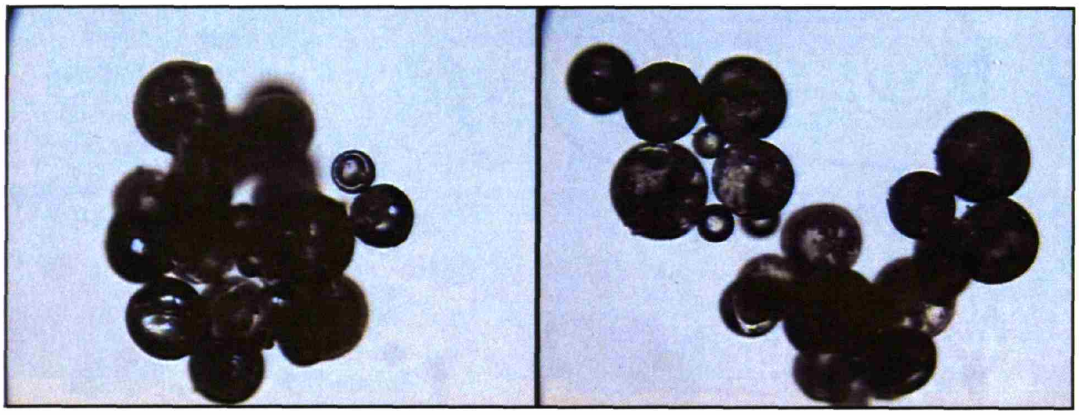

Figure 4-11: Dry PAA microspheres

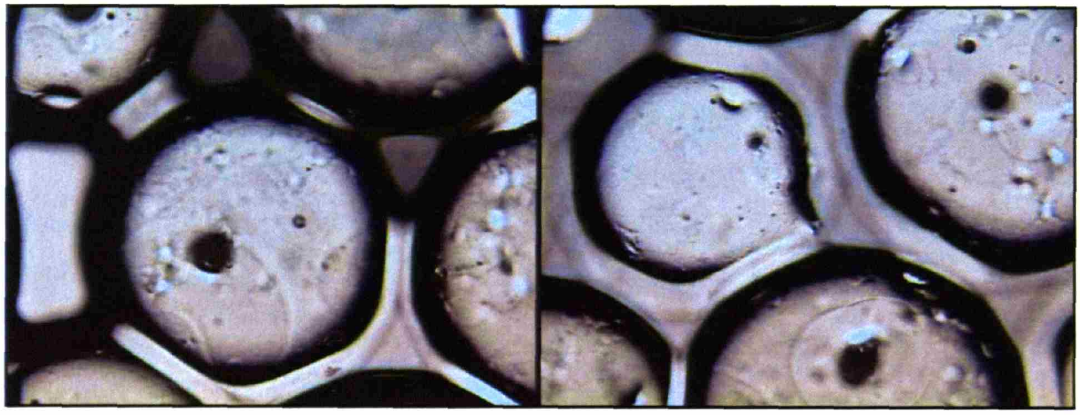

Figure 4-12: PAA microspheres following suspension in pure water. Note space filling properties

Conclusion

This study empirically demonstrates that PAA microspheres expand upon contact with whole blood. This result is in accordance with the PAA microsphere expansion observed during in-vivo testing. This result shows that the water-content of blood is sufficient to allow hydration of PAA microspheres. The microspheres also maintain their deformability in blood.

4.6.3 In-Vitro Cytotoxicity Testing of Bovine Aortic Endothelial Cells in Culture with PAA Microspheres and PAA Microsphere Fragments

Purpose

Assess the in-vitro response of bovine aortic endothelial cells (BAEC) cultured with both whole and fragmented PAA microspheres. Analyze cell cultures for signs of cell death or diminished functionality due to presence of PAA microspheres or microsphere fragments.

Hypothesis

PAA microspheres and/or fragments will have no effect on BAEC viability or functionality. Previous work has shown that PAA is a biocompatible material and has no observable effect on a variety of cell types[72, 73], including endothelial cells.

Materials

Bovine aortic endothelial cells (BAEC) were acquired at 4^{th} passage and were used as the biological testing cells. They were cultured with standard media (low glucose DMEM + 5% calf serum + 1% PSG). PAA microspheres of type E109572-25 were used in these experiments. A DiI-Ac-LDL uptake assay (BT-902), supplied by Biomedical Technologies Inc. was used to test cell function. A Live/Dead Viability/Cytotoxicity assay (L-3224), supplied by Molecular Probes was used to test cell viability.

Procedure

One vial of P4 BAEC was plated onto a P100 cell culture dish. The media was changed every two days. The plate was monitored daily for confluence. Once confluent,

the cells were passaged using trypsin to a stage of P5 (fifth passage) into five 6-well plates (30 total wells). The media was continually changed very two days.

200 mg of PAA microspheres in phosphate buffered saline (PBS) were fragmented by passing them through a 23 gauge needle. Another 200 mg of whole PAA microspheres were left whole and suspended in PBS. Whole and fragmented PAA microsphere samples were then filtered to remove PBS. The whole and fragmented PAA microspheres were then sterilized with exposure to UV light for 2 hours. When BAEC cells reached roughly 70-80% confluence, 20 mg of PAA microspheres were added per well to 10 wells and 20 mg PAA microsphere fragments per well were added to 10 other wells. The BAEC cells were then co-cultured with PAA microspheres and fragments for 48 hours. Concurrently, 10 wells of BAEC cells were cultured as control samples.

Following 48 hour of co-culture, the PAA microspheres and fragments were removed from all wells. The following assays were conducted on the cells. A Coulter Counter was used to count the cells from the control wells of BAEC only (n=3), the BAEC co-culture cells with whole PAA microspheres (n=3), and the BAEC co-culture cells with fragmented PAA microspheres (n=3). An LDL uptake assay was performed on the control wells of BAEC cells only (n=4), the BAEC co-culture cells with whole PAA microspheres (n=4), and the BAEC co-culture cells with fragmented PAA microspheres (n=4). Live/Dead assays were performed on the control wells of BAEC cells only (n=3), the BAEC co-culture cells with whole PAA microspheres (n=3), and the BAEC co-culture cells with fragmented PAA microspheres (n=3).
Analyze results of assays from each of the three culture types and note any difference between co-cultures and control wells.

Results

No significant difference was noted in the number of cells per well for each of the three culture conditions. The average and standard deviation of the cell counts for each culture condition overlapped and showed no statistical difference (Figure 4-13).

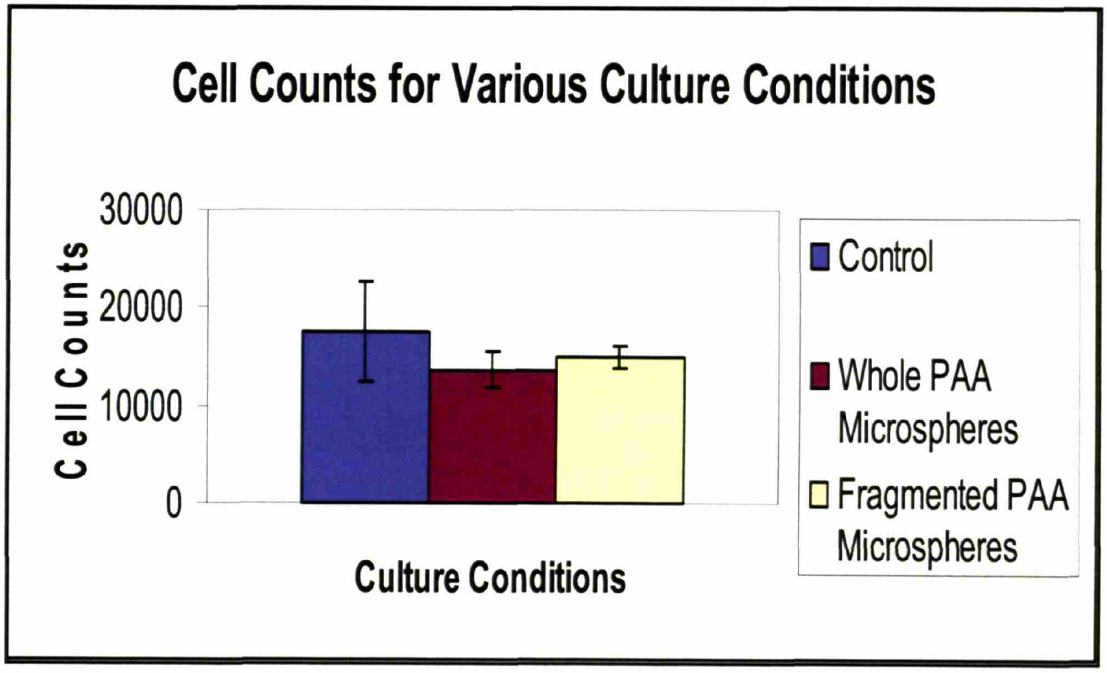

Figure 4-13: Cell counts for each of the three culture conditions.

LDL Uptake Assay: For all three culture conditions, there was indication of extensive LDL uptake for all wells when observed with fluorescence microscopy. BAEC in all culture fluoresced bright green, indicating that the cells were functioning bovine aortic endothelium. There was no observable difference in the samples between the various culture conditions.

Live/Dead Assay: For all three culture conditions, there was a similar profile in the percentages of live and dead cells. In all cases, the general health of the cultures was excellent, with > 90% survivability noted for all wells. There was no observable difference in the samples from the various culture conditions.

Conclusion

The results of this study indicate that both whole PAA microspheres and microsphere fragments have no observed detrimental effect on BAEC viability or functionality in-vitro. These findings suggest that PAA microspheres should not cause a cytotoxic reaction when in contact with the endothelium during endovascular embolization.

4.7 Discussion/Conclusion

This chapter outlined the techniques developed to monitor and improve upon the quality of microsphere batches. Sieving methods allowed for more precise control over the size range of PAA microspheres and tighter standard deviations. Light microscopy and SEM were performed to track fragmentation rates and to characterize the surface properties of the microspheres before and after injections or treatments. Microspheres were also shown to be resistant to degradation and fragmentation after they were modified to be smoother. Resistance to fragmentation will allow for the use of smaller-bore catheters and hence less invasive procedures while maintaining stable occlusions.

This chapter also describes the preliminary biocompatibility studies necessary to permit animal work and eventual clinical trials. Preliminary in-vivo functionality tests in blood were also demonstrated. These data show that PAA microspheres have passed preliminary biocompatibility and in-vitro functionality tests and are ready to be tested with more detailed methods and within long term animal models. Future work in this area will involve further precise molding of microsphere distributions to eliminate fragments and outliers as well as more stringent sterilization procedures such as Gamma radiation and/or Ethylene Oxide.

Chapter 5: Occlusive Efficacy

Abstract

PAA microspheres have been shown to expand roughly from 80 to 140 fold volumetrically when exposed to aqueous media. It had been hypothesized that this expansion will allow for greater occlusive efficacy while providing ease of delivery. However, expansion may also result in catheter occlusion. The upper-limit of concentrations that can go through various catheters must be determined to avoid catheter blockage. Initially, three different sized catheters (5 French, 6 French, and 7 French) were tested with different concentrations of PAA microspheres in their unexpanded state within DMSO. 250mg/mL concentrations could pass through 6F and 7F catheters with no fragmentation. 400mg/ml was over the saturation limit of DMSO. Mixtures up to 150mg/ml of PAA microspheres with average size of 250 micron were able to pass through 5 French catheters when MD-76R contrast was used as a delivery media for the microspheres. Microsphere concentrations of 200mg/mL saturated the MD-76R contrast (a high salt solution). It is important to note that the microspheres expand slightly (about 4X volumetrically) in contrast, which allows for some deformability and hence easier passage through small catheters at high concentrations. Small microspheres filtered within a range between 50 and 150 micron were able to pass through the 5 French catheters at 300mg/mL in MD-76R contrast.

After demonstrating the maximum concentrations that could pass through large-bore catheters, micro-catheters were studied. Expandable/deformable PAA microspheres suspended in their unexpanded state within high salinity (.3g sodium chloride per ml water) solution or DMSO were able to be delivered through a Boston Scientific 533 micron internal diameter three French hydrophobic-lined Renegade® microcatheter at concentrations previously shown to be sufficient to occlude 1.5mm internal diameter Tygon® tubing up to pressures beyond 1000mmHg. Furthermore, commercially available suspensions of PVA particulate and tris-acryl gelatin microspheres in saline were unable to pass through the microcatheter at concentrations recommended by the manufacturer for embolotherapy.

PAA microspheres have been able to selectively occlude both porcine renal and coronary vasculature. The results are reproducible and the occlusions are complete as observed under angiography. Using MD-76R contrast in the delivery media allows for visualization during the procedure. On histological examination, PAA microspheres were found to occlude the vasculature completely and were fully expanded. PAA expandable/deformable microspheres have been shown to perform better than non-expandable microspheres in flow loops by resisting much greater pressures once occlusion forms and requiring much less embolic mass to occlude the model flow system. Tris-acryl gelatin microspheres were not able to occlude the model flow system. More work must be done to conclusively demonstrate superiority in-vivo.

5.1 Quantification of Pressure Required to Dislodge Occlusions

Background and Purpose

Previous experiments have demonstrated that PAA microspheres can occlude tubing under static pressure and occlude flow in a constant pressure, single path flow loop. In order to more closely approximate the clinical implementation of microspheres for embolic procedures, a divergent flow loop was designed. The flow loop was designed to demonstrate that catheterization and microsphere injection upstream of a flow bifurcation can allow for selective tube occlusion.

A second study was conducted in order to quantify the pressure required to dislodge a given volume of both expandable and non-expandable microspheres from 1.5 mm internal diameter tubing. The purpose of this second study was to determine if expandable microspheres form a more robust and stable occlusion, which would suggest superiority for embolic applications.

Hypotheses

Divergent Flow Loop

The insertion of a 5F catheter beyond the primary bifurcation in a divergent flow loop will allow for selective tube occlusion. No significant backflow should occur due to the upstream applied pressure head, resulting in controlled microsphere placement. Flow in collateral tubes will persist following the occlusion of a targeted tube.

Dislodging Pressure

The pressure required to dislodge expandable microspheres from small diameter tubing will be much greater then for non-expandable microspheres. A smaller mass of expandable microspheres will be required for occlusion as compared to non expandable microspheres.

Materials and Methods

Divergent Flow Loop

A diverging flow loop was designed to provide constant pressure (approximately 147 mmHg static pressure head) flow to four symmetric Tygon® tubes (1.5 mm internal diameter, the lowest tubes in the diagram at right) with a cumulative flow rate of 560 ml/min (Figure 5-1). This flow rate is approximately 10% of the total flow rate of an adult male and is approximately the amount of flow delivered to a single kidney[74]. A catheter port located upstream of the initial tube bifurcation allowed for selective catheterization of one half of the flow system (2 of the 4 tubes). Expandable microspheres (E109572-25) and tris-acryl gelatin microspheres (500-700micron) were introduced into the flow system via 5F catheter in various delivery mediums. The injectable level of each prepared solution was qualitatively rated according to the following scale: 0-not injectable, 1-injection requires moderate force, 2-easily injectable with respect to how difficult the solution was to inject into the delivery catheter. Following microsphere delivery, all four terminal branching tubes were monitored for occlusion.

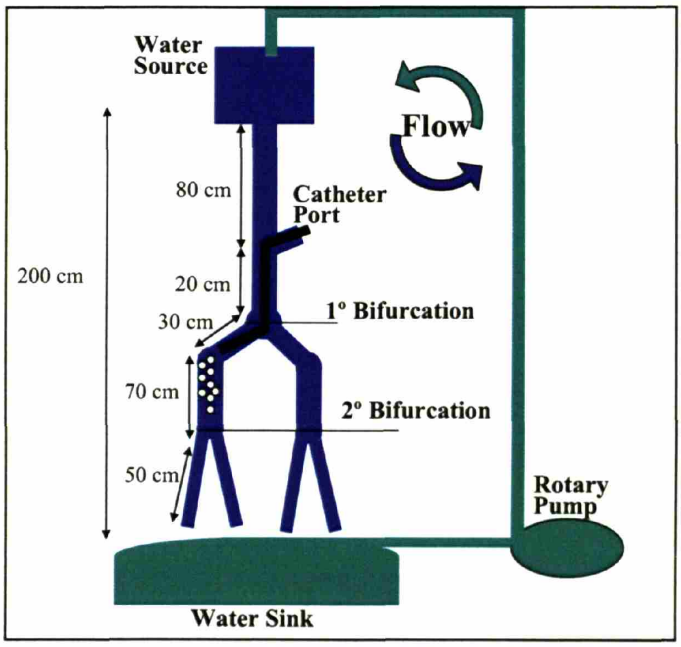

Figure 5-1: Schematic of Divergent Flow Loop System

A second study was performed similar to the first study except that the pressure head was dropped until the flow rate reached about 140ml/min. This is about $1/4^{th}$ the flow rate of the rate at the renal artery and would approximate what the flow rate might be like at the second bifurcation level off of the renal artery where the anatomy of the vessels approaches 1.5mm in diameter.

Dislodging Pressure

A linear tube system was used to apply internal pressure to a detachable Tygon® tube (1.5mm internal diameter) (Figure 5-2). The Tygon® tube was detached from the system and filled with a 2.5 ml aqueous suspension containing either expandable (E109572-25) or non expandable (E109573-3, 250-500 micron) PAA microspheres in water. A syringe was used to gradually impart internal pressure to the Tygon® tube. The pressure needed to dislodge the microspheres from the Tygon® tubing was recorded from a clinical grade pressure transducer (Harvard Apparatus). The experiment was repeated for various concentrations of expandable and non expandable microspheres. For the highest mass, 500mg, of non-expandable microspheres used in the experiment, 10ml of water was used to load the detachable occlusion tube because the concentration was too high to inject when 2.5ml of water was used.

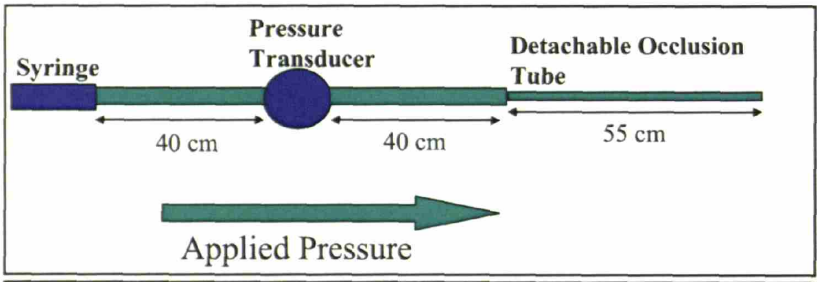

Figure 5-2: Schematic of Dislodging Pressure Flow System

Results

Divergent Flow Loop

The results of this experiment confirmed all three hypotheses: (i) selective tube occlusion was demonstrated with a 5F catheter (ii) no backflow of microspheres into untargeted tubing was observed and (iii) flow persisted in collateral tubing following microsphere introduction (Table 5-1). In all cases of noted occlusion, only one of the two tubes of the secondary bifurcation (on the side of the catheterized primary bifurcation) became occluded, with all other collateral flow persisting. The lower flow system was easier to occlude for most PAA microsphere suspensions. The tris-acryl gelatin microspheres were not able to occlude the flow system at the given dosage at either flow rate.

Table 5-1: Results of Divergent Flow Loop Occlusion Study (N/A means that either the solution did not inject properly or there was a difficulty with the injection that negated the data)

Expandable PAA MS					**Q=560 ml/min**	**Q=141 ml/min**
Delivery Solution	**Delivery Volume (ml)**	**Dry Volume of MS (ml)**	**Concentration (ml MS/ml)**	**Injection difficulty Rating**	**Occlusion**	**Occlusion**
5% Saline	5	0.5	0.10	1	N	Y
9% Saline	5	0.25	0.05	2	N	N/A
9% Saline	5	0.35	0.07	2	N	Y
9% Saline	5	0.5	0.10	1	N	Y
9% Saline	5	1	0.20	0	N/A	N/A
13% Saline	5	0.5	0.10	2	N	Y
13% Saline	5	1	0.20	0	N/A	Y
17% Saline	5	0.75	0.15	2	N	Y
3ml Contrast+2 ml 9% Saline	5	1	0.20	2	Y	Y
2.5 ml Contrast + 2.5 ml 9% Saline	5	1	0.20	2	N	Y
Contrast	5	0.1	0.02	2	N	N
Contrast	5	0.2	0.04	2	N	N
Contrast	5	0.3	0.06	2	N	N
Contrast	5	0.4	0.08	2	N	Y
Contrast	5	0.5	0.10	2	N	Y
Contrast	5	1	0.20	2	Y	Y
PBS	5	0.2	0.04	2	N	N
PBS	5	0.3	0.06	0	N/A	N/A
PBS	10	0.3	0.03	2	Y	Y
Embosphere® 500-700 MS						
0.9% Saline	6	1	0.17	2	N	N

Dislodging Pressure

Both hypotheses of the dislodging pressure study were confirmed; (i) a much greater force was required to dislodge expandable microspheres as compared to non expandable microspheres and (ii) a significantly smaller mass of expandable microspheres was required to induce tube occlusion (Table 5-2). It is important to note that these microspheres were introduced into the detachable occlusion tube in an aqueous medium, meaning the expandable microspheres were pre-expanded. We hypothesize that the occlusion formed by microspheres expanding within the tubing will be even more robust due to the effect of maximal packing and expansion within an elastic tube. This type of packing and expansion will induce maximal interfacial contact with deformable spheres while increasing normal recoil force by expanding the vessel walls radially outward.

Table 5-2: Results of Dislodging Pressure Study. Pressure given is pressure required to dislodge occlusion. All MS mixed with 2.5 ml water prior to introduction into occlusion tube

Expandable MS		
Dry MS Mass (mg)	**Run**	**Pressure(mmHg)**
15	1	140
	2	114
	3	126
18	1	570
	2	660
	3	588
20	1	max (>1000)
	2	max (>1000)
	3	max (>1000)
Non-expandable MS		
Dry MS Mass (mg)	**Run**	**Pressure(mmHg)**
20	1	<15
	2	<15
	3	<15
100	1	<18
	2	<15
	3	<15
500	1	43
	2	66
	3	37

Conclusion

Divergent Flow Loop

The results of the divergent flow loop study demonstrate that expandable PAA microspheres are capable of occluding high flow, low resistance systems. It is important to note that this system features a much lower level of resistance and much larger gauge terminal vessels than most physiologic arterial networks, and hence is much more difficult to occlude. This system most closely models the most difficult scenario to occlude, arterio-venous malformations, although flow-rate matching was used to approximate the shear forces experienced at the renal opening to compensate for the difference in resistance within the bed. The theory behind matching flow rates is that the shear forces from the flow are more important than absolute pressures and vascular resistances. The flow rate will be directly proportional to microsphere velocity and is a combination of several factors including viscosity of the delivery media, resistance in the flow bed, and the pressure gradient[68]. The flow rate is an easily controlled and quantifiable measure to approximate physiological systems.

Another important difference between this system and many physiological beds, such as hyper-vascular tumors, vessel diameter is constantly reduced in the target tissue, which virtually guarantees occlusion at some level in the vascular tree. In-vivo studies with PAA microspheres have shown that when injected into porcine renal vasculature the microspheres are capable of deep vessel penetration prior to occlusion due to high deformability. The deep penetration also leads to much greater packing of microspheres within the vessels as compared to non expandable microspheres, leading to more robust occlusions.

The results of this study also show that to achieve occlusion at high flow rates, the PAA microspheres had to be delivered at high concentration in a medium that allows some level of pre-expansion (either contrast or PBS). When attempts were made with a delivery medium that allows for minimal pre-expansion (high salinity aqueous solutions), no occlusion was realized. This is probably due to the high flow rate of the flow system not allowing sufficient time for microsphere expansion, which is typically complete in 3-5 seconds. At a lower flow rate, the expandable PAA microspheres were able to occlude at most concentrations delivered. These slower flow rates are more clinically applicable because the flow rate in the larger arteriole beds where microspheres are likely to occlude

is relatively slow. Furthermore, arteriole networks continue to bifurcate into sequentially smaller diameter vessels so occlusion by large microspheres is guaranteed once vessels on the order of magnitude of the sphere diameter are reached.

The concentrations used in this study were given in dry volume of microspheres (ml) per total wet volume of suspension. The density of PAA microspheres is between 5 and 10mg dry volume (depending upon packing density) to 1 ml wet volume in water. The significance of this is that although some of the dry volumes delivered were less than the dry volume of the non-expandable tris-acryl gelatin microspheres, the PAA microspheres were still able to occlude because a greater embolic load, i.e. greater expanded volume was delivered at the same or sometimes lower injection difficulty through the catheter.

Dislodging Pressure

The results of the dislodging pressure studies confirmed the previous qualitative assessment of the tighter packing of expandable microspheres forming a more robust occlusion. The robustness of the occlusion was quantified by identifying the pressure at which the occlusion would breakdown. In order to evaluate the dislodging pressure required for expandable microspheres that have expanded within the tubing (as opposed to the pre-expanded method used in this study), future studies will employ an aqueous flow loop and expandable microspheres delivered in an expansion-restrictive medium such as DMSO. A detachable occlusion tube will then be removed from the flow system and evaluated for dislodging pressure in a similar manner as used in this study.

5.2 Passage of PAA Microspheres through Catheters

Background

Delivery of expandable PAA microspheres through a catheter represents a minimally invasive technique to induce embolization and targeted occlusions. The delivery medium used in this study is dimethyl sulfoxide (DMSO), which has previously been shown to deliver microspheres in the unexpanded state. A critical factor for a catheter-based microsphere delivery procedure will be the concentration of microspheres injected through the catheter; high concentrations may occlude catheters while low concentrations may not effectively occlude the targeted vessel diameter.

Purpose

The purpose of this study was to determine the highest concentration of PAA microspheres that can pass through various sized catheters when PAA microspheres are suspended in DMSO. Catheters of size 5F, 6F, and 7F were tested.

Hypothesis

As catheter size is increased, denser concentrations of microspheres may pass without occluding the lumen. In all size catheters, an upper limit of microsphere concentration will be observed whereby further increase in concentration will occlude the catheter lumen.

Materials

Catheters

Three different catheters were used in this study: the Cordis PTA dilation catheter, Opta 5 - **5F catheter,** the Medtronic AVE Z^2 guiding catheter - **6F catheter**, and the Cordis Vistabritetip, guiding catheter - **7F catheter.**

DMSO/Microsphere Solutions

The delivery medium used in this study was dimethyl sulfoxide (DMSO), supplied by VWR. Two different types of expandable PAA microspheres were tested, referenced as batches E108302-12-1 and E108302-12-5. The size distributions of these microspheres in the unexpanded state are similar, with average unexpanded diameters of approximately 250 microns.

Procedure

Create various concentrations of DMSO/microsphere solutions by adding dry, unexpanded PAA microspheres to DMSO. Make five solutions of different concentrations with two types of microspheres. Mix the microspheres and DMSO in a 60 ml Falcon Tube for three minutes with a Vortex Touch Mixer at speed ten (Table 5-3). Attempt to inject the solutions through various sized catheters using a 10 ml syringe (Table 5-4). Collect samples of the PAA microspheres that passed through the smallest size catheter and observe under light microscopy. Search entire sample field for evidence of microsphere fragmentation. Capture representative frames with microscopic imaging software.

Table 5-3: DMSO/microsphere solutions for catheter passage experimentation

Solution	Microsphere Type	Volume DMSO (ml)	Mass Microspheres (mg)	Concentration in DMSO (mg/ml)
A	E108302-12-1	5	1000	200
B	E108302-12-1	10	1000	100
C	E108302-12-1	20	1000	50
D	E108302-12-5	5	2000	400
E	E108302-12-5	8	2000	250

Table 5-4: Description of trials for catheter passage experimentation

Trial	Microsphere type	Volume Injected	Catheter Size (F)	Concentration in DMSO (mg/ml)
1	E108302-12-1	2.5mL	5	200
2	E108302-12-1	2.5mL	5	100
3	E108302-12-1	2.5mL	5	50
4	E108302-12-5	2.5mL	6	250
5	E108302-12-5	2.5mL	6	400
6	E108302-12-5	2.5mL	7	250
7	E108302-12-5	2.5mL	7	400

Results

The results of this study demonstrate that of the examined PAA microsphere solutions, some can pass through 6F and 7F catheters, but none could pass through a 5F catheter (Table 5-5). The lumen of the 5F catheter was too small to allow passage of solutions with a concentration as low as 50 mg microsphere/ml DMSO. When any of the solutions were injected into the 5F catheter, the microspheres aggregated around the entry point of the lumen. No microspheres were carried by the DMSO as the fluid was passed through the 5F catheter. For both the 6F and 7F catheters, solutions with concentrations of 250 mg/ml could easily pass when injected with the 10 ml syringe. The most concentrated solution, solution D, could not pass through these catheters due to an over saturation of microspheres in DMSO, not to a luminal size limitation of the catheters. In other words, solution D could not even maintain homogeneity when injected from the 10

ml syringe with no associated catheter. This represents an upper limit of concentration for the microspheres that cannot be exceeded regardless of catheter dimensions.

Table 5-5: Summary of DMSO/microsphere solutions passage through various catheters

Trial	Microsphere type	Volume Injected	Catheter Size (F)	Concentration in DMSO (mg/ml)	Successful passage
1	E108302-12-1	2.5mL	5	200	No
2	E108302-12-1	2.5mL	5	100	No
3	E108302-12-1	2.5mL	5	50	No
4	E108302-12-5	2.5mL	6	250	Yes
5	E108302-12-5	2.5mL	6	400	No
6	E108302-12-5	2.5mL	7	250	Yes
7	E108302-12-5	2.5mL	7	400	No

The microspheres that were passed through the 6F catheter at a concentration of 250mg/mL were collected and observed under light microscopy (Figure 5-3). At 10 times magnification, no difference in the level of fragmentation was observed for passed microspheres when compared to controls. Overall, the level of fragmentation was low throughout the entire field and passage through the catheter had no apparent adverse effects on the microspheres.

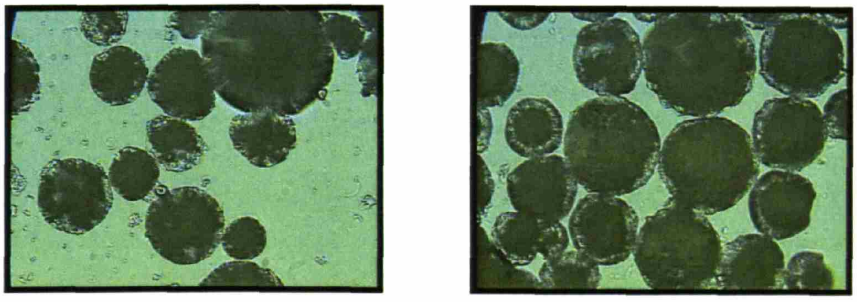

Figure 5-3: Left- Control (no attempted passage) **Right-** PAA-MS after passage through a 6 French catheter. No fragmentation was observed.

(Image scale 0.8 x 0.9 mm)

5.3 Candidate clinical suspension: MD76-R media, lower concentrations and a 5F catheter

A series of additional studies were conducted with 5F catheters to follow up on the initial findings described above. The purpose of these studies was to investigate the effect of different delivery media as well as more clinically relevant microsphere concentrations (the concentrations initially tested were determined to be much too high for in-vivo embolic applications). This study tests the hypothesis that (1) smaller microspheres can pass through 5F catheters at higher concentrations and (2) some expansion of microspheres actually allows for easier passage through 5F catheters (due to high deformability within rigid-walled catheters). Note: Microspheres undergo roughly 4X volumetric expansion when delivered in pure MD76-R contrast.

Procedure

Using contrast (MD76-R) as a delivery medium, determine the maximal mass of microspheres that can pass through a 5F catheter. Two different varieties of PAA microspheres were tested: E109317-129 (random size distribution, average dry diameter near 250 microns) and E105050-75 (50-150 micron dry diameter).

Results:

Both hypotheses were confirmed with this study (Table 5-6). The results suggest that it may be advantageous to deliver partially expanded microspheres to take advantage of deformability. Partially expanded microspheres can be delivered in pure contrast, a range of saline solutions, a cocktail of contrast and DMSO, or a cocktail of saline and contrast. Preliminary work (not shown) shows that fully hydrated microspheres are more readily passed through 5F catheters at high concentrations when compared to DMSO delivered microspheres because of their high deformability.

Table 5-6: Passage-ability of different microsphere concentrations in MD-76R contrast through a 5F catheter.

Microsphere type	MS Mass (mg)	Volume Contrast (ml)	Passage	Fragmentation	Notes
E109317-129	500	5	Y	N	Easy Passage
E109317-129	750	5	Y	N	Easy Passage
E109317-129	1000	5	N	N/A	Does not go into solution (not injectable through Syringe
E105050-75	1500	5	Y	N	Easy Passage (small MS; 50<D<150um

Conclusion

The delivery of expandable PAA microspheres through small bore catheters has great potential as a minimally invasive and highly effective procedure for embolic applications. The results of this study demonstrate that high concentrations of PAA microspheres suspended in DMSO can pass through catheters as small as 6F. Lower concentrations of microspheres in DMSO would likely pass through even smaller catheters. The ideal concentration will depend on the size of catheter needed for a given vascular bed as well as the amount of microspheres required to occlude. By allowing the microspheres to slightly expand in media such as MD-76R contrast, passage through 5F catheters is achievable at concentrations up to 150mg/ml. Smaller microspheres (50-150 micron) are able to pass through 5F catheters in even higher concentrations (300mg/ml) when suspended in MD-76R contrast. However, smaller microspheres have been shown to expand less when placed in water and hence may not be able to occlude as well in-vivo.

Future Work

In-vitro and in-vivo model systems will be used to determine the concentrations and catheter sizes required for given applications. If catheters smaller than 5F are indicated, lower concentrations may be used. We will determine the maximum passable microsphere concentrations and the most suitable delivery medium for use with these microcatheters. We suspect that fully hydrated microspheres may fracture with attempted passage through such a constricted catheter bore. It may be optimal to use partially

expanded microspheres in a low viscosity solution, i.e. contrast or a DMSO/contrast mixture. Delivery capabilities will be compared to various sizes of tris-acryl gelatin microspheres and PVA particulate.

5.4 Microcatheter passage of various microemboli

Background

For many embolic applications, it is preferential if not essential to use as small a catheter as possible to deliver enough embolic load to cease flow. There are several common scenarios that justify the use of microcatheters. Whenever vasospasm is an issue, a smaller catheter will result in less propensity for vascular irritation and hence less vasospasm. This is especially important for uterine artery embolization where vasospasm can be severe[22]. The vasospasm can cause erroneous endpoint determination by causing vascular beds to appear occluded when viewed via angiography, only to reopen after the spasm relaxes. Vasospasm can be so severe at times that further advancement of the catheter becomes impossible. A microcatheter is necessary when attempting to inject the embolic as close to the tumor as possible. If there are any anastomoses to other vascular beds, such as the ovarian artery or the cervicovaginal branch, there is a concern for unintentional embolization to the wrong site. By approximating the catheter tip as close as possible to the tumor's vascular bed, aberrant embolization can in be minimized. Another reason to use a microcatheter is that it will potentially allow for more controlled pruning of the tumor vasculature. Microcatheters allow for precise tailoring of the amount of devascularization in order to prevent overembolization and minimize any embolization to normal tissue. Serious complications of uterine fibroid embolization such as the post-embolic flu-like syndrome may be attenuated by precisely devascularizing the tumor bed no more than necessary to induce tumor regression. The following experiments investigate the use of small diameter catheters to deliver PAA microspheres in both expanded and unexpanded states as compared to delivery of commercially available concentrations of tris-acryl gelatin microspheres and PVA particulate suspensions.

Hypothesis

When suspended in highly ionic media or organic solvents, PAA microspheres remain unexpanded and are roughly 100 times smaller (roughly 200 micron average diameter) volumetrically than when suspended in water or other dilute solutions (roughly 1000 micron average diameter). Media such as low pH water, high salinity water, DMSO, MD-76R contrast or propylene glycol have all been shown to inhibit expansion of PAA microspheres, but to varying degrees (Table 3-2). We hypothesized that unexpanded microspheres (roughly 200 micron average diameter) in low viscosity media may be able to traverse small-bore microcatheters (533 micron inner diameter) in concentrations high enough to cause significant occlusion once the microspheres have expanded after leaving the catheter. Theoretically, some expansion may actually help microspheres pass through the microcatheter by allowing microspheres to deform slightly so they can assume smaller cross-sectional area. Because of this, both high-salt (which allows slight expansion similar to MD-76R contrast) and DMSO (which allows no expansion) were tested.

Expanded PAA microspheres, Non-expandable 500-700 micron diameter tris-acryl gelatin microspheres and 500 micron PVA particulate of standard diameters and concentrations for occlusion should not be able to traverse small bore (533 micron inner diameter) catheters due to size limitations.

Materials and Methods

Microcatheters

The microcatheters used in this experiment were 3-French Renegade® Fiber braided microcatheters from Boston Scientific. Lot # 7704153
The Renegade® design is most notable for its large .021 inch (533 micron) PTFE lined inner lumen, designed specifically for embolic applications.

Microembolic Suspensions

Ten different suspensions were injected into separate Renegade® microcatheters and the tips of the microcatheters were placed into collection beakers to monitor for any effluent. For all injections, the syringe was constantly agitated to promote adequate mixing of the slurry.

The following suspensions were prepared. The first suspension used 500-700 micron diameter tris-acryl Gelatin microspheres by Embosphere® Ref 5610GH, Lot 032BBS from Biosphere medical. One cubic centimeter of the Embospheres® comes prepackaged in a syringe diluted to 6ml total suspension volume with physiologic saline. The next suspension used PVA particulate, 500 micron average size diameter by Cook, lot 1485391. 1cc dry volume was diluted to 6ml with saline within a 6cc syringe. The particulate swelled to roughly 2cc when placed in saline. The rest of the suspensions were all made using Expandable/deformable PAA microspheres type E109572-25. The first of these suspension used 1cc wet volume (corresponds roughly to 10mg dry mass) diluted to 6ml with phosphate buffered saline within a 6cc syringe. The next used the same 10mg dry mass suspended in high salinity medium made to a concentration of .3g/ml sodium chloride in water to a total volume of 6ml within a 6cc syringe. At this concentration of sodium chloride, PAA microspheres do not appreciably expand. Suspensions of increasing PAA-MS concentration were made including: 30mg dry mass diluted to 6ml in .3g/ml high salinity solution within a 6cc syringe, 60mg dry mass diluted to 6ml in .3g/ml high salinity solution within a 6cc syringe, and 120mg dry mass diluted to 6ml in .3g/ml high salinity solution within a 6cc syringe. Using the same PAA-MS, three more suspensions were made with concentrations of: 10mg dry mass diluted to 6ml in DMSO within a 6cc syringe, 30mg dry mass diluted to 6ml in DMSO within a 6cc syringe, and 60mg dry mass diluted to 6ml in DMSO within a 6cc syringe. All of these solutions were injected through separate microcatheters as described above.

Results

500-700 micron diameter tris-acryl gelatin microspheres in saline fully occluded the Renegade® catheter. Saline was able to filter through the occlusion at high pressure, but greater than 99% of the microspheres remained within the syringe.

PVA 500 particulate in saline occluded the Renegade® catheter. Saline was able to filter through the occlusion at high pressure, but greater than 99% of the particulate remained within the syringe.

10mg PAA microspheres expanded in water occluded the microcatheter. Some microspheres passed through the Renegade® microcatheter, but the vast majority, greater than 95%, remained within the syringe. This experiment was repeated and the on the

second attempt the catheter was completely occluded after only a small amount of the suspension passed through the catheter.

The suspensions containing 10mg, 30mg, and 60mg of PAA microspheres within .3g/ml sodium chloride in water were all able to pass through the Renegade® microcatheter with very little injection pressure applied.

Although some of the suspension of 120mg PAA microspheres within .3g/ml sodium chloride in water passed through the Renegade® microcatheter, after approximately 3ml of suspension had been delivered the microspheres aggregated and occluded the microcatheter.

The suspensions containing 10mg and 30mg of PAA microspheres in DMSO passed through the Renegade® microcatheter with little injection pressure applied. Microspheres were clearly visible in the collection beaker and expanded after water was introduced into the beaker. Some microspheres remained in the syringe, however, due to static adherence to surfaces.

The suspension of 60mg PAA microspheres in DMSO did not pass though the microcatheter. After only about 1ml of fluid and few microspheres passed, the microcatheter became occluded such that no more fluid would pass.

Table 5-7: Passage of various suspensions through the Renegade® 533 micron internal diameter microcatheter

Suspension	Suspension media	Passage
1ml 500-700um tris-acryl gelatin microspheres siluted to 6ml	Saline	No
1ml PVA Particulate diluted to 6ml	Saline	No
10mg PAA-MS diluted to 6ml	Water	No
10mg PAA-MS diluted to 6ml	.3g/ml NaCl in water	Yes
30mg PAA-MS diluted to 6ml	.3g/ml NaCl in water	Yes
60mg PAA-MS diluted to 6ml	.3g/ml NaCl in water	Yes
120mg PAA-MS diluted to 6ml	.3g/ml NaCl in water	No
10mg PAA-MS diluted to 6ml	DMSO	Yes
30mg PAA-MS diluted to 6ml	DMSO	Yes
60mg PAA-MS diluted to 6ml	DMSO	No

Discussion/Conclusion

This experiment demonstrated that up to 60mg of expandable PAA microspheres can be delivered at a concentration of 10mg/ml through a three French Renegade® microcatheter when the diluent is .3g/ml high sodium chloride solution. When DMSO was used as the diluent, only 30mg was deliverable. This may be evidence that the slight expansion observed in high salt solutions may aid delivery by allowing greater deformations.

The experiment also indicated that expanded PAA microspheres could not be passed through the three-French Renegade® catheter at the low concentration of 10mg in 6ml saline. Furthermore, 500-700 micron tris-acryl gelatin microspheres could not be delivered through the Renegade® microcatheter at the prepackaged concentrations of 1cc in 6ml saline. PVA particulate at a concentration of 1cc dry volume per 6ml saline could not be delivered through the Renegade microcatheter.

These results are in accordance with the hypothesis that unexpanded PAA microspheres that have an average diameter near 200 microns will pass through the 533 micron bore of the Renegade® catheter while when in their expanded state where their average diameter can approach 1000 microns, they will not be able to pass. It is not surprising that neither the 500 to 700 micron tris-acryl gelatin Embospheres® nor the PVA 500 micron average diameter particulate are able to pass through the 533 micron inner diameter of the Renegade® microcatheter. It was somewhat surprising that the PAA microsphere suspended in DMSO occluded the catheter at 10mg/ml concentration, but this result is in accordance with the theory that some deformability of the microspheres aids transport through small bore catheters by allowing facial diameter to contract.

Previous experiments have shown that PAA microspheres can occlude 1.5mm inner diameter Tygon tubing up to pressures of greater than 1000mmHg with as little as 20mg of PAA microspheres. Non-expandable PAA microspheres of up to 500mg loaded into a 1.5mm tube could not withstand nearly the same pressure in previous experiments. These experiments demonstrate that a significant occlusive load of expandable PAA microspheres can be delivered through the three French Boston Scientific Renegade® microcatheter when suspended in .3g sodium chloride per ml water or DMSO. This has

important implications for embolization procedures because a microcatheter on the order of the 500 micron ovarian anastomoses can be used to deliver an embolic close to the target site, beyond cervicovaginal branches, and the expansion after delivery should prevent the particulate from regurgitation or embolization to distal sites.

5.5 In-vivo Occlusion of Porcine Vasculature with PAA Microspheres

Background

Expandable PAA microspheres are potential intravascular embolic agents. The porcine renal and coronary vasculature will serve as model systems for investigating intravascular occlusion using PAA microspheres.

Purpose

Demonstrate the ability of PAA microspheres to occlude renal and coronary vasculature in-vivo. Identify effective concentrations of microsphere/DMSO solutions for realizing complete occlusion, as indicated by angiographic observation. Compare the occlusive capabilities of expandable and non-expandable PAA microspheres. Attempt to deliver microspheres in a DMSO:contrast cocktail prepared in a 7:3 ratio. Determine if this cocktail allows for angiographic visualization of the microspheres forming an in vivo occlusion.

Hypothesis

Highly concentrated solutions of PAA microspheres in DMSO will be effective at occluding both the renal and coronary vasculature in a porcine study. The DMSO will serve as a convenient medium for microsphere delivery due to its low viscosity and organic composition (PAA microspheres remain unexpanded prior to blood contact). Expandable microspheres will form more robust occlusion as compared to non expandable microspheres due to their high deformability and the resulting stabilizing pressure exerted on the vessel wall. Delivery of microspheres in a DMSO:contrast cocktail will provide visualization of the procedure but should not decrease inject-ability (partial expansion will not affect microsphere passage thru the catheter lumen due to the accompanied increase in deformability).

Materials and Methods

A variety of 5ml DMSO/microsphere and DMSO:contrast/microsphere solutions were made prior to the experiments (Table 5-8). All solutions were made by adding the indicated mass of PAA microspheres to 5 ml of the described solution in a 15 ml Falcon tube. All solutions were made 48 hours before administration. Porcine studies were conducted on three separate days.

Table 5-8: DMSO/microsphere solutions prepared for porcine in-vivo study

Solution #	MS #	Mass MS (mg)	Solvent	Vol. Solvent (ml)
1	E108302-12-1	500	DMSO	5
2	E108302-12-1	1000	DMSO	5
3	E108302-12-5	200	DMSO	5
4	E108302-12-5	2000	DMSO	5
5	E108302-12-5	1000	DMSO	5

Adult male pigs were used for all occlusion studies with PAA microsphere solutions. A 12 ml syringe was used to inject the prepared solutions through a 6F catheter. Prior to each attempted injection, the catheter was angiographically guided to the target location. The first 2 injections were delivered as prepared; the third was diluted with 3ml DMSO (Table 5-9).

Table 5-9: Summary of in-vivo porcine occlusion experiment. All injections resulted in total occlusion of the target vessel

Injection	Solution #	Dilution	Volume Delivered	Vessel/Organ	Chase(10ml)
1	3	none	4.5cc	R. Kidney/Renal artery	DMSO
2	1	none	5.0cc	L. Kidney/Superior branch of Renal Artery	DMSO:saline.9:1
3	5	3ml DMSO	6.0cc	Heart/Right Coronary Artery	DMSO:saline.9:1

Results

The targeted vasculature was easily located in all attempted injections. The low viscosity of the delivery mediums (DMSO or DMSO:contrast) facilitated easy passage through the catheter by the technician in all attempts. One problem noted with DMSO is the tendency to degrade the plastic syringes and stopcocks used in catheterization.

Fracture of stopcock valve by DMSO may be due to DMSO freezing at lower room temp (freezing point of DMSO ~ 18° Celsius). To prevent this, DMSO/contrast combinations can be used to lower the freezing temperature of the DMSO. Following the injection of microspheres, contrast medium was injected to angiographically determine if the target vessel had been occluded (diversion of contrast indicated vessel occlusion). PAA microspheres selectively occluded the left superior renal artery bifurcation (Figure 5-4). Gross histological sections show fully expanded PAA microspheres occluding the renal vasculature (Figure 5-5).

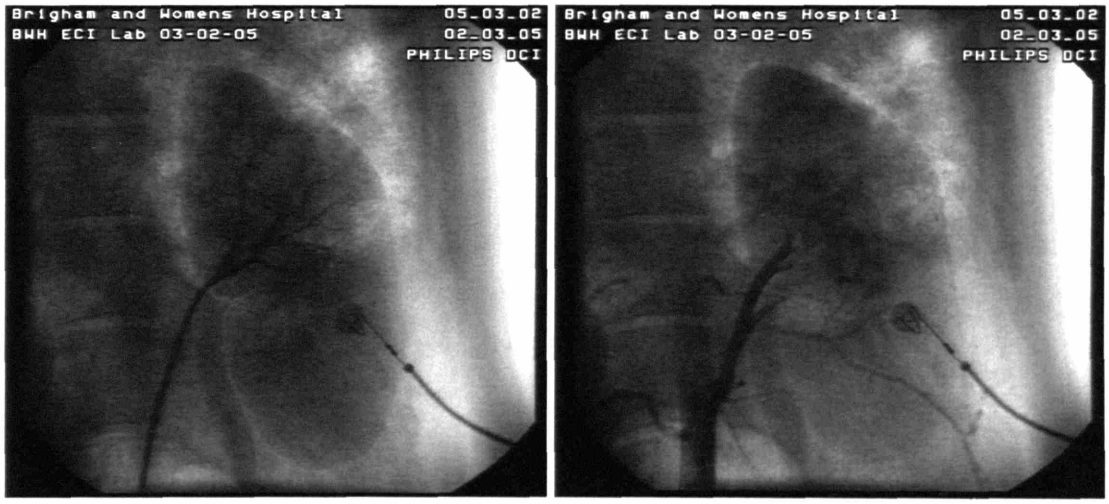

Figure 5-4: Left- Still image of patent left superior branch of the renal artery before embolization. Right- Still image of left superior branch of the renal artery after it has been successfully occluded by PAA microspheres

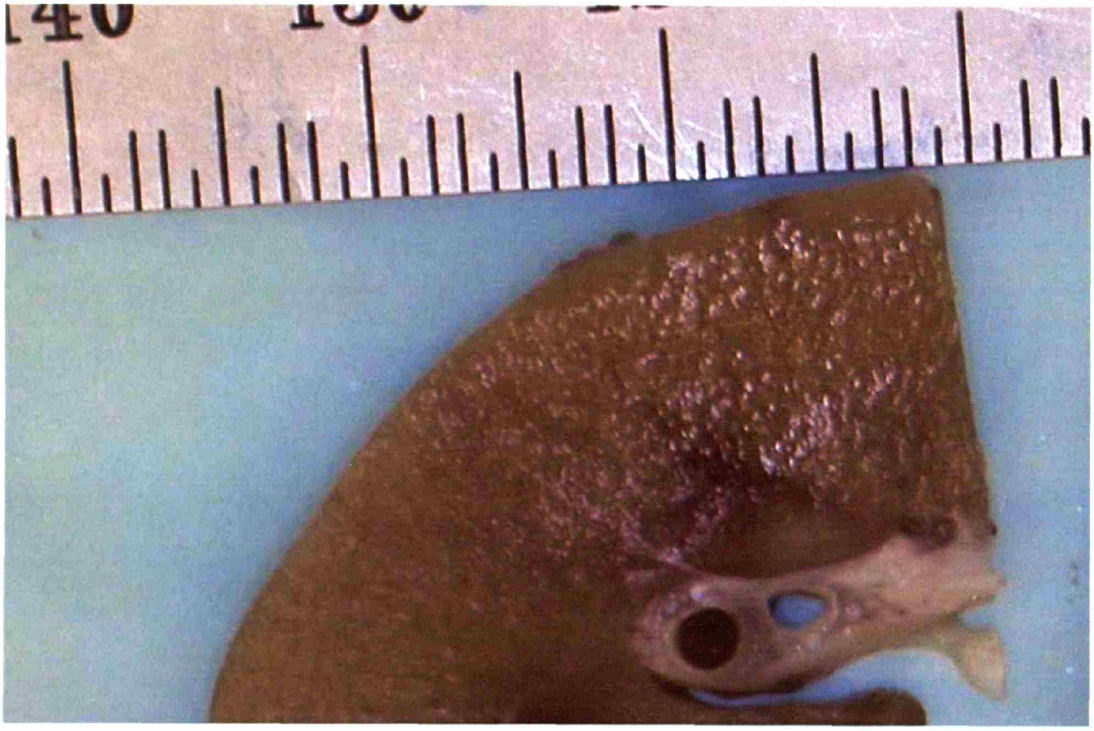

Figure 5-5: Superior Branch of L Kidney Renal Artery. Numerous microspheres are visible indicating that vessel was completely occluded (3/2/05).

Conclusion

Expandable/Deformable PAA microspheres can successfully occlude porcine renal vasculature. More work must be performed to optimize the concentrations and volumes of microspheres required for occlusion while limiting excess embolic delivery which may result in over-infarction or distal embolization.

5.6 Discussion/Conclusion

PAA microspheres can be injected in custom media that prevents expansion thereby allowing passage through both standard and micro-catheters without occluding the catheters. When the PAA microspheres enter the aqueous media within the blood stream, the 80 to 140 fold volumetric expansion can induce durable and lasting occlusions that will be less prone to disintegration, migration or recanalization than other occlusive technologies. The ability for PAA microspheres to traverse small-bore catheters that PVA particulate and tris-acryl gelatin microspheres cannot pass through is a significant advantage. The fact that these microspheres can also form occlusions that resist much greater pressures while requiring less embolic mass than other technologies is

even more impressive. This chapter also demonstrated proof of principle that PAA microspheres can selectively occlude both porcine renal and coronary vasculature in-vivo. Future work in this area will attempt to establish strong correlations between microsphere population statistics and occlusive properties both in-vitro and in-vivo.

Chapter 6: Thromboembolism

Abstract

Thromboembolism is the process where a blood clot dislodges from its site of origin and travels downstream where it eventually occludes a distal blood vessel. Clots that form thromboemboli can be large as in the case of deep venous thrombosis or they can be extremely small, such as the microemboli that form from during removal of large clots during interventional procedures. Previous investigators have used microspheres and microparticulate to simulate thromboembolism[3, 75]. Particle analysis of thromboembolism can give insight into relationship between thromboembolism and occlusive properties by correlating bulk and individual particulate properties with vessel occlusion. Model systems of microembolism can help determine what level of occlusion causes infarction and how anastomoses play a role. Studying synthetic thromboembolism may elucidate how the constituents of a thrombus contribute to distribution and occlusive properties.

The motivating hypothesis behind this work is that the constituents of a clot affect the size and shape distribution of particulate evolved during clot dissolution, the distribution and total volume directly relates to occlusive level within the vasculature, the occlusive level determines the amount of tissue infarction and the severity of tissue infarction and location of infarction determine patient outcome. This study begins the investigation of this process by modifying the system designed to study therapeutic embolism to study thromboembolism. A novel, ultrasonic clot dissolution device was used to break up both ex-vivo whole blood clots and synthetic fibrin only clots into clot dissolution byproducts that are analyzed in the RapidVUE® particle analysis system. Initial results show the average particle size for whole blood clots is less than 100 microns and synthetic clots produce significantly larger average emboli than whole blood clots, indicating that cellular components in the clot likely play an important role in limiting thromboembolic size.

6.1 Introduction

6.1.1 Background & Motivation

Vascular disease is the leading cause of mortality in the developing world [76]. Vessel stenosis and occlusion are often the culprits in life-threatening clinical syndromes such as angina, myocardial infarction, and pulmonary embolism among others. To treat the conditions the offending bolus is often removed either by surgical, mechanical or pharmacological means. However, over 80% of patients in a recent trial exhibit abnormal myocardial perfusion even when the offending occlusion appears to have been fully removed[77]. This situation has been dubbed the no-reflow phenomenon. One of the primary pathophysiological mechanisms of no-reflow is due to the presence of microembolic washout after interventional procedures[78].

Some of the interventional procedures designed to heal a patient often have embolic events with adverse and debilitating sequelae[79]. Procedures that remove clot burden from an occluded site can result in microembolic washout that can cause tissue damage even when macrovasculature appears patent on angiography[80]. For example, although microemboli can initially decrease flow through the coronary arteries of the heart, reactive hyperemia due to adenosine release from infarcted myocardium causes vasodilation of neighboring local vessels, resulting in normal or even elevated coronary blood flow[81]. Even though the superficial coronary flow is preserved, tolerance to ischaemia and regional contractile function decrease after microembolism[82, 83].

Almost any intravascular procedure will cause some microembolic evolution[84], but the impact of the microemboli depends crucially on several factors including but not limited to the type of vascular bed, the chemical compositions of the emboli, the size distribution of the emboli, the morphology of the emboli in addition to the total volume of emboli. For example, during deep vein thrombosis clot dissolution, large volumes of particulate may be produced because the size of the originating clot is rather large (several cubic centimeters), but the concern for microembolic damage is minor because emboli travel to the pulmonary vasculature where there is ample circulatory reserve to handle microvascular occlusion. On the other hand, even minute volumes of microemboli evolved from carotid or coronary stenting procedures could result in stroke

or myocardial infarction respectively. Some even theorize that microemboli can form spontaneously due to inflammatory processes and may be the causative agent in some forms of chronic heart failure[85, 86].

Microemboli can have many sources including air, fat, bone, necrotic debris and thrombus. Thromboemboli are likely the most prevalent form that cause disease and can be the most insidious of emboli because their source is from within the blood itself and emboli can be as small as a single nidus of activated thrombin to as large as saddle emboli or disseminated intravascular coagulation[2]. To understand the vascular complications caused by these microemboli, the nature of their composition and evolution must first be addressed.

Microemboli in the body are usually derived from breakdown of previously formed thrombus or formation of micro-thrombi within circulation. According to Virchow's triad, stasis, vascular injury and hypercoagulability are the three primary sources for thrombus formation in the body[1]. The unifying theme of this well know triad is that all three seemingly independent causes result in an imbalance between activation of thrombin and the subsequent polymerization of fibrin and the inactivation of thrombin and breakdown of fibrin polymer by natural thrombolytic mechanisms[87].

In the coronary circulation, the aforementioned no-reflow phenomenon has become of increasing interest as coronary stenting procedures become more common. Several flow scales and methodologies have been developed to quantify and characterize the amount of perfusion in the microvasculature following interventional procedures. The thrombolysis in myocardial infarction (TIMI) frame rate and Myocardial blush grade are two systems designed to gauge occlusion within the microvasculature[78]. These systems rely on the clearance of contrast from the tissue to measure the amount of occlusion in the microvasculature. Post-mortem histology has verified evidence of microembolic occlusion that correlates well with poor TIMI frame counts and poor Myocardial blush grades[78, 88].

Several treatments for microembolization have been attempted over the years with varying levels of success. Pharmacological dissolution of clot using drugs such as tissue plasminogen activator, works in some cases but not in others. When medical treatment alone does not work or is contraindicated because of hemorrhage risk, mechanical clot

dissolution has been used with some success[89]. These means are limited because microemboli penetrate deep into tissue where mechanical access is impossible and flow is limited such that pharmacological measures cannot convect to the sight of occlusion. Embolic protection devices were introduced as a possible solution for preventing microemboli from traveling downstream[90]. However, these devices remain controversial and have not been definitively shown to demonstrate a benefit to the patient[91]. Although embolic protection devices exist that demonstrate capture of microembolic material[65, 66, 92], most have significant design loop-holes that allow potentially harmful emboli to escape capture.

Because the evidence to date has been inconclusive, cardiologists have been reluctant to adopt the technology[78]. This presents a problem for the medical community that has not been properly addressed- over 80% of patients have flow abnormalities after coronary interventions yet there has been no preventative measure that works consistently, nor is there an understanding of which lesions are likely to result in microembolism and which ones will be in the small fraction that do not. Scant knowledge exists regarding the size, morphology, occlusive ability, and amount of embolic material evolved during various intravascular procedures. Furthermore, the precise amount of occlusion that can be tolerated by various vascular beds such as the heart, brain or ovaries remains elusive.

The system developed in this thesis to study the material properties, in-vitro function and in-vivo impact of therapeutic micro-emboli is ideally suited for studying aberrant natural microemboli that often result in tissue infarction and even death. This system can be used to study microemboli collected in-vivo or microemboli created ex-vivo. By applying the same rigorous and quantitative approach used to characterize therapeutic micro-emboli, a significant amount of new information can be discovered about harmful microemboli. Using a system designed to study synthetic micro-emboli for characterizing biological microemboli represents a complementary approach to the origins of synthetic microembolic research as a model for thromboembolism[3, 75]- in effect, the research as returned full circle to close the loop of investigation between synthetic and natural microemboli.

6.2 Objectives

The primary objective of these experiments was to design an in-vitro system for creating microemboli secondary to clot dissolution and to adapt the techniques developed to study therapeutic microembolism to the study of pathological microembolism. A secondary objective of these studies was to investigate the effects of clot constituents on clot dissolution embolic properties and distributions.

6.3 Theory & Hypothesis

The Clotting Cascade

The blood clotting cascade is an essential biological process that is necessary to prevent exsanguination after even the smallest trauma. The components of the clotting cascade are all found within the blood and many of them are produced by the liver. The clotting cascade can be activated by several different mechanisms as discussed previously, but the common end result is that the inactivated clotting factor prothrombin is converted to the active serine protease, thrombin. Thrombin is the primary enzymatic determinant and rate-limiting enzyme of the clotting cascade. It converts the blood plasma zymogen[3] fibrinogen into fibrin I and fibrin II monomers which rapidly and spontaneously polymerize to form a thrombus[87]. Thrombin also acts to activate another plasma protein, Factor XIII, which when activated acts as a cross-linking agent for the fibrin polymer. Factor XIII greatly increases the stability and strength of the forming thrombus.

While thrombus is forming, cellular components within the blood such as red blood cells, white blood cells and platelets become trapped within the fibrin polymer matrix as it is forming. Platelets can strengthen the thrombus because they bind to each other strongly. However, red blood cells and white blood cells do not enhance the strength of the thrombus and may actually be a vulnerability of its ultra-structure because the cellular components are fragile relative to the strong and stable fibrous quality of the fibrin polymer backbone in the thrombus.

[3] A zymogen is an inactivated precursor form of an enzymatic protein that can be activated by an enzymatic reaction or conformational change induced by another enzyme or some other environmental process

Clot dissolution

The blood system has natural methods to breakdown clots that form within circulation. The primary enzyme that breaks down fibrin clot is called plasmin and it is formed from the inactive zymogen, plasminogen. Tissue plasminogen activator and Urokinase are natural activators of plasminogen that are released within the body and act to keep the circulation free of thrombus. Anti-plasmin is a natural inhibitor of plasmin that rapidly degrades plasmin almost as soon as it is created from plasminogen. Because of this, plasmin activity is localized. It is competition between plasmin activity and thrombin activity that mediates whether fibrin will form a thrombus or not.

Most of the time a thrombus is formed as a protective measure and is beneficial; however, some thrombus formation is pathological. When a pathologic thrombus forms and the body is unable to break it down using natural means, intervention by a clinician may be the only way to prevent the thrombus from causing further damage and possibly even death. There are two primary classes of clot dissolution: pharmacological, and interventional. As mentioned in the introduction, pharmacological treatment with plasminogen activators may not always work and sometimes it is contraindicated because it can induce hemorrhage. In these cases interventions such as mechanical dissolution or surgery may be the only remaining options. Because surgery can be life threatening, especially in the older population, interest in mechanical dissolution by interventional means has grown into a burgeoning field. However, mechanical clot dissolution can create a wide range of particulate sizes depending upon method and conditions. Little is known about the total amount of emboli generated, the size distributions or the shapes of the emboli generated from mechanical dissolution. Furthermore, it is not known what impact the constituents of the clot have on dissolution.

In these experiments we used a novel device developed by Omnisonics ™ Corporation to generate clot dissolution byproducts. The Omnisonics™ Resolution® device is thin titanium wire that has a low-amplitude, ultrasonic frequency (20kHz) standing wave pattern generated along its length. The tip of the wire is loaded with tantalum and acts as a node of the standing wave. The theory behind the activity of the device is that shock-waves generated in the fluid around the anti-nodes of the wire, possibly from cavitation due to the high velocity of the wire, induce a high-frequency

impulsive force on rigid structures within the clot, causing them to disintegrate. The system is liquid cooled by the blood that surrounds the wire and a saline pump ensures that the interior of the introduction catheter for the wire remains lubricated.

Hypothesis

The ultrasonic waves generated on the Resolution® clot dissolution wire are low amplitude which limits the strains that can be developed when using such a device. Only relatively brittle materials that fail at low strains or under fatigue will be susceptible to such a device[93]. We posited that clots of different constituents would respond to ultrasonic clot dissolution differently depending upon the constituents. Our hypothesis was that cellular components such as red blood cells, white blood cells, and platelets would make in-vivo clots more susceptible to failure than the cross-linked fibrin polymer. The theory behind this postulate is that cellular components, with fragile cell walls, can rupture under high frequency, high impulse shock waves while fibrin polymer would be resistant to failure because it is a tough, well-hydrated, fibrous polymer with crosslinking. However, if the fibrin polymer were to fail it would likely fail at specific areas of weak crosslinking or at geometrically susceptible areas. The interstitial areas left after cellular components ruptured would result in geometrically weak areas with high stress concentrations within thrombus and therefore, the remaining fibrin matrix of a whole blood clot would disintegrate more readily than a solid fibrin clot and into smaller fragments due to the isolated islands of fibrin polymer between cellular components.

6.4 Materials and Methods

Two formulations of clots were studied, whole blood clots created from animal blood draws and synthetic clots synthesized from isolated and recombinant blood products. Whole blood clots were used to simulate clots that form in-situ, while the synthetic clots were utilized to investigate the dissolution of clots with no cellular components- i.e. pure crosslinked fibrin polymer. The clots were exposed to the active Omnisonics™ device and the particulate was analyzed in the RapidVUE® particle analyzer.

Clot construction

Ex-Vivo Whole blood clots

Blood was collected from adult male pigs. The pigs were not treated with heparin or any other anti-coagulants prior to phlebotomy. The blood was stored in sterile, untreated 15ml falcon tubes at room temperature for approximately 30 days to allow for curing of the fibrin polymer and hardening of the clot to simulate long-term indwelling clots such as those found in deep venous thrombosis. Because these clots were made from whole blood, they contain fibrinogen, thrombin, Factor XIII, plasminogen, all other plasma proteins, platelets, red blood cells, white blood cells, calcium,, antibodies, buffers, sodium, etc.

Synthetic blood clots

One ml synthetic clots were made using a protocol established previously in the literature.[94] The final concentrations of the constituents of each clot were as follows: 3 mg/ml fibrinogen, human plasma, plasminogen depleted (Calbiochem part # 341578) 6 Units/ml thrombin, citrate free, human plasma (Calbiochem part # 605206) 0.27 Units/ml Coagulation Factor XIII (Calbiochem part # 233501) and 40 mM CaCl2.

The materials are all pre-warmed in an incubator at 37° C for 15minutes prior to use and for 30 minutes after all materials were combined. Because fibrin polymerization is Calcium dependent, the initial fibrinogen was reconstituted in deionized water. Factor XIII was also reconstituted with the water and fibrinogen because Factor XIII has no effect on fibrinogen, nor can it have any effect on fibrin until it is activated by Thrombin. Thrombin was reconstituted with Calcium Chloride because Calcium has no effect on Thrombin by itself. Solutions were combined using a Duoflow dual syringe system (Hemaedics, Inc) designed to ensure equal mixing of both solutions. The Duoflow system was setup to deliver the materials in to a falcon tube identical to the tubes used to store the ex-vivo clots made from pig blood.

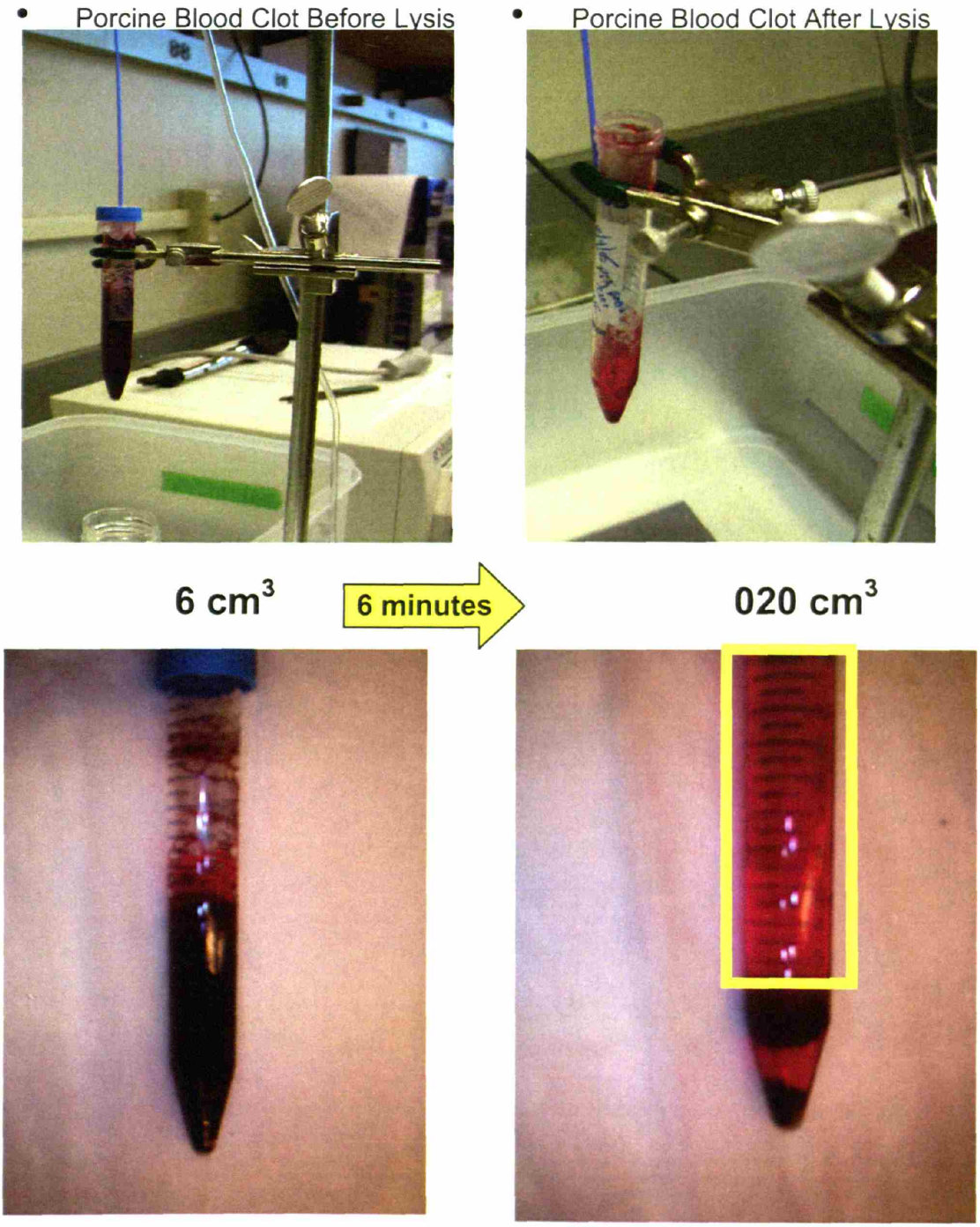

Figure 6-1: The images on the left shows a porcine clot before lysis, images at right show a clot after using the Omnisonics Resolution® system after six minutes.

Debris and liquid was poured out of the tube and analyzed. There was very little clot left in the tube and only a residue remained adherent to the walls of the tube. Because the tip of the Omnisonics device is not active some clot invariably remains in the location where the tip was located.

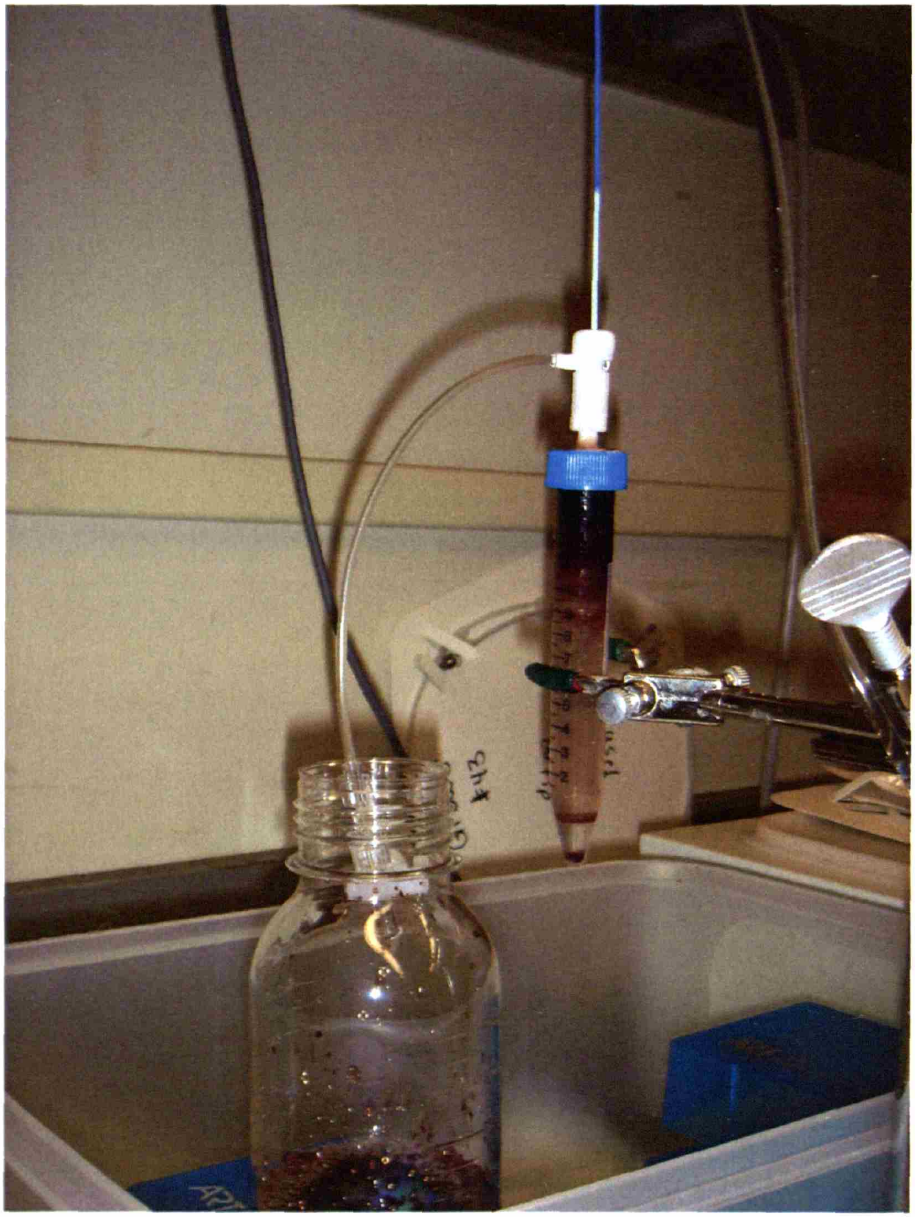

Figure 6-2: Modified system for total collection of debris and elimination of the problem associated with the inactive tip.

Clots for this configuration were made inverted so that no area of the clot was in the inactive region of the wire. The catheter port at the top of the device was used to introduce the catheter into the tube and the tube coming out the side allows for drainage of overflow from the water pumped through the catheter to cool the titanium wire.

Particle Analysis

Particulate was collected and diluted to 75ml samples from each clot and analyzed using the Beckman-Coulter™ RapidVUE® System. The settings specific for thrombus particulate were taken from the literature[65, 66] (Table 6-1). Unlike the settings for microsphere analysis, spherical objects are set for rejection so that bubbles are not counted. The output from the RapidVUE® software gives a table of least bound rectangular lengths for each particle detected. (Appendix A has a sample output file from an analysis of microspheres. See the Particle Analyzer chapter for a detailed description of the Beckman-Coulter™ RapidVUE®.)

Table 6-1: System settings for analyzing thromboembolic particulate

PARAMETERS	
* Focus rejection	On
* Border rejection	On
Edge correction	Off
* Repetition rejection	On
Fiber overlap rejection	Off
* Shape rejection	On
Background intensity rejection	Off
Background subtraction	Off
Area correction	Off
Shape rejection criteria	Sphericity > 0.90
Focus parameter	2256
Minimum particle area	4
Micron/pixel ratio	7.292
Maximum particle area	5000000
Threshold	Adaptive: 56
Magnification	2.74
Image size (microns)	4521 x 3354
Maximum edge correction factor	1.2
Shape model	Cylindrical

6.5 Results

Three different clots from the same animal were all exposed to the Omnisonics device for the same amount of time and the same procedure was followed for analyzing all three samples. The results show that there is no statistical difference between the means of each distribution and the distributions overlap considerably indicating that the system was reproducible (**Figure 6-3** and **Table 6-2**). A logistic curve was used to model

these distributions instead of a Normal distribution based upon log-likelihood calculations in Matlab. The deviation from Normal distribution results from the fact that particulate cannot be smaller than zero in size so outliers are truncated on the negative direction from the mean. The machine is also less accurate at the lower end of the size spectrum and tends to pick up more noise from the background. There may be an additional spike at the lower end of the spectrum due to debris created by lysis of cells and platelets that generates many small particles. The right skew of the distribution may be from particulate aggregation and outliers introduced by gross manipulation of the catheter. The underlying particulate distribution may approach a Gaussian based upon the central limit theorem which states that the sum of independent identically distributed random variables approaches a Gaussian distribution[67].

The clot debris collected off of filtered samples from the clot dissolution experiments are all approximately the same total volume and total particulate count (Table 6-3). The maximum particle size indicates the outliers present. Although not identical, the order of magnitude is reasonable considering all of the variables in a biological system. The maximum particle size range for particulate from synthetic clots is significantly higher than that of whole blood clots(Table 6-4). The control experiment with no power shows that the large maximum particulate sizes are related to the power delivery of the device and not to introduction of the catheter into the clot alone. Repeat experiments demonstrated the same pattern.

Results from whole blood clot dissolution versus a synthetic blood clot dissolution after exposure to the Omnisonics Resolution® System under identical treatments show that the distributions were both right skewed and most closely resembled Gamma distributions (Figure 6-4). As mentioned before, the rightward skew is partially due to aggregation of particles and is also due to the fact that particles cannot be less than zero diameter. The data clearly indicate that the synthetic clot distribution has a higher mean, a greater standard deviation and has much larger maximum sizes for particulate.

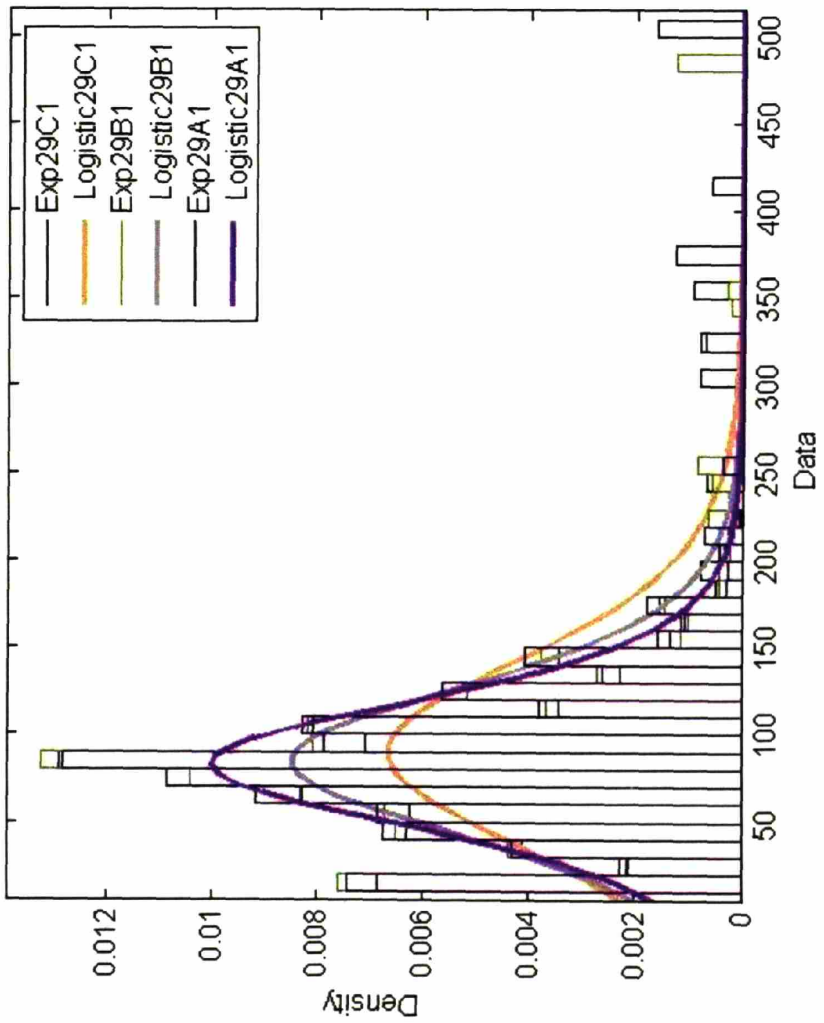

Figure 6-3: Particle counts from three different clots from the same animal that were all exposed to the Omnisonics device.

29A1	Length	Std. Error
mean	**83.0um**	0.4
sigma	**25.0um**	0.2
29B1		Std. Error
mean	**84.7um**	0.5
sigma	**29.5um**	0.3
29C1		Std. Error
mean	**89.8um**	0.6
sigma	**37.5um**	0.3

Table 6-2: Averages and standard deviations for three clots from the same animal that were all treated identically with the Omnisonics ultrasonic clot dissolution device.

Name	Total Count	Total Volume (cu mm)	Max. particle size range (um)
Filtered Clot 30A	182110	4.4	301-350
Filtered Clot 30B	182976	4.3	551-600
Filtered Clot 30C	175806	4.3	301-350

Table 6-3: Statistics for 36 Day old Porcine Blood clots in Falcon tubing

SYNTHETIC CLOTS	Clot type	Max Particle size range
Filtered Clot E	Synthetic	1301-1350
Filtered Clot F	Synthetic, Tubing,. Filter Paper put on bottom of tubing	1000-1050
Filtered Clot CONTROL G	Synthetic, Control as in no power	401-450

Table 6-4: Table of Synthetic clot dissolution data

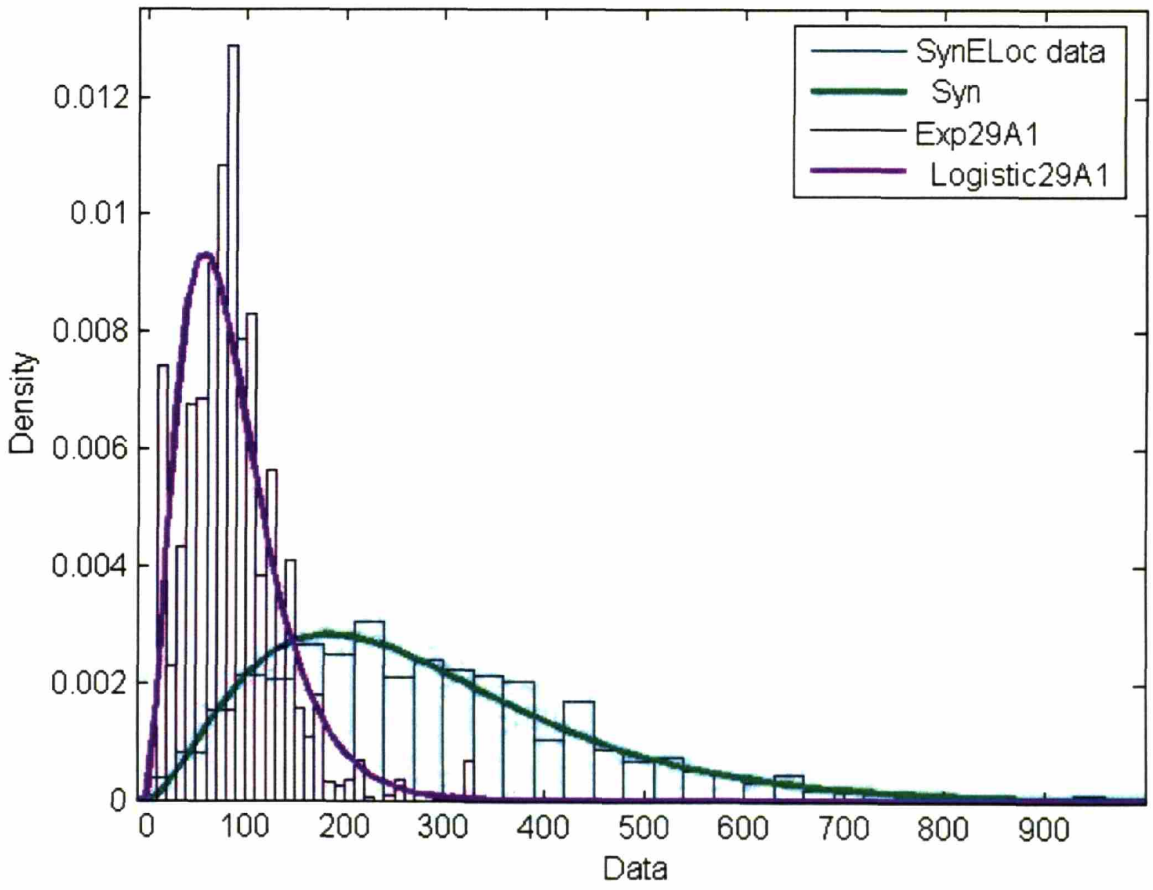

Figure 6-4: Whole blood Clot vs. Synthetic Clot probability Density curves with Gamma fits

6.6 Discussion/Conclusion

These preliminary studies of clot dissolution byproducts indicate that the system developed can generate reproducible results. The particulate generated from use of the Resolution® system on whole clots tends to average slightly less than 100 microns in least bounded rectangular length with a standard deviation around 30%. The distributions tend to be right skewed with outliers ranging on the order of between 300 and 600 microns in least bounded rectangular length. The significance of these numbers is not understood at this time[65, 66]. It has not been determined what is more detrimental: many particles that are small in diameter or fewer particles that have larger dimensions.

Synthetic clots treated with the Omnisonics device tended to generate distributions with higher means near 250 microns and larger standard deviations. The distributions for synthetic clots were most notable to be even further right skewed, with outliers far in excess of 1mm in least bounded length. This result is in agreement with the hypothesis posited previously. This means that clots with higher fibrin content are likely to generate larger particulate they are treated with this device. Clots that are found in arterial beds with lines of Zahn from platelet deposition have less red blood cell content than stasis clots formed in venous circulation[1] and would likely respond differently to the Omnisonics device. Studies must be performed with platelet only clots to see how a lack of red blood cells may affect clot dissolution.

It may seem intuitive to prefer smaller clot dissolution particulate; this is not necessarily valid in all circumstances. Large particulate can become lodged in vascular beds at locations where there is ample collateral circulation from neighboring arteries and little effect on the terminal vascular bed will occur. However, if that same volume of particulate were minced into smaller pieces and embolized downstream, the microcirculation could be cut off beyond where collateral circulation can supply a backup blood supply[95]. Future experiments correlating in-vivo results with particulate distributions and total volumes will be needed.

Chapter 7: Conclusion and Future Work

7.1 Thesis Summary and Accomplishments

This thesis work has established a comprehensive system for quantitatively analyzing the form and function of microembolic particulate. The experiments outlined in this document have established methods for testing the functionality of PAA microspheres both in-vitro and in-vivo. Advanced techniques including optical particle analysis, imaging, material characterization, size and morphological characterization, sieving, biocompatibility testing, custom flow systems and functional occlusion testing have been adapted and calibrated to reveal a wealth of information regarding microembolic particles.

The characteristics of novel expandable/deformable PAA microspheres were a focal point of the work. Based on results from this study, PAA microspheres may be able to produce more controlled occlusions in-vivo than have been previously attainable. The have been many notable results from the PAA investigation. Surface properties of PAA-MS were modified to prevent fragmentation. Microspheres were stained with cationic Acridine Orange to enable visualization. Microspheres were sieved into predictable probability distributions and analytical characterized into probability distributions. The expansion properties of PAA microspheres were quantified in various media including blood. Basic biocompatibility and chemical stability of PAA microspheres was demonstrated. Suitable delivery media of low viscosity and that prevent expansion were identified in addition to concentrations appropriate to deliver through large and small bore catheters. Substantial occlusive resistance to pressure with PAA microspheres when compared to other embolic materials was demonstrated. Finally, in-vivo occlusion of renal vasculature using PAA microspheres was demonstrated.

The techniques used to study therapeutic embolism were extended to investigate thromboembolism. The particulate size distributions of both whole blood clot dissolution byproducts and synthesized pure fibrin clot dissolution byproducts were compared and it was found that the cellular components of whole blood clots may contribute to smaller embolic size distributions. This result has implications for the use of mechanical clot

dissolution in arterial versus venous beds as the different cellular content of the clots will likely result in different particulate distributions.

7.2 Discussion

Whenever a clinician introduces microembolic particles into the body for therapeutic purposes, there is a finite probability that the emboli may track to an unintended location, possibly inducing infarction in a vital organ. The study of how thromboemobli infarct tissue has direct implications to the study of therapeutic embolism as well. These two areas of study are naturally associated and the techniques to investigate one process are equally applicable to the other. Previous to this work there was no systematic and quantitative approach to investigate microembolic phenomenon. Most studies were simple trial and error in large animal models or even human clinical trials. This work has established a system to study microembolic phenomenon in a quantitative and reproducible fashion. By furthering the investigation of how to make therapeutic embolism more effective at infracting tumor and causing microvascular occlusion, a wealth of knowledge can be learned about how to deal with thromboembolism. Similarly, investigations that show how thromboembolism impacts microvascular beds will help further the study of controlled therapeutic embolism.

7.3 Future Work

7.3.1 Further in-vitro characterization

Although much has been learned from the experiments presented in this work, with every answer many more questions have arisen. Experiments that precisely identify the correlations between distributions and occlusion must be developed. More microembolic materials variations must be studied. The following subsections identify some possible improvements upon microembolic technology.

7.3.2 Material-based improvements of PAA embolics

Further increase the continuity of the microsphere surface

Hypothesis: by increasing the continuity of the microsphere surface, the microspheres should be able to resist shear stress better so that fragmentation can be

completely avoided. This is important because fragmentation reduces embolic potential and could result in adverse biological events.

Foreseen undesirable side-effects: increasing the continuity of the capsule may strengthen the microsphere too much. It also may limit the ability for water to hydrate the spheres. These factors may result in spheres that do not expand as much as the original iterations. We would like to reduce fragmentation as much as possible without sacrificing the expandability of the spheres.

Proposed initial experiments: retest the new spheres for fragmentation and expansion. Test for occlusion ability and dye adherence. If they are superior to previous spheres use them in animal studies of occlusion

Increase the size of microspheres

Hypothesis: Larger microspheres will be able to occlude larger vessel beds and should be able to encapsulate more drug for drug delivery applications.

Foreseen undesirable side-effects: Large microspheres may be difficult to deliver and may lose physical integrity.

Proposed initial experiments: Repeat in-vitro material characterization on large spheres. Test their occlusion capabilities in tubing within static and under flow conditions. Test the larger spheres in-vivo.

Colored microspheres to improve imaging and particle analysis

Hypothesis: Currently we dye the spheres with cationic dye. The dye may interfere with charged drugs or adsorbed proteins. If the spheres could have color built-in it would decrease possible artifact due to the cationic dying process

Foreseen undesirable side-effects: built-in dye may alter polymer structure and could affect hydrogel performance

Proposed initial experiments: validate that microsphere properties are not altered and that dye is sufficient for particle analysis

Microspheres featuring an additional surface coating to promote delayed expansion

Hypothesis: Dayed expansion could allow for a more robust occlusion to form because microspheres that are loosely aggregated in small vessels will expand and

provide radial force on the occluded artery. The delay will also allow the spheres to travel downstream to smaller vessel beds prior to expansion and subsequent occlusion. It would be preferable if the delay could be modulated for different applications. A soluble coating such as a polysaccharide that could have varying thickness may allow for modulated delay of expansion.

Foreseen undesirable side-effects: Coating process may alter microsphere integrity

Proposed initial experiments: correlate coating thickness to delay amount. Characterize occlusion strength of new spheres vs. old spheres.

7.3.3 Biologically-inspired PAA Microsphere augmentation

Encapsulate FITC labeled dextrans and albumin for drug delivery studies

Hypothesis: PAA microspheres may be able to encapsulate drugs. Because of the porous nature of the capsule, diffusion should occur through the capsule. When the microspheres expand and the capsule is stretched the size of the pores should increase and allow for greater transport. There are many factors that must be explored regarding encapsulation of various species within microspheres: Does charge affect retention- i.e. positively charged dextrans may be retained more than negatively charged dextrans within the negatively charged microsphere interior. Hydrophilic drugs may be encapsulated easily, hydrophobic drugs may not be retained well within microspheres and may elute into delivery medium. How does molecular weight affect transport- large molecules may retain better in unexpanded spheres vs. expanded while small molecules may not differ in transport.

Foreseen undesirable side-effects: There may not be enough space within the microsphere to accommodate therapeutic doses of candidate drugs. Manufacturing process may denature proteins or damage dextrans.

Proposed initial experiments: First create microspheres with varying species encapsulated. Test for transport in expanded state and quantify delivered dose. Dextrans/albumin may not stay within spheres when suspended within delivery medium so tests should be designed for elution in delivery medium. Delivery

medium may alter dextrans/albumin so tests for molecular stability must be performed

Spheres coated with active biologicals: i.e. fibrinogen

Hypothesis: Microsphere efficacy may be increased by coating with biologically active substances. For example, coating with fibrinogen will promote platelet adhesion and will enhance clot formation around the occlusion formed by the microspheres. Platelet to platelet binding via GP IIIa/IIb may act to promote microsphere aggregation and inhibition of GP IIIa/IIb should lessen this enhanced effect.

Foreseen undesirable side-effects: Proteins may not adsorb well to smooth microsphere surface. Fibrinogen may promote too much clotting.

Proposed initial experiments: Perform an in-vivo study of clot formation with and without fibrinogen coating. Repeat previous studies on modified spheres. Inhibit GPIIIa/IIb in whole blood and rate microsphere aggregation.

Anti-Occlusion	Pro-Occlusion	Anti-Tumor
TPA/Urokinase/StreptoKinase/Tenecteplase	Theophylline	Paclitaxol
Plasmin/Plasminogen	Thrombin	Rapamycin
GP IIB/IIIA inhibitors	Fibrinogen	
Verapamil/nicorandil/Nitroglycerin	ADP/PAF	
Heparin		
Coumadin		
Adenosine		

Table 7-1 Table of drugs and proteins that will be used to modify microparticulate.

Anti-occlusion drugs/proteins are used to mitigate the effect of micro-particulate washout after interventions while pro-occlusion drugs/proteins are used synergistically to increase the efficacy of embolic therapy. Anti-tumor drugs may also be implemented in conjunction with vessel occlusion to further enhance tumor destruction.

7.3.4 In-vivo experiments and correlation

The most important subsequent step to in-vitro characterization is to bridge the gap to in-vivo relevancy. Although proof of principle has been demonstrated in-vivo; safety, efficacy, and superiority of PAA microspheres must be shown in long-term animal models. By studying the precise histopathological effects of microvascular occlusion, much can be learned about the nature of infarction caused my microemboli of all types.

This knowledge can be extended into modifying and directing therapies designed to prevent unwanted microembolism secondary to intravascular treatments.

7.3.5 Computer modeling of microvascular networks

A theoretical model of microvascular occlusion would allow repeated experiments on an identical, virtual vascular bed. This would be the ideal "gedanken" or thought experiment model system because it would eliminate the vast noise and heterogeneity inherent to in-vivo systems. This section outlines the construction of a computer model based upon a combination of results from this thesis and detailed microvascular anatomy data available in the literature. This model could potentially shed light upon many questions that would be much more difficult if not impossible to answer using in-vivo tests.

Using morphometric data obtained from the investigation of microparticulate and occlusion correlates, combined with vascular tree models from the literature[96-104], a lumped parameter model of microvasculature tailored to study microembolic occlusions will be constructed. The model will include tissue elements that will emulate diffusion and partitioning of oxygen and other nutrients. Tissue oxygen tension will be calculated as a percentage of initial oxygen tension determined from the pre-embolism state. Tissue infarction will be correlated with in-vivo models of controlled microembolization in the porcine heart to calibrate the oxygen tension percentage threshold for infarction. The model will monitor oxygen tension and will simulate reactive hyperemia by reducing resistance in nearby vessels once oxygen tension drops below an experimentally validated threshold. Vessels closest to the infarction will dilate most with transport limited dilation of more distal vessels. Flow, pressure and oxygen tensions will then be recalculated and hence a feedback loop will be established between tissue perfusion alterations and flow alterations. Once flow reaches levels in accordance with the reactive hyperemia condition[49] or neighboring vessels become maximally dilated within physiologic limits the feedback loop will be halted and steady state will ensue.

Emboli will be modeled by removing resistors from the connectivity matrix of the model at the vascular tree level that correlate with where that type of embolic load appears in histological specimens after in-vivo embolization. Total embolic volume will be matched to in-vitro and in-vivo data that indicate volumes required for occlusion.

Occlusions will be positioned stochastically and will be more likely to occur where more flow has been delivered. Pressures will be calculated throughout the network and occlusion will not be allowed to occur if pressure drops are too high based on in-vitro data of occlusion. Once the model has been calibrated using physiological parameters, flow alterations can be studied to determine optimum occlusion levels for tissue death as well as maximum allowable occlusion level for adequate tissue survival. Mittal et al.[104], outlines the explanation of major assumptions regarding linear resistive modeling of the vasculature. The model will be based on the Mittal & Kassab model and will add in the assumption of Fick's law of oxygen diffusion into tissue elements while interstitial oxygen concentration will be ignored. As the model is constructed more assumptions will be incorporated and justified. Matlab and C++ will be used for implementation of this model. The development of a computer model based upon microembolic data will allow a reproducible, high-throughput method for analyzing the impact of microembolism on vascular beds as well as providing a theoretical framework for assessing embolic protection/prevention strategies.

By implementing in-vitro, in-vivo, and computational model systems with cross-validation, a framework for elucidating the intricacies of microembolic mechanics will be established. Results of this study should contribute to the design and implementation of improved embolic protection devices as well as optimal protocols for therapeutic embolism.

7.4 Thesis Web

The Thesis web (Figure 7-1) outlines the interconnection of the work presented in this thesis with work in the literature and planned future work. The central theme of this research is the understanding of intravascular occlusion at the microvascular level.

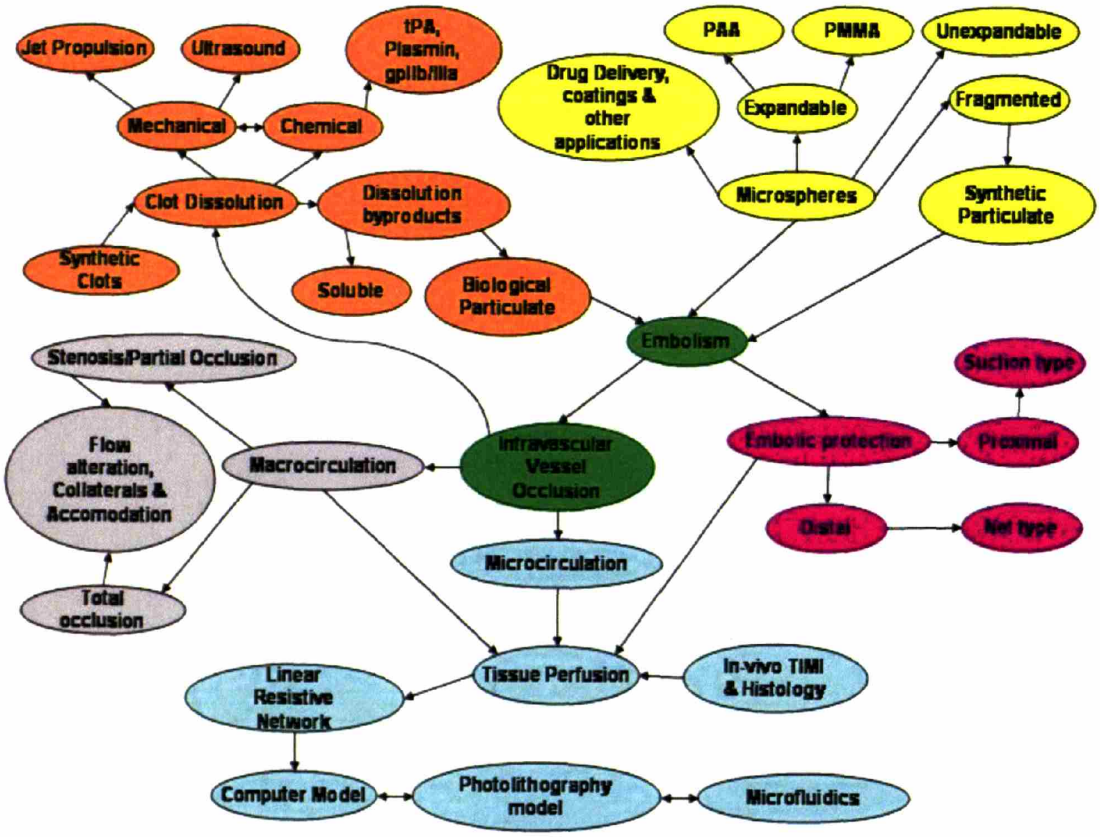

Figure 7-1: Thesis web and flow matrix of research and future work

Key: Green- Central focus of research is on microembolism and how it relates to intravascular occlusion. Orange- Biologic emboli generation Yellow- Synthetic polymer emboli generation. Gray- relation to work done in the literature and elsewhere. Cyan- future work will develop theory of microvascular occlusion using in-vitro and in-vivo data to develop computer simulations and model systems of microvascular occlusion and infarction. Purple- purpose of this work is to help understand the source and consequences of microemboli so that preventative measures can be intelligently engineered.

Appendices

Appendix A: RapidVUE® Output file

Below is an example of a text output from the RapidVUE® software a produced from one of the three runs of an analysis of one sample of microspheres in suspension.

```
SIXTY1
RapidVUE® 2.03
C:\PROGRAM FILES\RAPIDVUE®\DATA\SIXTY1.DAT

18 Jan 2005  11:55 AM
"",""
"",""
"",""
"",""
"",""
"",""
"",""
"",""
"",""
"",""
"",""

SAMPLE ANALYSIS SUMMARY (sizes in microns)

EQUIVALENT CIRCULAR AREA DIAMETER
"Count",76
"Minimum",80.6
"Maximum",1131.4
"D1,0",660.4
"D3,2",784.7
"D4,3",824.3
"Geometric volume std. dev.",0.205
Number percentiles:
"10%",442.2
"25%",528.5
"50%",680.3
"75%",827.2
"90%",941.9
Area percentiles:
"10%",560.6
"25%",671.1
"50%",797.4
"75%",928.2
"90%",1003.5
Volume percentiles:
"10%",585.3
"25%",724.3
"50%",849.4
"75%",947.3
"90%",1044.9
"Total volume (cu mm)",1.56E+01
```

```
SPHERICITY
"Count",76
"Minimum",0.93
"Maximum",1.00
Number percentiles:
"10%",0.94
"25%",0.95
"50%",0.96
"75%",0.98
"90%",0.98

PERFORMANCE SUMMARY
"In-focus count",76
"Video frames",2768
"Run time (sec)",101
"Focus reject %",1.4
"Shape reject %",44.7
"Border reject",144
"Fiber overlap reject %",0.0
"Contrast",0.00
"Background intensity",144
"Micron/pixel ratio",7.292
"Magnification",2.74
"Image size (microns)","4521 x 3354"

PARAMETERS
*   Focus rejection
*   Border rejection
    Edge correction
*   Repetition rejection
    Fiber overlap rejection
*   Shape rejection
    Background intensity rejection
    Background subtraction
    Area correction
"Horizontal indents","10, 10"
"Shape rejection criteria","Sphericity < 0.90"
"Vertical indents","10, 10"
"Focus parameter",500
"Minimum particle area",4
"Micron/pixel ratio",7.292
"Maximum particle area",5000000
"Background rejection limits","180, 255"
"Threshold","Adaptive: 56"
"Maximum edge correction factor",1.2
"Shape model","Cylindrical"

EQUIVALENT CIRCULAR AREA DIAMETER TABLE

DIAMETER,,COUNT,% NUMBER,% AREA,% VOLUME,CUM % VOLUME
   80.2,    83.3,      1,   1.32,   0.02,   0.00, 0.0018,
   83.3,    86.5,      1,   1.32,   0.02,   0.00, 0.0038,
   86.5,    89.8,      1,   1.32,   0.02,   0.00, 0.0060,
   89.8,    93.3,      1,   1.32,   0.02,   0.00, 0.0085,
   93.3,    96.9,      0,   0.00,   0.00,   0.00, 0.0085,
   96.9,   100.6,      0,   0.00,   0.00,   0.00, 0.0085,
```

```
100.6,   104.5,      0,   0.00,   0.00,   0.00, 0.0085,
104.5,   108.5,      0,   0.00,   0.00,   0.00, 0.0085,
108.5,   112.7,      0,   0.00,   0.00,   0.00, 0.0085,
112.7,   117.0,      0,   0.00,   0.00,   0.00, 0.0085,
117.0,   121.6,      0,   0.00,   0.00,   0.00, 0.0085,
121.6,   126.2,      0,   0.00,   0.00,   0.00, 0.0085,
126.2,   131.1,      0,   0.00,   0.00,   0.00, 0.0085,
131.1,   136.2,      0,   0.00,   0.00,   0.00, 0.0085,
136.2,   141.4,      0,   0.00,   0.00,   0.00, 0.0085,
141.4,   146.9,      0,   0.00,   0.00,   0.00, 0.0085,
146.9,   152.5,      0,   0.00,   0.00,   0.00, 0.0085,
152.5,   158.4,      0,   0.00,   0.00,   0.00, 0.0085,
158.4,   164.5,      0,   0.00,   0.00,   0.00, 0.0085,
164.5,   170.9,      0,   0.00,   0.00,   0.00, 0.0085,
170.9,   177.5,      0,   0.00,   0.00,   0.00, 0.0085,
177.5,   184.3,      0,   0.00,   0.00,   0.00, 0.0085,
184.3,   191.4,      0,   0.00,   0.00,   0.00, 0.0085,
191.4,   198.8,      0,   0.00,   0.00,   0.00, 0.0085,
198.8,   206.5,      0,   0.00,   0.00,   0.00, 0.0085,
206.5,   214.4,      0,   0.00,   0.00,   0.00, 0.0085,
214.4,   222.7,      0,   0.00,   0.00,   0.00, 0.0085,
222.7,   231.3,      0,   0.00,   0.00,   0.00, 0.0085,
231.3,   240.2,      1,   1.32,   0.15,   0.05, 0.0538,
240.2,   249.5,      0,   0.00,   0.00,   0.00, 0.0538,
249.5,   259.1,      0,   0.00,   0.00,   0.00, 0.0538,
259.1,   269.1,      0,   0.00,   0.00,   0.00, 0.0538,
269.1,   279.5,      0,   0.00,   0.00,   0.00, 0.0538,
279.5,   290.3,      0,   0.00,   0.00,   0.00, 0.0538,
290.3,   301.5,      0,   0.00,   0.00,   0.00, 0.0538,
301.5,   313.1,      0,   0.00,   0.00,   0.00, 0.0538,
313.1,   325.2,      0,   0.00,   0.00,   0.00, 0.0538,
325.2,   337.7,      0,   0.00,   0.00,   0.00, 0.0538,
337.7,   350.7,      0,   0.00,   0.00,   0.00, 0.0538,
350.7,   364.3,      0,   0.00,   0.00,   0.00, 0.0538,
364.3,   378.3,      0,   0.00,   0.00,   0.00, 0.0538,
378.3,   392.9,      0,   0.00,   0.00,   0.00, 0.0538,
392.9,   408.1,      2,   2.63,   0.85,   0.43, 0.4856,
408.1,   423.8,      0,   0.00,   0.00,   0.00, 0.4856,
423.8,   440.1,      0,   0.00,   0.00,   0.00, 0.4856,
440.1,   457.1,      5,   6.58,   2.71,   1.54, 2.0296,
457.1,   474.8,      2,   2.63,   1.19,   0.71, 2.7385,
474.8,   493.1,      0,   0.00,   0.00,   0.00, 2.7385,
493.1,   512.1,      0,   0.00,   0.00,   0.00, 2.7385,
512.1,   531.8,      6,   7.89,   4.39,   2.91, 5.6494,
531.8,   552.3,      0,   0.00,   0.00,   0.00, 5.6494,
552.3,   573.6,      2,   2.63,   1.64,   1.15, 6.8042,
573.6,   595.8,      9,  11.84,   8.22,   6.09, 12.8904,
595.8,   618.8,      3,   3.95,   2.89,   2.19, 15.0851,
618.8,   642.6,      2,   2.63,   2.16,   1.74, 16.8290,
642.6,   667.4,      0,   0.00,   0.00,   0.00, 16.8290,
667.4,   693.1,      4,   5.26,   4.97,   4.30, 21.1252,
693.1,   719.9,      2,   2.63,   2.70,   2.43, 23.5530,
719.9,   747.6,      7,   9.21,   9.90,   9.13, 32.6847,
747.6,   776.5,      3,   3.95,   4.71,   4.58, 37.2628,
776.5,   806.4,      3,   3.95,   4.91,   4.87, 42.1303,
806.4,   837.5,      3,   3.95,   5.33,   5.51, 47.6415,
837.5,   869.8,      3,   3.95,   5.90,   6.41, 54.0515,
```

```
  869.8,    903.4,      2,    2.63,    4.26,    4.81, 58.8635,
  903.4,    938.2,      5,    6.58,   11.30,   13.17, 72.0295,
  938.2,    974.4,      4,    5.26,    9.79,   11.87, 83.8946,
  974.4,   1012.0,      1,    1.32,    2.53,    3.12, 87.0110,
 1012.0,   1051.0,      1,    1.32,    2.76,    3.55, 90.5568,
 1051.0,   1091.6,      0,    0.00,    0.00,    0.00, 90.5568,
 1091.6,   1133.7,      2,    2.63,    6.67,    9.44, 100.0000,

SPHERICITY TABLE

SPHERICITY,,COUNT,% NUMBER
   0.93,     0.93,      2,    2.63,
   0.93,     0.93,      1,    1.32,
   0.93,     0.94,      4,    5.26,
   0.94,     0.94,      1,    1.32,
   0.94,     0.94,      2,    2.63,
   0.94,     0.95,      5,    6.58,
   0.95,     0.95,      6,    7.89,
   0.95,     0.95,      5,    6.58,
   0.95,     0.95,      3,    3.95,
   0.95,     0.96,      2,    2.63,
   0.96,     0.96,      4,    5.26,
   0.96,     0.96,      9,   11.84,
   0.96,     0.97,      4,    5.26,
   0.97,     0.97,      3,    3.95,
   0.97,     0.97,      4,    5.26,
   0.97,     0.98,      3,    3.95,
   0.98,     0.98,      6,    7.89,
   0.98,     0.98,      3,    3.95,
   0.98,     0.99,      2,    2.63,
   0.99,     0.99,      2,    2.63,
   0.99,     0.99,      0,    0.00,
   0.99,     0.99,      0,    0.00,
   0.99,     1.00,      0,    0.00,
   1.00,     1.00,      5,    6.58,
```

Appendix B: Bibliography

1. Kumar, V., N. Fausto, and A. Abbas, *Robbins & Cotran Pathologic Basis of Disease*. 7th ed. 2004, Philadelphia, PA: W.B. Saunders Company.
2. Saldeen, T., *The Microembolism Syndrom*. 1979, Stockholm, Sweden: Almqvist & Wiksell.
3. Hori, M., et al., *A possible model of the anginal syndrome with normal coronary arteriograms: microembolization of canine coronary arteries.* Heart Vessels, 1987. **3**(1): p. 7-13.
4. Rosch, J., C.T. Dotter, and M.J. Brown, *Selective arterial embolization. A new method for control of acute gastrointestinal bleeding.* Radiology, 1972. **102**(2): p. 303-6.
5. Berenstein, A. and Kricheff, II, *Catheter and material selection for transarterial embolization: technical considerations. II. Materials.* Radiology, 1979. **132**(3): p. 631-9.
6. Ryu, R.K., et al., *Comparison of pain after uterine artery embolization using tris-acryl gelatin microspheres versus polyvinyl alcohol particles.* Cardiovasc Intervent Radiol, 2003. **26**(4): p. 375-8.
7. Andrews, R.T. and C.A. Binkert, *Relative rates of blood flow reduction during transcatheter arterial embolization with tris-acryl gelatin microspheres or polyvinyl alcohol: quantitative comparison in a swine model.* J Vasc Interv Radiol, 2003. **14**(10): p. 1311-6.
8. Siskin, G.P., et al., *Pathologic evaluation of a spherical polyvinyl alcohol embolic agent in a porcine renal model.* J Vasc Interv Radiol, 2003. **14**(1): p. 89-98.
9. Chiesa, A.G. and W.R. Hart, *Uterine artery embolization of leiomyomas with trisacryl gelatin microspheres (TGM): pathologic features and comparison with polyvinyl alcohol emboli.* Int J Gynecol Pathol, 2004. **23**(4): p. 386-92.
10. Spies, J.B., et al., *Polyvinyl alcohol particles and tris-acryl gelatin microspheres for uterine artery embolization for leiomyomas: results of a randomized comparative study.* J Vasc Interv Radiol, 2004. **15**(8): p. 793-800.
11. Chua, G.C., et al., *Comparison of particle penetration with non-spherical polyvinyl alcohol versus trisacryl gelatin microspheres in women undergoing premyomectomy uterine artery embolization.* Clin Radiol, 2005. **60**(1): p. 116-22.
12. Lupattelli, T., et al., *Percutaneous uterine artery embolization for the treatment of symptomatic fibroids: current status.* Eur J Radiol, 2005. **54**(1): p. 136-47.
13. Spies, J.B., *Uterine artery embolization for fibroids: understanding the technical causes of failure.* J Vasc Interv Radiol, 2003. **14**(1): p. 11-4.
14. Osuga, K., et al., *Embolization of high flow arteriovenous malformations: experience with use of superabsorbent polymer microspheres.* J Vasc Interv Radiol, 2002. **13**(11): p. 1125-33.
15. Laurent, A., et al., *Trisacryl gelatin microspheres for therapeutic embolization, I: development and in vitro evaluation.* AJNR Am J Neuroradiol, 1996. **17**(3): p. 533-40.

16. Beaujeux, R., et al., *Trisacryl gelatin microspheres for therapeutic embolization, II: preliminary clinical evaluation in tumors and arteriovenous malformations.* AJNR Am J Neuroradiol, 1996. **17**(3): p. 541-8.
17. Bendszus, M., et al., *Efficacy of trisacryl gelatin microspheres versus polyvinyl alcohol particles in the preoperative embolization of meningiomas.* AJNR Am J Neuroradiol, 2000. **21**(2): p. 255-61.
18. Basile, A., et al., *Trisacryl gelatin microspheres versus polyvinyl alcohol particles in the preoperative embolization of bone neoplasms.* Cardiovasc Intervent Radiol, 2004. **27**(5): p. 495-502.
19. Jiaqi, Y., et al., *[A new embolic material: super absorbent polymer (SAP) microsphere and its embolic effects].* Nippon Igaku Hoshasen Gakkai Zasshi, 1996. **56**(1): p. 19-24.
20. Osuga, K., et al., *[A new embolic material: SAP-microsphere].* Nippon Rinsho, 2001. **59 Suppl 6**: p. 534-8.
21. Khankan, A.A., et al., *Embolic effects of superabsorbent polymer microspheres in rabbit renal model: comparison with tris-acryl gelatin microspheres and polyvinyl alcohol.* Radiat Med, 2004. **22**(6): p. 384-90.
22. Spies, J.B. and J.P. Pelage, *Uterine Artery Embolization and Gynecologic Embolotherapy*. 2005, Philadelphia, PA: Lippincott WIlliams & Wilkins.
23. Ravina, J.H., et al., *[Arterial embolization of uterine myoma: results apropos of 286 cases].* J Gynecol Obstet Biol Reprod (Paris), 2000. **29**(3): p. 272-5.
24. Bakal, C.W., et al., *Vacular and Interventional Radiology: Principles and Practice*. 2002, New York, NY: Thieme Medical Publishers, Inc.
25. de Blok, S., et al., *Fatal sepsis after uterine artery embolization with microspheres.* J Vasc Interv Radiol, 2003. **14**(6): p. 779-83.
26. Simon, J. and M. Silverstein, *Uterine artery embolization for fibroids: Procedure, results, and complications.* SUPPLEMENT TO APPLIED RADIOLOGY, 2001.
27. Vogl, T.J., et al., *[Embolization of symptomatic myomas (UAE): technique, indication and results].* Rofo, 2003. **175**(8): p. 1032-41.
28. Joffre, F., J.M. Tubiana, and J.P. Pelage, *FEMIC (Fibromes Embolises aux MICrospheres calibrees): uterine fibroid embolization using tris-acryl microspheres. A French multicenter study.* Cardiovasc Intervent Radiol, 2004. **27**(6): p. 600-6.
29. Richter, G.M., et al., *[Uterine fibroid embolization with spheric micro-particles using flow guiding: safety, technical success and clinical results].* Rofo, 2004. **176**(11): p. 1648-57.
30. Takano, M., et al., *Successful management of cervical pregnancy by selective uterine artery embolization: a case report.* J Reprod Med, 2004. **49**(12): p. 986-8.
31. Marret, H., et al., *Late leiomyoma expulsion after uterine artery embolization.* J Vasc Interv Radiol, 2004. **15**(12): p. 1483-5.
32. Rajan, D.K., et al., *Risk of intrauterine infectious complications after uterine artery embolization.* J Vasc Interv Radiol, 2004. **15**(12): p. 1415-21.
33. Lefebvre, G.G., G. Vilos, and M. Asch, *Uterine fibroid embolization (UFE).* J Obstet Gynaecol Can, 2004. **26**(10): p. 899-911, 913-28.

34. Phelan, J.T., 2nd, J. Broder, and P.A. Kouides, *Near-fatal uterine hemorrhage during induction chemotherapy for acute myeloid leukemia: a case report of bilateral uterine artery embolization.* Am J Hematol, 2004. **77**(2): p. 151-5.
35. Hovsepian, D.M., et al., *Quality improvement guidelines for uterine artery embolization for symptomatic leiomyomata.* Cardiovasc Intervent Radiol, 2004. **27**(4): p. 307-13.
36. Helmberger, T.K., T.F. Jakobs, and M.F. Reiser, *Embolization of uterine fibroids.* Abdom Imaging, 2004. **29**(2): p. 267-77.
37. Smith, W.J., et al., *Patient satisfaction and disease specific quality of life after uterine artery embolization.* Am J Obstet Gynecol, 2004. **190**(6): p. 1697-703; discussion 1703-6.
38. Kim, M.D., et al., *Uterine artery embolization for adenomyosis without fibroids.* Clin Radiol, 2004. **59**(6): p. 520-6.
39. Leonhardt, H., et al., *[Embolization of uterine arteries yields good results in symptomatic myoma].* Lakartidningen, 2004. **101**(13): p. 1208-14.
40. Kroncke, T.J., et al., *[Transarterial embolization for uterine fibroids: clinical success rate and results of magnetic resonance imaging].* Rofo, 2005. **177**(1): p. 89-98.
41. Nikolic, B., et al., *Ovarian artery supply of uterine fibroids as a cause of treatment failure after uterine artery embolization: a case report.* J Vasc Interv Radiol, 1999. **10**(9): p. 1167-70.
42. Pelage, J.P., et al., *Uterine artery embolization in sheep: comparison of acute effects with polyvinyl alcohol particles and calibrated microspheres.* Radiology, 2002. **224**(2): p. 436-45.
43. Weichert, W., et al., *Uterine Arterial Embolization With Tris-acryl Gelatin Microspheres: A Histopathologic Evaluation.* Am J Surg Pathol, 2005. **29**(7): p. 955-961.
44. Iwase, K., et al., *Laparoscopically assisted splenectomy following preoperative splenic artery embolization using contour emboli for myelofibrosis with massive splenomegaly.* Surg Laparosc Endosc Percutan Tech, 1999. **9**(3): p. 197-202.
45. Nakamura, H., et al., *[Transcatheter arterial embolization for advanced hepatocellular carcinoma--indications and limitations].* Gan To Kagaku Ryoho, 2000. **27**(10): p. 1509-15.
46. Osuga, K., et al., *Transarterial embolization for large hepatocellular carcinoma with use of superabsorbent polymer microspheres: initial experience.* J Vasc Interv Radiol, 2002. **13**(9 Pt 1): p. 929-34.
47. Takeda, T., et al., *A case of generalised oedema secondary to uterine artery embolisation for leiomyomata.* BJOG, 2004. **111**(2): p. 179-80.
48. Takeda, T., et al., *Changes of plasma vascular endothelial growth factor level after uterine artery embolisation for leiomyomata.* BJOG, 2005. **112**(10): p. 1437-9.
49. Jeremy, R.W., et al., *Preservation of coronary flow reserve in stunned myocardium.* Am J Physiol, 1989. **256**(5 Pt 2): p. H1303-10.
50. Chilian, W.M., et al., *Microvascular occlusions promote coronary collateral growth.* Am J Physiol, 1990. **258**(4 Pt 2): p. H1103-11.

51. Tulandi, T., *Uterine Fibroids: Embolization and other treatments*. 2003, New York, NY: Cambridge University Press.
52. Healey, S., et al., *Ovarian function after uterine artery embolization and hysterectomy*. J Am Assoc Gynecol Laparosc, 2004. **11**(3): p. 348-52.
53. Meriam, J.L. and L.G. Kraige, *Engineering Mechanics: Dynamics*. Vol. 2. 2002, New York, NY: John Wiley and Sons.
54. Fung, Y.C., *Biomechanics: Motion, Flow, Stress, and Growth*. 1990.
55. Fung, Y.C., *First Course in Continuum Mechanics*. 3rd ed. 1994, New Jersey: Prentice-Hall.
56. Coxeter, H.S.M., *Introduction to Geometry*. 1961, New York, NY: John Wiley and Sons.
57. Black, J., *Biological Performance of Materials: Fundamentals of Biocompatability*. 3rd ed. 1999, New York, NY: Marcel Dekker, Inc.
58. Peppas, N.A., *Physiologically responsive hydrogels*. J. Bioact. Compat. Polym., 1991.
59. Ratner, B., et al., *Biomaterials Science*. Second ed. 2004, San Diego, CA: Elsevier Academic Press.
60. Kronenthal, R., Z. Oser, and E. Martin, *Polymer Science and Technology: Polymers in Medicine and Surgery*. 1975. **8**.
61. Oxtoby, D. and N. Nachtrieb, *Principles of Modern Chemistry*. 3rd ed. 1996, Orlando, FL: Saunders College Publishing.
62. Fishbane, P., S. Gasiorowicz, and S. Thorton, *Physics for Scientists and Engineers*. 2 ed. Vol. 2. 1996, New Jersey: Prentice Hall.
63. Beckman-Coulter, *RapidVUE Particle Analysis System User's Reference PN 8321490B*.
64. Beckman-Coulter, *RapidVUE Fluid Sample Module Reference Manual PN 8321519A*.
65. Rogers, C., et al., *Embolic protection with filtering or occlusion balloons during saphenous vein graft stenting retrieves identical volumes and sizes of particulate debris*. Circulation, 2004. **109**(14): p. 1735-40.
66. Quan, V.H., et al., *Morphometric analysis of particulate debris extracted by four different embolic protection devices from coronary arteries, aortocoronary saphenous vein conduits, and carotid arteries*. Am J Cardiol, 2005. **95**(12): p. 1415-9.
67. Hayter, A.J., *Probability and Statistics for Engineers and Scientists*. 2nd ed. 2002, Pacific Grove, CA: Duxbury Thomas Learning.
68. Sabersky, R., et al., *Fluid Flow*. 4th ed. 1999, New Jersey: Simon & Schuster.
69. Kurkuri, M.D. and T.M. Aminabhavi, *Poly(vinyl alcohol) and poly(acrylic acid) sequential interpenetrating network pH-sensitive microspheres for the delivery of diclofenac sodium to the intestine*. J Control Release, 2004. **96**(1): p. 9-20.
70. Jack, C.R., Jr., et al., *Polyvinyl alcohol sponge for embolotherapy: particle size and morphology*. AJNR Am J Neuroradiol, 1985. **6**(4): p. 595-7.
71. Kusano, S., et al., *Low-dose particulate polyvinylalcohol embolization in massive small artery intestinal hemorrhage. Experimental and clinical results*. Invest Radiol, 1987. **22**(5): p. 388-92.

72. Ghavamzadeh, R., V. Haddadi-Asl, and H. Mirzadeh, *Bioadhesion and biocompatibility evaluations of gelatin and polyacrylic acid as a crosslinked hydrogel in vitro.* J Biomater Sci Polym Ed, 2004. **15**(8): p. 1019-31.
73. Dimitrov, M., et al., *Hydrogels based on the chemically crosslinked polyacrylic acid: biopharmaceutical characterization.* Acta Pharm, 2003. **53**(1): p. 25-31.
74. Berne, R.M., et al., *Physiology*. 5th ed. 2004, St. Louis, Mo: C.V. Mosby.
75. Hori, M., et al., *Adenosine-induced hyperemia attenuates myocardial ischemia in coronary microembolization in dogs.* Am J Physiol, 1989. **257**(1 Pt 2): p. H244-51.
76. Murray, C.J. and A.D. Lopez, *Mortality by cause for eight regions of the world: Global Burden of Disease Study.* Lancet, 1997. **349**(9061): p. 1269-76.
77. Costantini, C.O., et al., *Frequency, correlates, and clinical implications of myocardial perfusion after primary angioplasty and stenting, with and without glycoprotein IIb/IIIa inhibition, in acute myocardial infarction.* J Am Coll Cardiol, 2004. **44**(2): p. 305-12.
78. Alfayoumi, F., et al., *The no-reflow phenomenon: epidemiology, pathophysiology, and therapeutic approach.* Rev Cardiovasc Med, 2005. **6**(2): p. 72-83.
79. Grube, E., et al., *Prevention of distal embolization during coronary angioplasty in saphenous vein grafts and native vessels using porous filter protection.* Circulation, 2001. **104**(20): p. 2436-41.
80. Heusch, G., et al., *Coronary microembolization.* J Mol Cell Cardiol, 2004. **37**(1): p. 23-31.
81. Grund, F., et al., *Microembolization in pigs: effects on coronary blood flow and myocardial ischemic tolerance.* Am J Physiol, 1999. **277**(2 Pt 2): p. H533-42.
82. Skyschally, A., et al., *Reduced coronary and inotropic reserves with coronary microembolization.* Am J Physiol Heart Circ Physiol, 2002. **282**(2): p. H611-4.
83. Dorge, H., et al., *Perfusion-contraction mismatch with coronary microvascular obstruction: role of inflammation.* Am J Physiol Heart Circ Physiol, 2000. **279**(6): p. H2587-92.
84. Grube, E., et al., *Evaluation of a balloon occlusion and aspiration system for protection from distal embolization during stenting in saphenous vein grafts.* Am J Cardiol, 2002. **89**(8): p. 941-5.
85. Topol, E.J. and J.S. Yadav, *Recognition of the importance of embolization in atherosclerotic vascular disease.* Circulation, 2000. **101**(5): p. 570-80.
86. Erbel, R. and G. Heusch, *Spontaneous and iatrogenic microembolization. A new concept for the pathogenesis of coronary artery disease.* Herz, 1999. **24**(7): p. 493-5.
87. Beck, W.S., *Hematology*. 5th ed. 1991, Cambridge, MA: The MIT Press.
88. Erbel, R. and G. Heusch, *Coronary microembolization--its role in acute coronary syndromes and interventions.* Herz, 1999. **24**(7): p. 558-75.
89. Atar, S. and U. Rosenschein, *Perspectives on the role of ultrasonic devices in thrombolysis.* J Thromb Thrombolysis, 2004. **17**(2): p. 107-14.
90. Ohki, T., et al., *Efficacy of a proximal occlusion catheter with reversal of flow in the prevention of embolic events during carotid artery stenting: an experimental analysis.* J Vasc Surg, 2001. **33**(3): p. 504-9.

91. Schomig, A. and A. Kastrati, *Distal embolic protection in patients with acute myocardial infarction: attractive concept but no evidence of benefit.* Jama, 2005. **293**(9): p. 1116-8.
92. Taguchi, I., et al., *Comparison of the effects of a distal embolic protection device and an aspiration catheter during percutaneous coronary intervention in patients with acute myocardial infarction.* Circ J, 2005. **69**(1): p. 49-54.
93. Fung, Y.C., *Biomechanics: Mechanical Properties of Living Tissues*. Second Edition ed. 1993, New York: Springer-Verlag.
94. Hwang, C.W., et al., *Thrombosis modulates arterial drug distribution for drug-eluting stents.* Circulation, 2005. **111**(13): p. 1619-26.
95. Fung, Y.C., *Biomechanics: Circulation.* 2nd ed. 1997, New York, NY: Springer-Verlag.
96. Kassab, G.S., et al., *Morphometry of pig coronary arterial trees.* Am J Physiol, 1993. **265**(1 Pt 2): p. H350-65.
97. Kassab, G.S., D.H. Lin, and Y.C. Fung, *Morphometry of pig coronary venous system.* Am J Physiol, 1994. **267**(6 Pt 2): p. H2100-13.
98. Kassab, G.S. and Y.C. Fung, *Topology and dimensions of pig coronary capillary network.* Am J Physiol, 1994. **267**(1 Pt 2): p. H319-25.
99. Kassab, G.S., D.H. Lin, and Y.C. Fung, *Consequences of pruning in morphometry of coronary vasculature.* Ann Biomed Eng, 1994. **22**(4): p. 398-403.
100. Kassab, G.S. and Y.C. Fung, *The pattern of coronary arteriolar bifurcations and the uniform shear hypothesis.* Ann Biomed Eng, 1995. **23**(1): p. 13-20.
101. Kassab, G.S., J. Berkley, and Y.C. Fung, *Analysis of pig's coronary arterial blood flow with detailed anatomical data.* Ann Biomed Eng, 1997. **25**(1): p. 204-17.
102. Zhou, Y., G.S. Kassab, and S. Molloi, *On the design of the coronary arterial tree: a generalization of Murray's law.* Phys Med Biol, 1999. **44**(12): p. 2929-45.
103. Kassab, G.S., *The coronary vasculature and its reconstruction.* Ann Biomed Eng, 2000. **28**(8): p. 903-15.
104. Mittal, N., et al., *Analysis of blood flow in the entire coronary arterial tree.* Am J Physiol Heart Circ Physiol, 2005. **289**(1): p. H439-46.